THE MOBILITY OF ELECTRONS

IN

HYDROGEN AT LOW PRESSURES

being

a thesis on the motion of electrons in
pure hydrogen at moderate values of E/p.

by

D.K. BEDFORD, B.Sc., A.Inst.P.

and

submitted to the University of Keele for
the degree of Ph.D.

Department of Physics
University of Keele.

Department of Physics
LaTrobe University.

July 1970

ACKNOWLEDGEMENTS

I wish to express my thanks to -

Professor D.Elwyn Davies, my supervisor, for his help and guidance, and for the provision of facilities at LaTrobe University,

Professor D.J.E.Ingram for the provision of facilities at the University of Keele,

Dr D.Smith for many invaluable and stimulating discussions at all stages of this work,

Dr N.A. Surplice for his interest, and to many colleagues at Keele, LaTrobe and Birmingham Universities for helpful discussions,

Mr F.Rowerth, Mr C. Ducza and Mr K. Flisikowski and their technical staffs, and Mr H.Nielissen for their willing and skilled assistance,

Miss C.Wilkinson for her care in typing this thesis,

My wife for her patient encouragement.

SYNOPSIS

Measurements of the electron drift velocity at room temperature in pure molecular hydrogen have been made for the E/p range between 40 and 360 volts.cm^{-1}.torr^{-1}. Experimental conditions were arranged to minimise the effects of space charge distortion of the applied electric field, of secondary processes, and of the time for initial equilibrium of the avalanche to be established.

The progress of single avalanches was monitored by photomultipliers and an electron-multiplier in a pulsed time-of-flight method. The scattering of resonance radiation in the gas caused erroneous results to be recorded by the photomultiplier technique, but the electron-multiplier measurements yielded reliable data.

The v_- values show fair agreement with those obtained previously by Schlumbohm(3.46), but are higher up to a maximum of 17%. It is shown that the relationship between v_- and E/p is given by the expression

$$v_- \propto (E/p)^{\nu}$$

where, if all the electron-multiplier data is considered,

$$\nu = 0.9 \quad \text{for } E/p = 40 \text{ to } 360 \text{ volts.cm}^{-1}\text{.torr}^{-1}.$$

These values for ν can be compared with those from (3.46), ranging from 1.65 at E/p = 30 to 0.5 at E/p = 1500. An adequate theoretical treatment is not available for the E/p range covered by the present invest-

-igation; at low E/p, theory shows $\nu = 0.5$.

Further data, of poor quality, is presented for electron energy distributions in the anode region of a glow discharge in hydrogen, and for positive ion drift velocities in helium. The development of a fast triggered ultra-violet light source is also described.

CONTENTS

CONTENTS Cont'd

LIST OF FIGURES

Table

INTRODUCTION

The importance of the energy distribution in all phenomena associated with the motion of charged particles in a gaseous medium has been recognised at least since 1930 (2.15), and there has been adequate consideration of the interdependence of the electron drift velocity and energy distribution in most of the theoretical and experimental investigations at low E/p, where only momentum-transfer collisions need be included. At moderate E/p, many types of collision are possible and the problem becomes difficult to manage theoretically; reliable experimental values for the electron drift velocity are available for E/p < 40 volts.cm^{-1}.torr^{-1}, but little attention has been paid to the determination of the electron energy distribution. At higher E/p, up to 1700 volts.cm^{-1}.torr^{-1} for hydrogen, there has been only one successful determination of electron drift velocities (3.46), and no attempt has been made to measure the energy distribution or to apply a rigorous theoretical treatment. Thus there exists a need for electron drift velocities to confirm the existing set for E/p > 40, and for electron energy distributions in this same region. These complementary data would also permit a proper evaluation of any theoretical solutions of the problem that might become available.

Conflicting measurements of the first Townsend coefficient α have led to uncertainty and speculation about the possible onset of non-equilibrium conditions above E/p $\sim$ 150 volts.cm^{-1}.torr^{-1}, a situation in which a swarm of electrons, drifting in a uniform electric

field, never comes to equilibrium with the field and the gas, but continues to accelerate until the anode is reached. In the measurement of drift velocities, such an effect would be manifested by a dependence on the drift distance d, and on the applied voltage V_a, for conditions of constant E/p.

In this investigation, electron drift velocities have been obtained, for the E/p range 40 to 360 volts.cm^{-1}.$torr^{-1}$, which substantially confirm the existing values, and no evidence of non-equilibrium has been observed in this region. A technique, potentially capable of determining electron energy distributions at high E/p, was not developed sufficiently to yield useful data.

Chapter 1 introduces the basic physics of the Townsend discharge, with the emphasis on pulsed single avalanches, and considers the effects of diffusion, space charge and impurities on such avalanches. There is no satisfactory theory available for the E/p range in which this investigation was conducted, but some of the theories for low E/p are discussed in Chapter 2. In Chapter 3, the methods for determining electron drift velocities are classified, previous work is reviewed, and the motives for selecting the pulsed time-of flight are outlined. The experimental procedures and apparatus, both for the principal experiment in hydrogen and for a preliminary investigation in helium, are detailed in Chapter 4, and a fast pulsed ultra-violet source light source is described in Appendix 4.

In Chapter 5 the early helium data is briefly considered, followed by a critical assessment of the electron drift velocity values of Schlumbohm (3.46) and Dawson (3.58). Anomalous v_- values in hydrogen were obtained in this investigation by a technique employing photomultipliers, and much of this chapter is devoted to determining whether these values are real or spurious. It is concluded that resonance scatter of photons is leading to false data, and only the independent values obtained by an electron-multiplier technique appear to be reliable. The electron energy measurements are briefly considered, and the possibilities for further work are explored.

The word "molecules" is frequently used in this thesis to describe both atomic and molecular neutral particles when the discussion is general, and it will be clear from the context whether the term should be interpreted in its general or specific sense.

The relationship between the electron mobility μ_- and the drift velocity v_- is $v_- = \mu_- E$ (by definition), and between v_- and the fundamental parameter E/p is $v_- \alpha (E/p)^{\nu}$ (by experiment and theory), where $\nu = \frac{1}{2}$ at low E/p and $\nu \sim 1$ for the E/p range of this investigation. The resultant relationship $\mu_- \alpha E^{(\nu-1)}/p^{\nu}$ is inconvenient, particularly if the value of ν is not known, and therefore the dependence of v_-, rather than μ_-, on E/p is investigated throughout this thesis.

CHAPTER 1

TOWNSEND DISCHARGES, WITH PARTICULAR REFERENCE TO PULSED SINGLE AVALANCHES

1.1. Introduction.

1.2. Primary Processes.

1.3. Secondary Processes.

1.4. Self-sustained Currents and Paschen's Law.

1.5. The Currents due to an Avalanche.

1.6. Diffusion and Space Charge.

1.7. The Effects of Impurities.

1.1. Introduction.

This investigation is concerned solely with the motion of charged particles in gases, particularly hydrogen, under the conditions of a Townsend type of discharge. This is not to say that the same type of motion does not occur in other classes of discharge, but that a Townsend discharge was selected because the quantities to be measured are well defined under these conditions, and the mechanism of the Townsend discharge is clearly understood. Considerable care is taken experimentally to ensure that the conditions are those of the simple Townsend mechanism, and to preclude any complicating conditions.

To precisely define a Townsend discharge is difficult, but the most important condition is that the electric field in the discharge region should only be that applied externally, unmodified to any appreciable extent by ionisation space charge; this condition can be imposed by keeping current densities to the minimum practical value. Usually Townsend conditions also imply gases at fairly low pressures of less than about 500 torr, and uniform electric fields between plane-parallel or Rogowski electrodes, the fields being either steady or pulsed, though these conditions reflect the bulk of experimental work rather than fundamental boundaries of the Townsend regime. It might be mentioned that some of the concepts and terminology of the

Townsend discharge have been borrowed in the analogous field of the study of the motion of charges in semi-conductors.

1.2. Primary Processes.

Consider a region of uniform electric field E volts. cm^{-1}, bounded by two plane parallel electrodes of potential difference V_a volts and separation d cm, filled with a pure gas at pressure p_o torr, where p_o is the pressure reduced to 0^oC (Appendix I). If an electron appears in this region it is accelerated by the field until it makes a collision with a neutral gas molecule; this collision may be elastic, or inelastic resulting in excitation or ionisation of the molecule. If the collision is elastic the electron will retain most of its kinetic energy, losing on the average only $2Mm/(M+m)^2 \simeq 2m/M$ per collision, and the instantaneous scattering angle of the electron is expected to be isotropic. After an elastic collision the electron will continue to acquire energy from the electric field until it has sufficient energy to cause either excitation or ionisation. For theoretical convenience, it is usually assumed that, after an exciting or ionising collision, the electron starts from rest.

Townsend's first ionisation coefficient α is defined as the number of ionising collisions per electron per cm path length in the field direction. Thus, if n_o electrons are released from the cathode, either steadily per second or as a short pulse, the electron current or number of electrons, respectively, at a distance x from the cathode is given by

$$n = n_o \exp(\alpha x) \quad (1.1)$$

if α is constant. This exponentially increasing bunch of electrons is known as an avalanche or, if $\alpha \simeq 0$, a swarm. It is sometimes more convenient to express this in terms of conventional current, $I = I_o \exp(\alpha x)$, and if the initiating electrons are released as a pulse, it is frequently useful to invoke the electron drift velocity v_- to give

$$n = n_o \exp(\alpha v_- t) \quad (1.2)$$

This expression is not entirely sufficient, since it is probable that the n_o initiating electrons will not be in equilibrium with the electric field and the gas, thus modifying the value of α until equilibrium is attained; α, or more precisely α/p, is only constant if E/p (Appendix 1) is constant. This deviation is most easily taken into account by rewriting the equation (1.2) thus

$$n = n_o \exp[\alpha v_- (t-t_o)] \ldots \quad (1.3)$$

where t_o is a function of the time taken to come to equilibrium. It is sometimes convenient to write this expression as $n = n_o \exp\eta(V-V_o)$, where $\eta = \alpha/E$ is the number of ionising collisions per volt.

A qualitative model readily shows that α/p must depend on E/p, since the energy acquired by the electron per cm travelled in the field direction is determined by E, and the distance between collisions is proportional to 1/p, so that the energy gained between collisions, and therefore the number of ionisations per collision (which is proportional to α/p) will be some function of E/p. Townsend (1901)[1.1] confirmed experimentally that $\alpha/p = f(E/p)$, and von Engel (1956)[1.2] and Smith (1965)[1.3] have shown that

$$\alpha/p = A.\exp(-B.p/E)$$

in agreement with experimental data for a number of gases over the approximate range E/p = 100 to 800 volts.cm^{-1}.torr^{-1} (for hydrogen A = 5, B = 130 for E/p = 150 to 600, and for helium A = 3, B = 34 for E/p = 20 to 150)[1.4]. This expression was derived by consideration of the average energy of the electron swarm, but it is more rigorous to use an energy distribution (Chapter 2). Emeleus, Lunt and Meek (1936)[1.5] assumed a

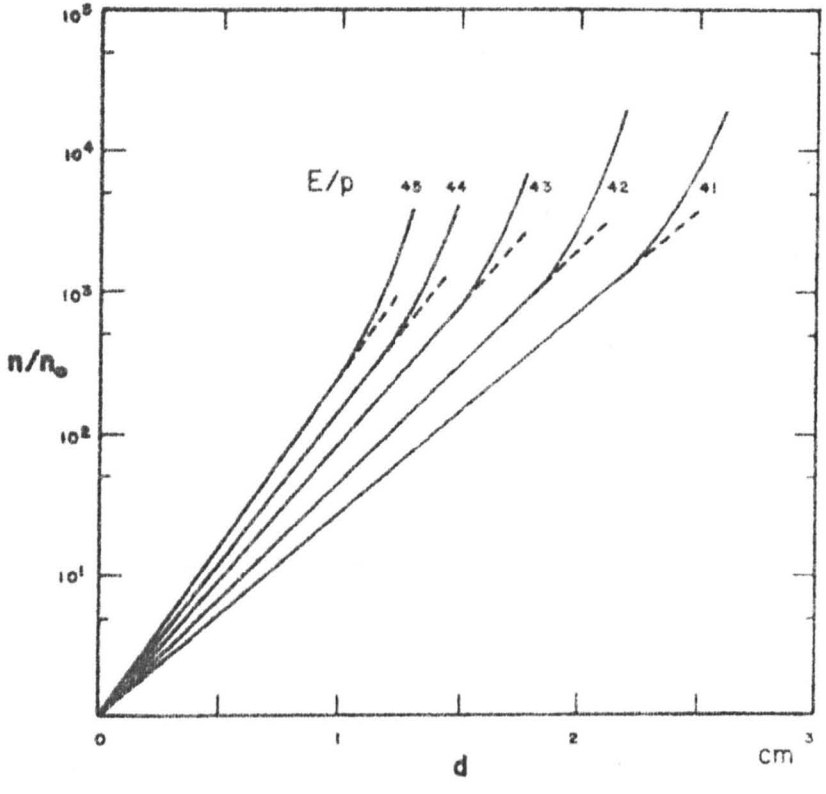

Fig. 1.1

The variation of $\log(n/n_o)$ with the interelectrode distance d.

Maxwellian distribution to obtain the expression

$$\frac{\alpha}{p} = \frac{1.23\times10^{8}}{v_-} (\bar{V})^{-3/2} \int_{V_i}^{\infty} \alpha'(V).\exp -\frac{3V_i}{2V} . dV,$$

where $\bar{V}$ is the mean electron energy in eV, $\alpha'(V)$ is the number of ionising collisions per cm of actual path at 1 torr by an electron of energy V, and V_i is the ionisation potential. This showed some agreement with experimental data for the diatomic gases hydrogen, oxygen and air, but not for the monatomic gas argon. Blevin and Haydon (1957)[1.6] later used this expression to show good agreement with the experimental values of Blevin, Haydon and Somerville (1957)[1.7] and Rose, DeBitetto and Fisher (1956)[1.8] for α/p in hydrogen over the range E/p = 30 to 150 volts. $cm^{-1}.torr^{-1}$.

1.3. Secondary Processes.

There are two reasons to suspect that the mechanism detailed above does not fully describe the Townsend process. Firstly, if experimental values of the ratio $\log(n/n_o)$ are plotted against d for constant E/p, as in fig.1.1, a straight line is not obtained for large values of d. Secondly, it is observed that it is possible to obtain a self-sustained discharge whilst rigidly maintaining Townsend conditions, and also that, if

all external restraints are removed, the current in the gap will increase rapidly with time under certain conditions until it is no longer possible to maintain the potential across the electrodes. The simple expressions previously stated predict a linear $\log(n/n_o)$ - d graph, and that n is proportional to n_o at all times.

As a consequence, Townsend modified his equation to include the generalised secondary ionisation coefficient γ, defined as the number of secondary electrons produced per primary electron, leading to the modified expression

$$n' = n_o \frac{\exp\alpha v_-(t-t_o)}{1-\gamma[\exp\alpha v_-(t-t_o)-1]} \quad .. \qquad (1.4)$$

at constant E/p.

There are six possible classes of mechanism whereby secondary electrons might be produced, namely

the interaction of

{ positive ions, photons, excited molecules } with the { gas, cathode } .

Gas processes are not normally of importance, since positive ions do not acquire sufficient energy in moderate electric fields to cause ionisation, and the probability for photo-ionisation by recombination photons is small (section 5.4.1). Excited molecules

have very short lifetimes, $\sim 10^{-8}$ sec, which make such a process unlikely except for metastable states, for example

$$He_m^* + He \rightarrow He_2^+ + e.$$

However, all three classes of cathode process are important, positive ions readily ejecting electrons from a metal surface if $eV_i > 2e\phi$, as will incident photons if $h\nu > \phi$ (ϕ is the work function). The work of Schram et al (1966)[1.9] on the incidence of multiply-charged noble gas ions on a copper-beryllium surface showed that γ is approximately linearly dependent on the velocity of the ion, and is independent of the charge, implying that it is the kinetic rather than the potential energy of the ion that determines the value of γ. Photon action is important whether the photons arrive directly, and therefore virtually instantaneously at the cathode, or are delayed in the gas by the process of resonance radiation (section 5.5). Whilst most excited molecules still have too short a lifetime to be effective, the millisecond or greater lifetimes of metastable states make them highly efficient producers of secondary electrons.

The hydrogen molecule has no metastable states (the ^2P state of the hydrogen atom is metastable, but the lifetime of the atom is short and the probability of incidence at the cathode is

small), so the mechanisms that must be considered are the incidence at the cathode of photons and positive ions. The relative proportions of these processes are not of importance in this work, but a qualitative measure can be obtained by observation of the variation of γ with E/p. As E/p increases up to a value of about 150 volts.cm^{-1}. torr^{-1}, there are relatively more ionising than exciting collisions, so that an increase in γ with increasing E/p would indicate predominantly positive ion production of secondaries, a decrease in γ photon produced secondaries. It is possible to evaluate the relative contributions of the secondary processes by measurement of the formative time lags (f.t.l.) of slightly overvolted pulsed discharges. The magnitude of the f.t.l. provides an immediate indication of the predominant secondary process, values in the 10^{-7} sec range indicating photon action, in the 10^{-5} sec range positive ion action, and in the milli-second range metastable action, for overvoltages of a few percent and anode-cathode separations of a few centimetres. An analysis developed by Bartholomeyczyk (1940)[1.10], and later refined and modified by Davidson (1953)[1.11], permits an accurate evaluation of the relative contributions of the secondary processes, but it is necessary to know which processes are active and the values of α, γ, v_- and v_+ appropriate to the experimental conditions, and the overvoltage

is restricted to less than 5% of the sparking potential. This analysis has been criticised on the grounds that no allowance is made for the effects of space charge, which must be present at least during the final portion of the f.t.l. period, but it appears that a satisfactory alternative in this respect is not at present available. The Davidson-Bartholomeyczk analysis has been successfully applied to the study of secondary processes in hydrogen, helium, neon and argon[1.12-16].

1.4. Self-sustained Currents and Paschen's Law.

The threshold conditions for a self-sustained current and for sparking or breakdown are the same, a self-sustained current normally implying the use of external restraints to prevent the current from increasing to a value where space charge effects become significant, and breakdown that the current is allowed to develop until the source of potential fails. For either to occur, it is only necessary that the rate of production of secondary electrons should at least be equal to the rate at which electrons are removed from the discharge region, or that n should be independent of n_o. This condition is fulfilled if the denominator in equation (1.4) is set equal to zero, i.e.

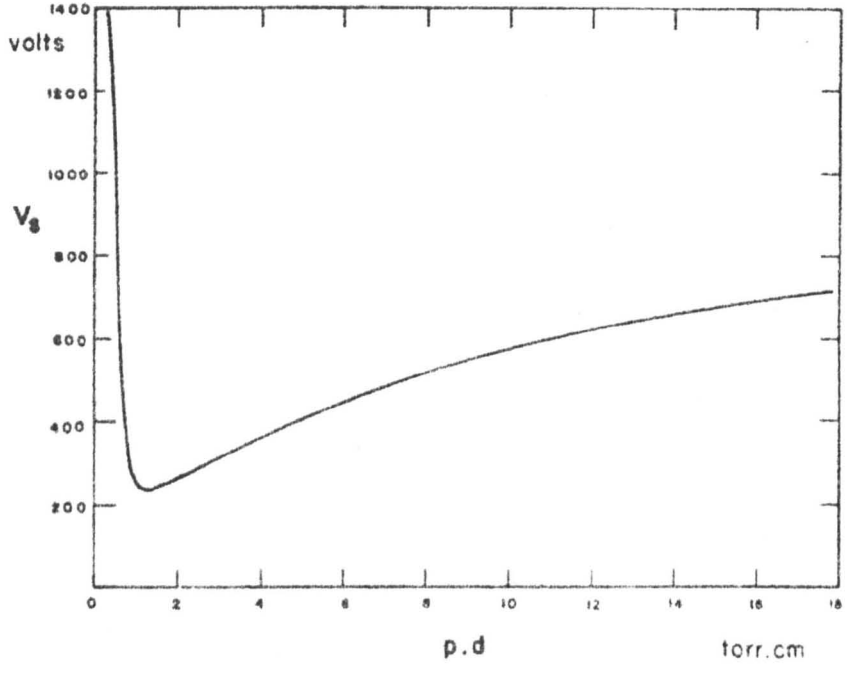

Fig. 1.2

Paschen curve for Hydrogen with a Nickel cathode.

$$1 - \gamma\left[\exp \alpha v_{-} (t-t_{o}) - 1\right] = 0 \qquad (1.5)$$

Thus, neglecting t_o, a knowledge of α and γ for the experimental conditions permits $v_-.t$, and thus d to be calculated for the onset of breakdown; at this value d_s, the potential across the gap $V_s = E/p.pd_s$ is known as the sparking potential.

It has been established experimentally that V_s is a function of (pxd_s) only, this relationship being known as Paschen's Law. The Paschen curve for Hydrogen (fig. 1.2) is typical of that for most gases in that, as (pxd_s) increases, V_s decreases sharply at low pxd_s, finds a minimum in the region of a few torr.cm, and then increases again less steeply. It is important to specify the cathode material and condition as well as the gas when presenting Paschen curves, since the appearance of γ in equation (1.5) means that breakdown is dependent on the nature of the cathode surface. Deviations from Paschen's law have been reported (e.g. Davies, Smith and Myatt (1961)[1.17], Overton, Smith and Davies (1965)[1.18]), these being attributed to the use of gaps of variable geometry under conditions where field-independent photon and metastable secondary processes are important, and where the loss of these agencies from the gap must be considered. It is perhaps of interest to mention that in some circumstances a glow discharge is observed to take a path between the electrodes which is not

the shortest, due to the tendency for the discharge to seek the value of (pxd_s) which corresponds to the lowest sparking potential.

1.5. The Currents due to an Avalanche.

If a potential V_a is applied across the electrodes, and a current measuring device is placed in series with the gap, a current will be observed to flow as a result of a number of possible processes. Firstly, if the applied voltage is pulsed, a momentary displacement current will flow as the self-capacity of the gap is charged - this effect can be used to provide a timing mark in pulsed experiments. Secondly, as the charged particles produced in the gap drift under the influence of the applied field, a conduction current will be observed. The greatest contribution to this current is made by the electron component because of the relatively high drift velocity of the electrons ($\sim 10^2$ times that of the ions), and it is frequently permissible to neglect the effect of positive ions. In the case of electro-negative gases it may be necessary to allow for the negative ion contribution also.

Only the electron component is of importance in the present investigation, since secondary processes have been controlled so that single avalanches can be studied, and in Appendix 2 the currents flowing between the electrodes are

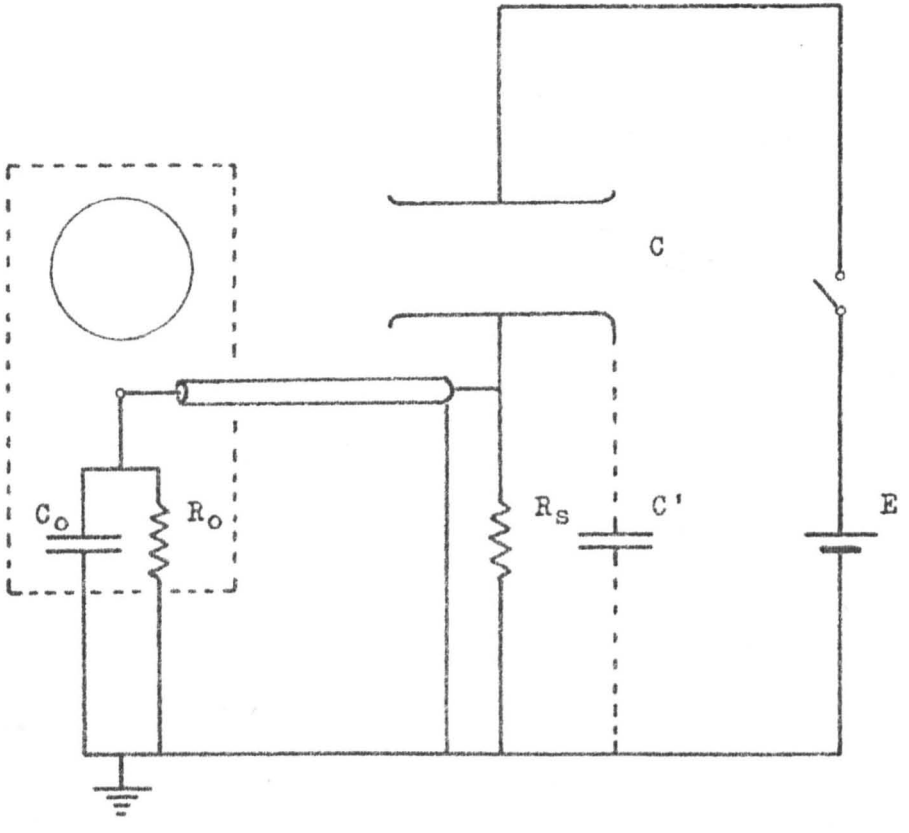

Fig. 1.3

Typical experimental circuit.

calculated for the various components under conditions where the development of the discharge can be completely described in terms of the first Townsend coefficient α, where α is constant throughout the electron transit time.

The effects observed in the external circuit will depend on the choice of circuit components; in particular, it is necessary to carefully choose the time constants. The basic circuit which is almost invariably used is shown in fig.1.3, where R is the resistance across which the signal voltage is developed, comprising the series resistance R_s in parallel with the oscilloscope input resistance R_o, and C is formed by the self-capacitance C_e of the electrodes, in parallel with the input capacitance C_c of the oscilloscope and the capacitance C'_e of the cathode to earth (important if the discharge gap is screened). Thus

$$R = R_s R_o/(R_s + R_o) \; ; \quad C = C_e + C_o + C'_e \; .$$

In addition to the electron and ion currents derived in Appendix 2, there is the displacement current due to charging and discharging of C as the signal voltage varies, given by

$$I_d(t) = C. \; \frac{dV_C}{dt} \; .$$

V_C , V_R and V_a are the voltages across C,R and the terminals of the power supply. Then

$$V_R(t) = R\left[I(t) + C.\ \frac{dV_C}{dt}\right]$$

$$= R\left[I(t) - C.\ \frac{dV_R}{dt}\right]$$

$$= R\left[I(t) + C.\ \frac{d}{dt}(V_a - V_R)\right].$$

If the applied voltage is a step function, then at time $t = 0$, $I(t) = 0$ to give

$$V_R(t) + RC.\ \frac{dV_R(t)}{dt} = 0 \ ,$$

which is frequently used to provide a timing mark, the shape depending on the value of RC.

It is usually desirable to choose R such that the time constant RC is short compared with the I(t) time constant, so that the actual variation of I(t) with t is shown on the oscilloscope. Under these conditions the displacement current is negligible as long as I(t), and hence $V_R(t)$, does not become too great, and also the voltage source is able to maintain V_a. Then $V_R(t)$ is given simply by

$$V_R(t) = R.I(t)$$

where $RC \ll 1/\alpha v_-$ for non-attaching gases,

$RC \ll 1/(\alpha-\eta')v_-$ for electronegative gases.

The less useful cases where $RC = 1/\alpha v_-$ and $RC >> 1/\alpha v_-$ can be similarly treated, the latter condition giving an integrated signal.

Apart from time-constant considerations, the value of R is also governed by the sensitivity of the oscilloscope pre-amplifier, as sufficient voltage must be developed across R to drive the oscilloscope, and, in cases where very fast transients are to be studied, impedance matching of cables imposes a further limitation on the choice of values.

1.6. Diffusion and Space Charge.

The diffusion through a neutral gas of charged particles at low concentrations can be treated as the thermal diffusion of two non-interacting neutral gases, in which case Fick's Law will apply -

$$\underline{v}\, N = -D.\underline{\nabla}N \qquad (1.6)$$

where $\underline{\nabla}N$ is the concentration gradient, D is the diffusion coefficient, and $\underline{v}N$ is the electron flux per unit area in the direction of $\underline{\nabla}N$. If charges are allowed to diffuse from a point in the absence of an electric field, the spatial distribution at any time will be Gaussian, with the total number of charges and therefore the area under the distribution

constant at all times. According to Loeb (1955)[1.19], the radius r of a diffusing sphere of charge at time t is given by

$$\bar{r} = (12Dt/\pi)^{\frac{1}{2}} \qquad (1.7)$$

where $$D = \lambda\bar{c}/3 \qquad (1.8)$$

(λ is the electron mean free path, $\bar{c}$ the mean velocity). It is shown in section 5.4.2 that for 35 eV electrons in hydrogen at 1 torr, λ = 0.36 cm. If it can be assumed that the electrons have thermal energies ($\sim$ 0.04 eV) for diffusion purposes (i.e. that the elevated velocities have components in the field direction only), then $\bar{c} = 1.2\text{x}10^{7}$ cm.sec^{-1} at 300°K. Thus D is calculated to be $1.4\text{x}10^{6}$ cm^{2}.sec^{-1}, and substituting in equation (1.7) it is found that, for the shortest and longest electron transit times measured in this investigation,

$\bar{r}$ = 0.95 cm for t = 50 nsec (c.f. Δl = 3.0 cm)

$\bar{r}$ = 2.30 cm for t = 300 nsec (c.f. Δl = 0.5 cm)

where $\Delta l = v\Delta t$, Δt is the halfwidth of the pulse of initiating electrons. It is calculated that for E/p > 75 volts.cm^{-1}.torr^{-1} the diffusion radius is less than the spatial halfwidth of the initiating pulse; for E/p < 75, diffusion should become increasingly important with decreasing E/p, though no clear evidence of diffusion has been observed in the data.

Measurements of the ratio μ/D, where μ is the electron mobility, are often made in the Townsend magnetic deflection type of experiment (section 3.2). This ratio can be shown to be a function of the electron temperature only by substituting for μ from equation (2.2) and for D from equation (1.8), to give

$$\frac{\mu}{D} = \frac{(e\lambda/m\bar{c})}{(\bar{c}\lambda/3)} = \frac{e}{kT} ,$$

since $\frac{1}{2}mc^2 = 3kT/2$.

Mutual electrostatic repulsion of the electrons causes a similar effect to diffusion expansion of the swarm. If there is a sphere of radius r containing n electrons then, by Gauss' theorem, the field at the surface is

$$E_r = ne/4\pi r^2 .$$

Now $$\frac{dr}{dt} = \mu E_r = \frac{ne\mu}{4\pi r^2}$$

to give $$r^3 - r_o^3 = \frac{3ne\mu}{4\pi} t \qquad (1.9)$$

since $r = r_o$ at $t = 0$.

The effects of electrostatic repulsion will be important if, at the time t_- that the avalanche reaches the anode, the radius r in equation (1.9) is greater than the thermal diffusion radius $\bar{r}$ in equation (1.7), that is if

$$\frac{3ne\mu t_-}{4\pi} \geq \left(\frac{12Dt_-}{\pi}\right)^{\frac{1}{2}}$$

i.e. $$n \geq \frac{8}{3e\mu}\left(\frac{\pi\lambda\bar{c}}{t_-}\right)^{\frac{1}{2}} \qquad (1.10)$$

Typical values for these parameters in hydrogen are $\mu \simeq 1.5\text{x}10^{8}$ $cm^{2}.sec^{-1}(esu\ of\ potential)^{-1}$, $\lambda = 0.36$ cm, $\bar{c} = 1.2\text{x}10^{7} cm.sec^{-1}$, $t \sim 1.0\text{x}10^{-7}$ sec, and substitution in equation (1.10) gives

$$n \geq 4\text{x}10^{8} \text{ electrons}$$

as the value for expansion of the avalanche by electrostatic repulsion. Experimental confirmation of this value is afforded by cloud chamber photographs by Raether (1939)[1.20], which show marked expansion of the avalanche at $n \simeq 10^{8}$.

Ambipolar diffusion will occur in any situation where there is separation of positive and negative charges, provided the Debye length is much less than the dimensions of the experimental vessel. In the absence of an applied field, electrons tend to diffuse more rapidly down the concentration gradient than ions because of their higher mobility; however, as soon as there is charge separation, coulombic attraction couples the ions and the electrons so that they diffuse at the same rate. From Fick's Law, equation (1.6), for electrons and

ions respectively

$$\begin{aligned} \underline{v}_e N_e &= -D_e \underline{\nabla} N_e - N_e \mu_e \underline{E}' \\ \underline{v}_i N_i &= -D_i \underline{\nabla} N_i + N_i \mu_i \underline{E}' \end{aligned} \qquad (1.11)$$

where $\underline{E}'$ is the ambipolar field. Since, if there is overall charge neutrality, $N_e = N_i = N$, $v_e = v_i$

$$\underline{E}' = \left(\frac{D_i - D_e}{\mu_i + \mu_e} \right) \frac{\underline{\nabla} N}{N} \quad ; \quad \underline{v} N = \left(\frac{\mu_e D_i + \mu_i D_e}{\mu_i + \mu_e} \right) \underline{\nabla} n = -D_a . \underline{\nabla} N,$$

where D_a is the ambipolar diffusion coefficient.

In the case of a Townsend discharge, there is an applied field E, and usually $E > E'$. Equations (1.11) become

$$\begin{aligned} \underline{v}_- N &= \pm \left(-D_e \underline{\nabla} N - N \mu_e \underline{E}' \right) - N \mu_e \underline{E} \\ \underline{v}_+ N &= \pm \left(-D_i \underline{\nabla} N + N \mu_i \underline{E}' \right) + N \mu_i \underline{E} \end{aligned}$$

where N and E' are not stationary with time. An assessment from these equations of the effects of space charge on the electron drift velocities in the present investigation is not attempted, but instead evidence for the extent of the effect will be adduced from the work of several authors.

Hasted (1964)[1.21] quotes a value of 10^8 ions per cm^3 as the point at which space charge distortion becomes important. Experimental and theoretical investigations of the streamer

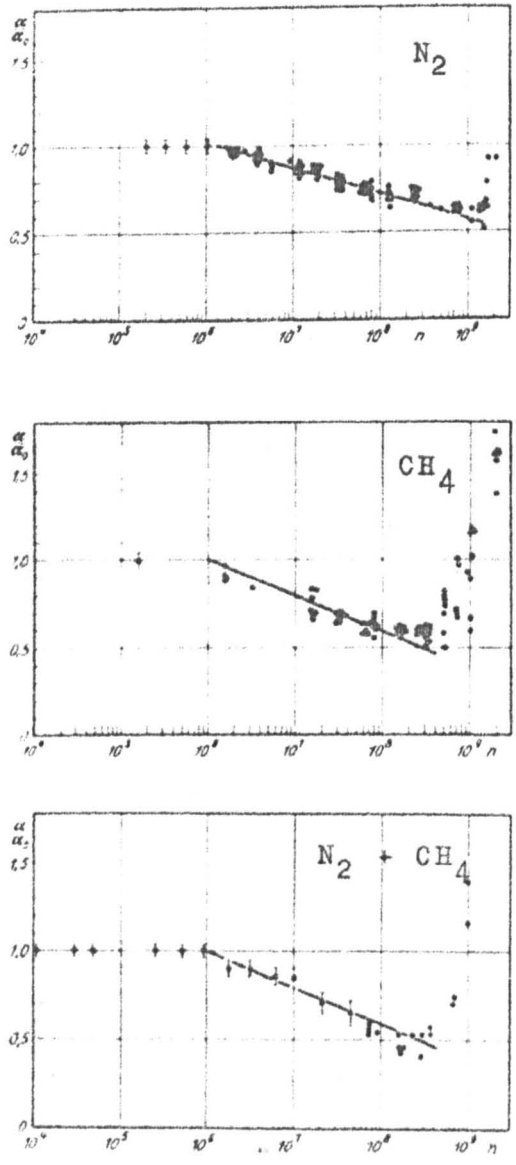

Fig. 1.4

The effect of space charge on the value of α.

mechanism, a space charge controlled process, lead to positive ion concentrations $\sim 10^8$ within a sphere of radius $\sim 10^{-3}$ cm as the criterion for streamer propagation (e.g. Dawson (1965)[1.22], Dawson and Winn (1965)[1.23]), under which conditions the Townsend mechanism is grossly disturbed.

Tholl (1963)[1.24] has measured the variation with n of α/α_o, the ratio of the values of the first Townsend coefficient at n and at very small n, in N_2, $N_2 + CH_4$ and CH_4 (fig. 1.4), and it is seen that in all cases there is a sudden decrease in α/α_o' at $n = 10^6$, followed by a rapid increase at $n \simeq 5 \times 10^8$ as the streamer mechanism becomes operative. Thus, if the effects of space charge are to be avoided, n must be kept less than 10^6, and it is shown in section 4.1 that a design criterion for this experiment was $n \simeq 10^4$.

1.7. The Effects of Impurities.

Many of the discrepancies for values of α determined by various authors have since been attributed to the presence of impurities in the gas under investigation. Mercury contamination, which can arise from inadequate trapping between the experimental volume and the diffusion pump or a McLeod gauge, readily leads to false values of α, since the vapour pressure of mercury at room temperature ($\sim 10^{-3}$ torr at 20°C) can result in typical impurity

levels of 10^2 to 10^3 p.p.m., and the ionisation potential of mercury is only 10.4 eV, which is less than the ionisation potentials of any of the monatomic or diatomic gases commonly investigated. Thus large numbers of mercury atoms are readily ionised, both by electron impact, and by inelastic collisions of the second kind, such as

$$Hg + Ne_m^* \ (16.6 \text{ eV}) \rightarrow Hg^+ + Ne + e,$$

to give higher α values than in the pure gas. The presence of mercury contamination is also liable to lead to erroneous results in positive ion mobility measurements because of the readiness of the mercury atom to lose an electron in charge exchange reactions of the type

$$H_2^+ + Hg \rightarrow H_2 + Hg^+.$$

The Penning effect [1.25], of which the Hg/Ne_m^* reaction above is an example, was first observed to yield erroneously high α values in 1936, in a Neon/Argon mixture, where one reaction is

$$Ar + Ne_m^* \rightarrow Ar^+ + Ne + e,$$

and will occur in any gas mixture in which the ionisation potential of one constituent is less than a metastable level of another constituent. A metastable atom in a gas at a pressure of

1 torr makes 10^5 to 10^8 collisions during its lifetime, and will therefore have a very high probability of making an ionising collision with a low ionisation potential constituent present in small concentrations. An analogous process occurs when there is photoionisation of one constituent by radiation emitted from another. The presence of readily ionisable minority constituents is not always deleterious, and is used in some gas-filled valves to obtain α coefficients higher than those of either of the constituents (e.g. He/H_2 mixtures - Chanin and Rork (1964)[1.26]), and in the "seeding" of flames with alkali salts to enhance the conductivity.

In the measurement of electron drift velocities, the effects of impurities would be important in the exponential current growth method (section 3.4) because of the need to substitute a value for α in the expression for the time constant $1/\alpha v_-$. In the time of flight methods it is probably sufficient to consider only the relative numbers of electron collisions with impurity and principal constituents, and to postulate that the drift velocities are unaffected if this ratio is sufficiently small. In the present investigation, where the number of electron-neutral collisions between the cathode and the anode is only about 35 and the impurity level is $\sim$0.1 p.p.m., there is a negligible probability of a collision with an impurity atom, though the effect of such a collision on

the transit time of an individual electron might be appreciable because of the small number of free paths between the electrodes. Spurious drift velocities could be observed in situations where the Penning type photoionisation process described above can occur (section 5.4.1).

CHAPTER 2

SOME THEORETICAL ASPECTS OF DRIFT VELOCITIES AND VELOCITY DISTRIBUTION FUNCTIONS OF ELECTRONS IN GASES

2.1 Introduction

The problem of ion drift velocities, where the term ion embraces all types of charged particle, can in general be approached in two ways. Either it may be assumed that all parameters with distributed values, such as ion drift velocities, molecular and ion thermal velocities, ion free paths and scattering angles, can be ascribed a mean value at the commencement of the analysis, or that a distribution function may be assumed or calculated at least for some of the parameters, to permit the effects of the distribution to be assessed. Whilst it would appear that the latter will lead to a more meaningful result, the use of this procedure by several authors has shown that the simplifying assumptions, which are necessary to allow the analysis to proceed, result in a physical model with little advantage over that which takes average values as a starting point. In particular, the derivation of a suitable velocity distribution presents considerable difficulties, and those which are most commonly used are the Maxwellian and Druyvesteyn distributions.

In this chapter several simple theories of the average value type and one distribution theory are presented in some detail, and attention is drawn to other recent treatments of the problem. The applicability of the available theories to the present investigation is discussed, and a simple treatment of the problem of attainment of equilibrium by the initial photoelectrons is presented.

The terms 'low E/p' and 'high E/p' are used loosely in the literature, and are quoted frequently in this work. There are three distinct regions into which the E/p spectrum can be subdivided. The first, low E/p, is the regime in which only momentum transfer collisions occur; the second, which might be termed 'moderate E/p', embraces all classes of collision process; the third, high E/p, is the largely unexplored region in which the avalanche fails to come to equilibrium with the applied electric field and the gas. The low E/p region alone is amenable to theoretical treatments, and satisfactory analysis of moderate and high E/p models is difficult because of the large number of possible collision processes. The term 'high E/p' is often applied, in the presentation of experimental data, to what is here called 'moderate E/p'. The transition from low to moderate E/p will depend on the nature of the gas, and particularly on whether it is monatomic or polyatomic, since it is determined by the position of the lowest excited state. In hydrogen, the threshold for vibrational excitation is at 1 eV, with a peak cross-section of $6 \times 10^{-17} cm^2$ at 2.3eV (Schulz (1964)[2.1]), the threshold corresponding to $E/p \sim 2$ volts.cm^{-1}.$torr^{-1}$. Excitation of rotational levels requires about 10^{-2} of the energy for vibrational excitation (Herzberg (1950)[2.2]), corresponding to $E/p \sim 2 \times 10^{-2}$.

2.2. Ion Drift Velocities using Mean Values.

2.2.1. The general case.

The mean value methods have been reviewed by von Engel (1965) [2.3], and his treatment is followed here.

The most simple approach, first used by Langevin (1903)[2.4] assumes that -

1. neutral molecules and ions have the same energy, so that thermal equilibrium exists.

2. velocities are completely randomised on impact, so that ions have zero drift velocity after each collision.

3. impacts can be described as perfectly elastic encounters.

If λ is the ion mean free path and c is the mean ion speed, then

$$v = \tfrac{1}{2} \frac{eE\lambda}{mc} = \tfrac{1}{2} \frac{e\lambda}{mc} E = \mu E \qquad (2.1)$$

since $\frac{1}{2}m\overline{c^2} = \frac{1}{2}M\overline{C^2}$ for thermal equilibrium. v is the ion drift velocity and μ is the mobility, where

$$\mu = \tfrac{1}{2} e\lambda/m\bar{c} \qquad (2.2)$$

Langevin's approach can be extended by assuming that there is a mean fractional energy loss f on collision. In the steady state,

the rate at which energy is gained from the electric field is equal to the rate at which it is lost by collision, so that

$$eEv = f.\tfrac{1}{2}mc^{\overline{2}}.\bar{c}/\lambda$$

hence $$\bar{c}^3 \simeq 2eE\lambda v/fm \ .$$

Now $$\bar{c}^3 = (\tfrac{1}{2}eE\lambda/mv)^3 \quad \text{from equation (2.1),}$$

to give $$v = \tfrac{1}{2} f^{1/4}(Ee\lambda/m)^{\frac{1}{2}} \ .$$

Thus $$v \propto (E/p)^{\frac{1}{2}} \qquad (2.3)$$

since $\lambda \propto 1/p$.

A more sophisticated approach was adopted by Langevin (1905)[2.5] and Thomson (1924)[2.6] in their induced dipole theories, where the electrostatic interaction between the ion and the induced dipole moment μ' of the molecule is considered.

$$\mu' = (\epsilon/N)E_i = (D - 1)e/4\pi Nr^2 \text{ (c.g.s. units)}$$

where, in the usual notation, $D = 1 + 4\pi\epsilon$, N is the molecular number density, and $E_i = e/r^2$ is the ion field at a distance r. The field due to a dipole is

$$E_{\mu'} = 2\mu'/r^3 = (D - 1)e/2\pi Nr^5 \qquad (2.4)$$

Now, from equation (2.2)

$\mu = \frac{1}{2}e\tau/m$ where τ is the time between collisions. If it is assumed that λ is equal to the distance between molecules, then $\lambda \simeq N^{-1/3}$ and

$$\tau = \int_0^{\lambda} dr/v = \int_0^{\lambda} dr/\mu E_{\mu}, \quad .$$

Substituting for E_{μ}, from equation (2.4), and integrating

$$\tau = \frac{\pi N \lambda^6}{\mu e(D-1)} \simeq \frac{1}{N\mu e(D-1)}$$

Hence $$\mu = \frac{e}{m}\tau \simeq \left(\frac{1}{Nm(D-1)}\right)^{\frac{1}{2}} \qquad (2.5)$$

For molecular and atomic ions, since $Nm \propto p$,

$$v = \mu E \propto E/(p)^{\frac{1}{2}} . \qquad (2.6)$$

2.2.2. The case for electrons.

It is again assumed that there are elastic collisions with a fractional energy loss f, and additionally that the applied electric field is very weak to maintain condition (1) that there is thermal equilibrium ($v_- << \bar{c}$). As before (equation 2.1), $v_- = \frac{1}{2}\, eE\lambda/m\bar{c}$. The net rate at which an electron gains energy is given by

$$\frac{d}{dt}\left(\tfrac{1}{2}m\bar{c}^2\right) = eE.\tfrac{1}{2}\frac{e\bar{E}\lambda}{m\bar{c}} - f.\tfrac{1}{2}m\bar{c}^2.\frac{\bar{c}}{\lambda} \qquad (2.7)$$

At equilibrium $\frac{d}{dt}\left(\tfrac{1}{2}m\bar{c}^2\right) = 0$ and $t = \infty$

so that $c_\infty = (1/f)^{1/4}(eE\lambda/m)^{\frac{1}{2}}$

Thus $v_{-\infty} = \tfrac{1}{2}\frac{eE\lambda}{mc_\infty} = \tfrac{1}{2}f^{1/4}\left(\frac{eE\lambda}{m}\right)^{\frac{1}{2}}$

so that, at equilibrium

$$v_- \propto (E/p)^{\frac{1}{2}} \qquad (2.8)$$

The limitations of the mean values approach, and its relevance to the present investigation are discussed in Section 2.4.

2.3. Velocity Distribution Functions.

2.3.1. Early Approaches to the Problem.

Any theoretical approach to this problem must take into account the energy gained by the ions from the applied field, the fractional energy loss f on collision, and the interaction between the ions at high ion concentrations. f depends on the relative probabilities for elastic and inelastic encounters, and these probabilities are functions of the ion energy; if one type of collision only is important, f can be assigned a definite value (for instance, $f = 2m/M$ for elastic impacts, averaged over all scattering angles), but the ion mean free path λ will still be a function of the ion energy. Collision cross-section data is available for most monatomic and diatomic gases including hydrogen (e.g. Frost and Phelps

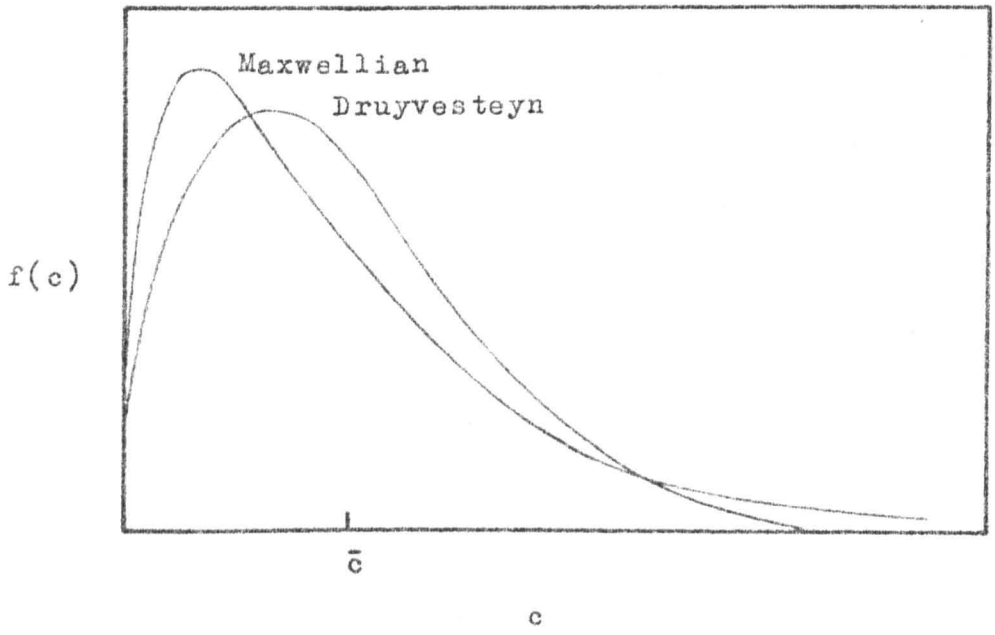

Fig. 2.1

The form of the Maxwellian and Druyvesteyn velocity distribution functions.

(1962)[2.7] for rotational and momentum transfer cross-sections in hydrogen and nitrogen; Englander-Golden and Rapp (1964)[2.8] for total ionisation cross-sections in hydrogen and other gases), and there is a number of theoretical treatments (e.g. Morse (1953)[2.9], Gerjuoy and Stein (1955)[2.10], and Frost and Phelps (1961)[2.11]).

Pidduck (1913)[2.12] was the first to attempt to tackle the distribution function problem and obtained a Maxwellian distribution, on the assumption of perfectly elastic collisions and f = 0. Compton (1918)[2.13] used a finite value for f, and also arrived at a Maxwellian distribution. Hertz (1925)[2.14] failed to achieve a useful result when considering elastic impacts in a uniform field between parallel plates, but Druyvesteyn (1930)[2.15] followed a similar approach to derive the well-known distribution that bears his name, based on the following assumptions -

1. elastic collisions,
2. energy independent mean free paths,
3. f = 2m/M, the momentum transfer value,
4. the ions had reached their terminal velocity,
5. no interaction between ions,
6. molecules at rest.

This distribution has the form

$$f_D(c).c^2dc = A \exp(-Bc^4).c^2dc \qquad (2.9)$$

compared with the Maxwellian distribution

$$f_M(c).c^2dc = A \exp(-Bc^2).c^2dc \qquad (2.10)$$

and fig. 2.1 shows the shape of these distributions for the same mean electron velocity $\bar{c}$. It is seen that the Druyvesteyn distribution has a higher peak energy, but that its high energy tail decreases more rapidly. This comparative depletion of high energy electrons is of significance in that there is a reduction in the probability of occurrence of processes requiring more energetic electrons.

Subsequently the literature begins to proliferate, and only a few of the many contributions are briefly mentioned. Morse, Allis and Lamar (1935)[2.16] confirmed the Druyvesteyn distribution employing a different approach, and this work was later extended by Allis and Allen (1937)[2.17] to include the effects of inelastic collisions, yielding results in agreement with the reliable experimental data of Bradbury and Nielsen (section 3.3). Davydov (1935)[2.18] confirmed the Druyvesteyn distribution, and Smit (1937)[2.19] took into account inelastic collisions and the variation of mean free path. Amongst other theories are those of Healey and Reed (1941)[2.20], Yarnold (1947)[2.21], Holstein (1951)[2.22], Barbiere (1951)[2.23] and Huxley (1960)[2.24,2.25]. The approach most generally and productively employed uses the Boltzmann transport theory, first applied in (2.16); Huxley, and Huxley and Crompton (1962)[2.26] have presented a fairly

complete treatment which is closely followed in Appendix 3, and the salient points of which are outlined in section 2.3.2. It will be seen that the result obtained differs from the Maxwellian and Druyvesteyn distributions, but that its form is inconvenient to apply although many simplifying assumptions are retained. The extreme difficulty of setting up the equations for electron transport using a realistic model, even at low E/p, is thus emphasised.

2.3.2. Huxley's Derivation of the Electron Velocity Distribution Function.

An entirely general electron velocity distribution function f(c) is defined for field free conditions, upon which is superimposed a drift velocity v = v(c) in the x direction, to give a new distribution function $F(c,\dot{x})$. Thermal equilibrium is assumed, in which is implicit a restriction to very low E/p, and the general distribution function in the presence of very low electric fields follows (equation (A3.2)) -

$$F(c,\dot{x}) \simeq f(c) - \frac{v\dot{x}}{c} \cdot \frac{df(c)}{dc} \qquad (2.11).$$

This cannot be evaluated until the zero field distribution f(c) and the electron drift velocity v(c) have been determined.

A mean drift velocity $\bar{v}$ is calculated in terms of v(c), c and f(c), using the relationship of equation (2.11), and the expression derived by Langevin for the drift velocity (equation (2.1))

is substituted for the function v(c), introducing the further assumptions that the velocities are completely randomised on impacts which are always perfectly elastic. It is also assumed that the Ramsauer effect does not exist, so that the electron mean free path λ is constant, to give the mean electron drift velocity (equation (A3.3)) for electrons as

$$\bar{v}_- = - \frac{4\pi e E \lambda'}{3m} \int_0^\infty c^2 . \frac{df}{dc} . dc \qquad (2.12)$$

where λ' is the effective mean free path.

f(c) is evaluated by equating the rate of energy gain from the field to the rate of loss by collision. It is assumed again that collisions are elastic, and also that the neutral molecules are stationary, that the collision rate is determined by f(c) rather than $F(c,\dot{x})$, and that the electrons are isotropically scattered, to give equation (A3.6). This equation is then adjusted so that for non-stationary molecules and zero drift velocity, f(c) becomes Maxwellian, which leads to the final expression for f(c) in equation (A3.7) -

$$f(c) = \text{constant} \times \exp\left[- \int^c \frac{mc.dc}{2M(eE\lambda')^2/3(mc)^2 + kT} \right] \qquad (2.13).$$

If inelastic collisions are to be considered , the fractional energy loss term f in the energy loss rate expression must be modified. In these circumstances $f = f(\frac{1}{2}mc^2)$, where this function is unlikely to be simple and will exhibit resonances for $\frac{1}{2}mc^2 \approx h\nu$, where ν has values corresponding to the excitation and ionisation potentials. It is feasible to use an estimated mean value for f, when a similar analysis yields, for the case of electrons

$$f(c) = \text{constant} \times \exp\left[- \int^{c} \frac{mc.dc}{(eE\lambda')^2/3fmc+kT} \right]$$

It is evident that the use of distributed parameters produces unwieldy expressions, even though a number of severe simplifying assumptions has been adopted and several procedures of apparently dubious validity have been executed. Simplification of the expression for the zero field distribution for electrons (equation (2.13)) gives

$$f(c) \propto \exp(Ac^2 - B \ln c^2) \text{ for constant } T,$$

and substitution in (2.11) yields the general distribution function

$$F(c,\dot{x}) \propto (1-D+E/c).\exp(Ac^2-B \ln c^2),$$

which may be compared with the distributions due to Maxwell

$$f_M(c) \propto \exp(B'c^2)$$

and Druyvesteyn $$f_D(c) \propto \exp(B'c^4) .$$

2.4. The Validity of Existing Theories at Low E/p, and Their Extension to Moderate and High E/p.

The application of the Boltzmann transport method has been reviewed by Allis (1956)[2.27], since when the work of Huxley[2.24,2.25] and a number of other authors has been published. Arthurs and Dalgarno (1960)[2.28] calculated the mobility of diatomic ions at $0^{\circ}K$ in terms of the dipole moment and the polarizability, and Heylen (1960)[2.29] considered rotational and vibrational excitation to obtain an electron energy distribution that was approximately Maxwellian, and showed that the substitution of a Maxwellian distribution and experimental cross-sections in Allis' expression for v_- gave good agreement with the data of Bradbury and Nielsen (section 3.3). Demetriades and Hill (1965)[2.30] analysed the motion of pulses of charged particles under space charge limited conditions, neglecting diffusion effects, and Ward (1965)[2.31] solved the continuity equations, allowing for diffusion, ionisation and space charge, to show that $v_- \propto \mu E + \alpha D_-$ at low E/p. Lawson and Lucas (1965)[2.32,2.33] have calculated the ratio D/μ using a model that takes into account positive ion and direct photon secondary effects at the cathode, and have supported the calculations by experimental measurements in $(H_2 + 0.01\%N_2)$ for the moderate E/p range 15 to 350 volts.cm^{-1}.$torr^{-1}$.

The conditions existing in the electron avalanches of the present investigation may be summarised as follows -

1. thermal equilibrium does not exist $v_- \geq c$.

2. $\lambda = \lambda(v_-, c)$

3. non-stationary molecules, except at very high E/p, where $v_- >> c$ and it is reasonable to assume stationary molecules

4. inelastic collisions of many types

5. probably non-isotropic scatter of electrons

6. diffusion can be ignored for E/p > 75 volts.cm^{-1}.$torr^{-1}$ (section 1.6)

7. negligible electrostatic interaction between the particles (section 1.6).

8. non-Maxwellian velocity distribution.

Of all these conditions, probably the greatest obstacle to a satisfactory theoretical treatment is the need to include different types of inelastic collision. An appropriate analysis of the problem has not been found, and Huxley's work represents an attempt to solve the problem, subject to the assumptions -

1. thermal equilibrium exists $v_- << c$.

2. λ is independent of c.

3. stationary molecules for part of the treatment

4. momentum transfer collisions only

5. isotropic scatter

6. diffusion can be ignored

7. non-interacting particles.

From equations (A3.3) and (A3.7)

$$v_- \propto A \int_0^\infty c^2 . \frac{d}{dc} \left[\exp \int^c \frac{c.dc}{A^2/c^2+B} \right] .dc$$

(where $A = \lambda E$, $B = kT$), which becomes

$$v_- \propto A \int_0^\infty (A^2+Bc^2)^{2B^2/A^2} \left[\frac{c}{B} + \frac{4B^3}{A^2} (A^2+Bc^2)^{-1} \right] . \exp \frac{c^2}{2B} .dc \qquad (2.14)$$

From which it is clear that v_- depends on E/p in a complex manner (since $E/p \propto E\lambda = A$). The agreement of this theory with experimental data at low E/p has not been investigated.

The mean values approach in section 2.2 makes the same assumptions as Huxley's model, except for the Langevin-Thomson treatment, which considers the polarisation attraction between ions and molecules but still retains non-interacting ions, and yields a relationship

$$v_- \propto E/(p)^{\frac{1}{2}} \qquad \text{from equation (2.6).}$$

This relationship does not give the observed functional dependence of v_- on E/p, but yields numerical values of the correct magnitude for positive ions at low E/p.

Otherwise, the mean values method produces the relationship, from equation (2.8),

$$v_- \propto (E/p)^{\frac{1}{2}} \quad ,$$

which gives numerical values that are a factor of about five too large for ions, but are correct for electrons at low E/p. The functional dependence is also valid for electrons at low E/p and for ions at E/p ≈ 5 to 15 volts.cm^{-1}.torr^{-1}, but not for E/p < 5.

Langevin's original method can be extended naïvely to high values of moderate E/p, where $v_- \gtrsim \bar{c}$. Then, equating the rate of energy loss to the rate of energy gain

$$eEv_- = f.\ \tfrac{1}{2}m(\overline{c^2} + v_-^2).(\overline{c^2} + v_-^2)^{\frac{1}{2}}/\lambda \quad ,$$

where f is the mean fractional energy loss factor. If $v_- >> \bar{c}$, this becomes

$$v_- = (2e/fm)^{\frac{1}{2}}(E\lambda)^{\frac{1}{2}} \propto (E/p)^{\frac{1}{2}} \qquad (2.15)$$

2.5. The Attainment of Equilibrium by Initiating Electrons.

It has long been recognised that an end-effect exists in the Townsend discharge, because the initiating electrons leave the cathode with a velocity distribution which differs from that of electrons in equilibrium with the applied field and the gas, and a correction term

t_o is often included in the current growth expression $i = i_o.\exp \alpha\, v_-(t - t_o)$ - see section 1.2. This problem has been treated by von Engel[2.3], subject to the same conditions that were applied in section 2.2, in the following manner.

The net rate at which an electron acquires energy is

$$\frac{d}{dt}\left(\tfrac{1}{2}m\bar{c}^2\right) = eEv_- - f.\tfrac{1}{2}m\bar{c}^2.\frac{\bar{c}}{\lambda} \qquad (2.16)$$

Substitution for $\bar{c}$ from equation (2.1), and integration gives

$$t/t_o = \tfrac{1}{2}.\ln\left[\,(1 + c/c_\infty)(1 - c/c_\infty)\,\right] - \tan^{-1}c/c_\infty,$$

where $$t_o = (1/16)(e/m)^{-\frac{1}{2}}(f)^{-3/4}(E/\lambda)^{-\frac{1}{2}} \alpha\, (f)^{-3/4}(Ep)^{-\frac{1}{2}} \qquad (2.17)$$

is a time constant, corresponding to the time taken for an electron to acquire 94% of its final value v_-. c_∞ is the value of c when the left hand side of equation (2.16) is equal to zero. If the value of c_∞ is put into equation (2.1), the expression obtained for v_- is

$$v_- = (1/16)(e/m)^{\frac{1}{2}}(f)^{1/4}(E\lambda)^{\frac{1}{2}} \alpha\, (E/p)^{\frac{1}{2}} \qquad (2.18)$$

Values for v_- calculated from equation (2.18) show poor agreement with the experimental values from (3.48) -

E/p volts.cm^{-1}.torr^{-1}	30	50	100	200	400
v_-(calc.)cm.sec^{-1}x10^{-7}	41	53	75	106	150
v_-(3.48)cm.sec^{-1}x10^{-7}	0.5	2.2	4.8	8.1	12.5

This approach can be extended to the case for $v_- >> \bar{c}$, at high values of moderate E/p, when equation (2.16) becomes

$$\frac{d}{dt}\left(\tfrac{1}{2}mv_-^2\right) = eEv_- - f.\frac{1}{\lambda}.\tfrac{1}{2}mv_-^3$$

Integration gives, using $v_- = 0$ when $t = 0$,

$$t = (\lambda/fa).\ln\left[(a + v)/(a - v)\right]$$

or $$(a + v)/(a - v) = \exp(t/t_o)$$

where $$a = (2\lambda eE/fm)^{\frac{1}{2}},\ t_o = \lambda/fa.$$

Thus $$t_o = (\lambda m/2feE)^{\frac{1}{2}} \qquad (2.19)$$

The significance of t_o under the conditions of this investigation is discussed in section 5.4.2.

CHAPTER 3

PREVIOUS DETERMINATIONS OF ELECTRON DRIFT VELOCITIES, WITH PARTICULAR REFERENCE TO HYDROGEN.

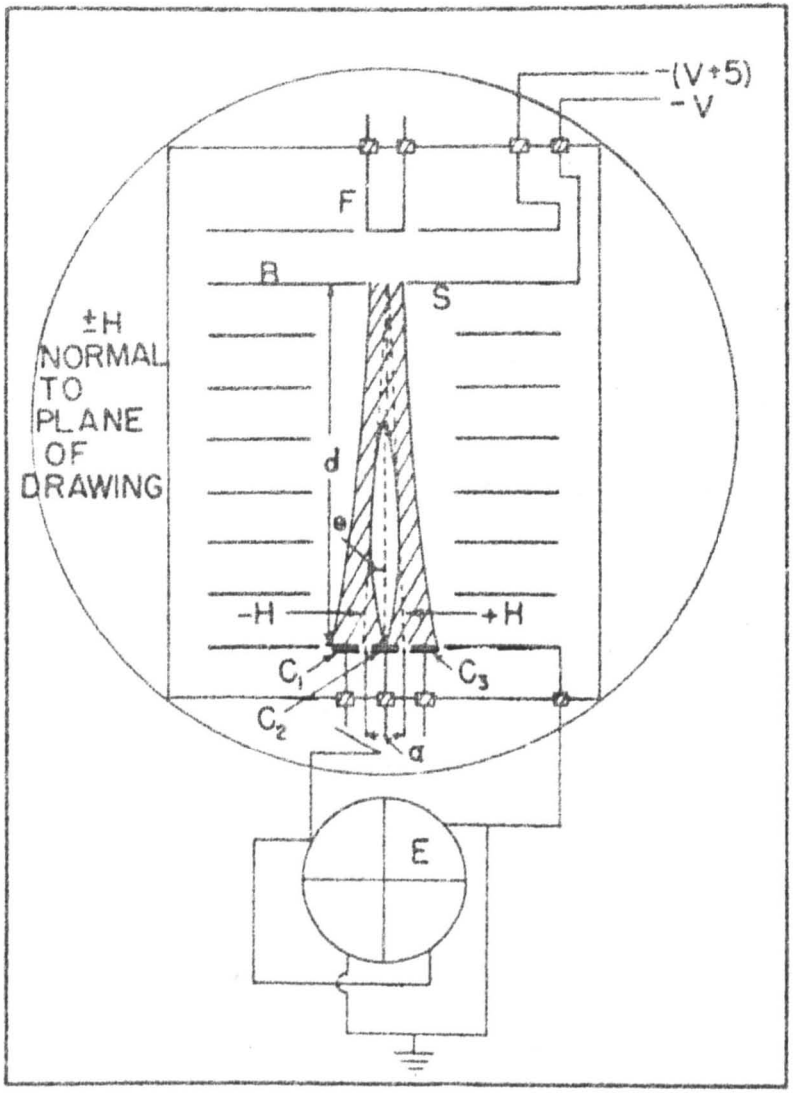

Fig. 3.1

Townsend and Tizard's magnetic deflection method.

3.1 Introduction.

The methods available for the measurement of electron drift velocities can be classified into four main groups -

1. Magnetic deflection
2. Shutter methods
3. Exponential growth of electron current
4. Pulsed time of flight.

These categories are not exclusive and there is a certain amount of overlap; for instance, the shutter methods are essentially a time of flight determination. In general, the shutter and magnetic deflection methods are confined to equilibrium d.c. experimental conditions, but the exponential growth and time of flight techniques can also be applied to above-breakdown pulsed conditions.

3.2 Magnetic Deflection Method.

Townsend and Tizard (1913)[3.1] obtained values for v_- by measuring the magnetic deflection of electrons drifting in a uniform electric field. Their equipment (fig. 3.1) used a hot filament electron source behind a slit in the cathode. In the absence of a magnetic field, electrons passing through the slit drifted in the electric field to the centre strip C_2 of the anode, which was parallel to the cathode slit, and the current was measured with the electrometer; the smaller currents to the strips C_1 and C_3, due to

lateral diffusion, were neglected.

A magnetic field H_{12} was applied, parallel to the slits, until equal currents to C_1 and C_2 were obtained, and then a magnetic field H_{23} in the reverse direction until the currents to C_2 and C_3 were equal. A mean field $H = \frac{1}{2}(H_{12} + H_{23})$ was said to give a deflection $\theta = a/2d$, where a was the separation of the anode strips and d the separation of the cathode and the anode. Equating $\tan\theta$ to the ratio of the magnetic and electrostatic forces acting on an electron, it follows that $v_- = Ea/2Hd$.

This technique has a poor resolving power because of the finite size of the anode strips, and the difficulty in determining precisely the point at which the currents are equal. Nevertheless, it has been extended and improved and is still in use in a modified form. Hershey (1938)[3.2] extended the technique by the use of a large and powerful magnet to obtain magnetic fields of up to 5000 oersteds, compared with Townsend's fields of a few oersteds. Huxley[3.3] and Bailey[3.4] have both progressively improved the technique over a period of years. Huxley used a circular hole in the cathode, and two concentric discs split on a diameter for the anode, and related the currents collected by the different points of the anode to the applied magnetic field, to obtain values for the ratio v_-/D, where D is the diffusion coefficient (which was ignored in Townsend's original experiment). Huxley's group continue actively to apply and develop this method - e.g. Crompton, Elford and Gascoigne (1965)[3.5]

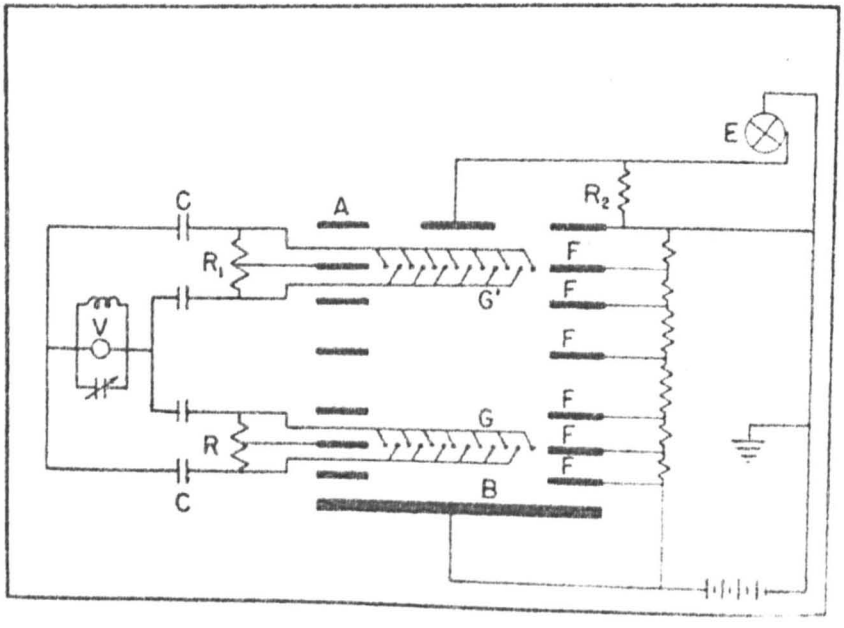

Fig. 3.2

Bradbury and Nielsen's electron shutter apparatus.

and Liley (1967)[3.6] - and obtain results of high precision.

3.3. Shutter Method.

Measurements of v_- were first made using the shutter technique in 1936 by Bradbury and Nielsen[3.7], and this method has served as a model for a number of subsequent investigations by several workers. Bradbury and Nielsen used as shutters the electron filter designed by Loeb (published 1935)[3.8], and later developed by Lusk (1927)[3.9] and Cravath (1929)[3.10], in a method previously used by Van de Graaff (1929)[3.11] to measure ion mobilities. Photoelectrons, released from the zinc cathode by a mercury arc u.v. source, drifted to the anode under the influence of the uniform field (fig. 3.2). A potential, varying sinusoidally about the ambient uniform field potential, was applied between alternate wires of the grids, to both grids simultaneously. As the potential between adjacent wires was increased, an increasing fraction of the electrons passing through the grids was collected, thereby reducing the transmitted current. Thus when the electron transit time between grids was equal to a multiple of a half period of the applied frequency, the instantaneous maximum current transmitted by the first grid at zero potential difference was also allowed to pass with minimum attenuation by the second grid, so that the electrometer, (which was insensitive to the high frequency variations), recorded a maximum for the anode current. In practice it was found most convenient to fix

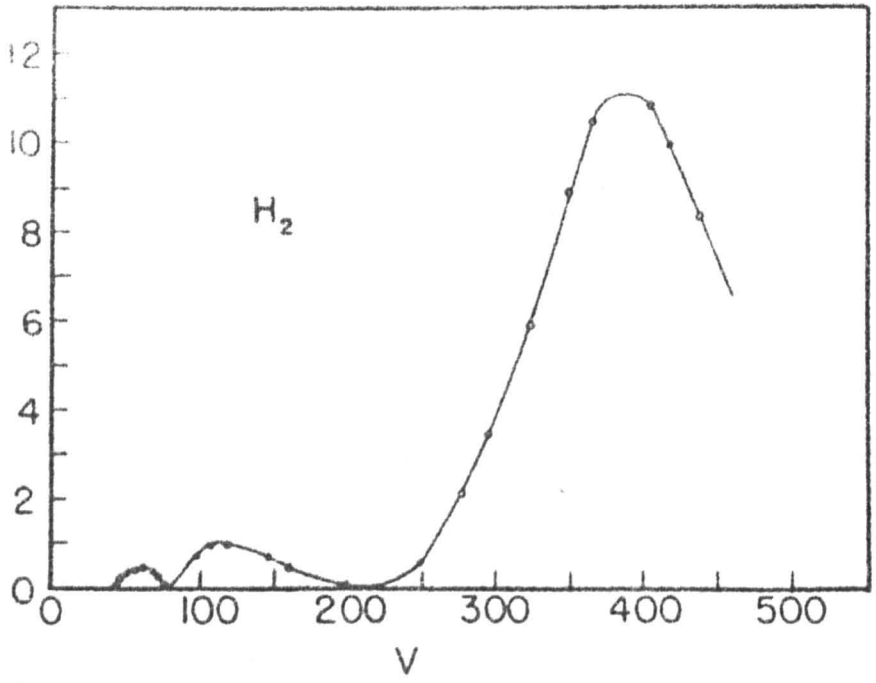

Fig. 3.3

1st, 2nd & 3rd order resonances in Bradbury and Nielsen's experiment.

the amplitude and frequency of the alternating voltage, and to locate the resonances by sweeping the applied field E, keeping the pressure constant. Usually 1st, 2nd and 3rd order resonances could be located, corresponding to $t_- = \frac{1}{2}\tau, \tau$ and $3/2\tau$ (fig. 3.3). It was found that the larger the amplitude of the alternating potential, the sharper were the resonances and therefore the more precisely they could determine t_-.

Their background pressure before admission of hydrogen was stated to be less than 10^{-7} torr, but gas purity was probably not of the standard achieved in later experiments, as cylinder hydrogen was purified by passing over a hot copper gauze and through liquid nitrogen traps. Measurements were made in the E/p range 0.03 to 20 volts.cm^{-1}.$torr^{-1}$, and in the pressure range 1.5 to 50 torr (pd = 9 to 300 torr.cm. approximately), and values for v_- were obtained that were consistent, at a given E/p, for readings at varying pressure and of different order. The graph of v_- plotted against E/p, which is reproduced in fig. 3.4, shows that their values lay between the earlier values of Loeb (1922)[3.12] and Townsend and Bailey (1921)[3.4].

Bradbury and Nielsen also calculated momentum transfer cross-sections using the theoretical treatment due to Compton (1930)[3.13], which assumed elastic collisions between hard spheres. Poor agreement was obtained using the classical energy loss factor $f = \frac{2m}{M}$, but there was fair agreement if it was assumed that rotational and vibrational excitations were important and that the fractional energy

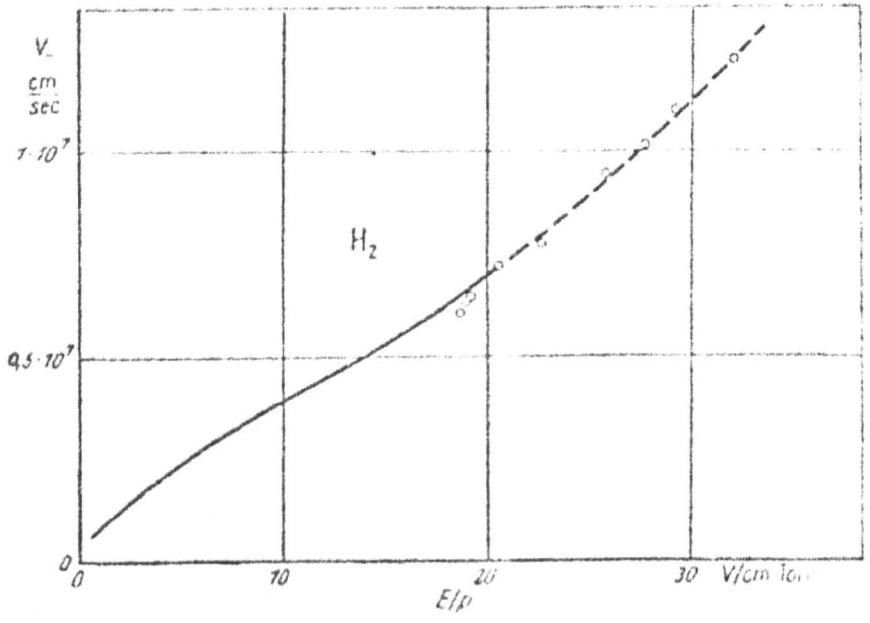

Fig. 3.4

Electron drift velocities in Hydrogen

(— Bradbury & Nielsen, ◦ Frommhold).

loss could be described, rather arbitrarily, by an f factor that varied linearly with E/p and had the value $f = 16 \times \frac{2m}{M}$ at E/p = 20volts.cm^{-1}.torr^{-1}.

Aspects of this experiment are open to criticism. The amplitude of the alternating potential applied between the grid wires, maximum 200 volts, would have destroyed the uniformity of the field applied to the drift space, particularly in the low E/p range where the applied voltage could not have been greater than 10 volts. Gas purity and the use of sinusoidal rather than square wave forms on the shutters reflect the technology of the time. But subsequent measurements have verified the v_- values from this experiment, and the technique has been refined and extended by many later workers over a period of more than thirty years. Its particular advantages are that the velocity of the bunch of electrons is determined after time has been allowed for equilibrium to be attained between the electrons and the gas and the applied field, and that an essentially pulsed measurement produces data in d.c. form, which permits rapid data acquisition, in contrast to the present investigation.

Amongst the later investigations of v_- using the Bradbury-Nielsen technique are those of Pack and Phelps (1961)[3.14] and Prasad and Smeaton (1967)[3.15]. Pack and Phelps measured v_- in helium, neon, argon, hydrogen and nitrogen in the E/p range 10^{-4} to 10 volts. cm^{-1}.torr^{-1} and the temperature range 77°K to 373°K, and also derived momentum transfer cross-sections, but only at very

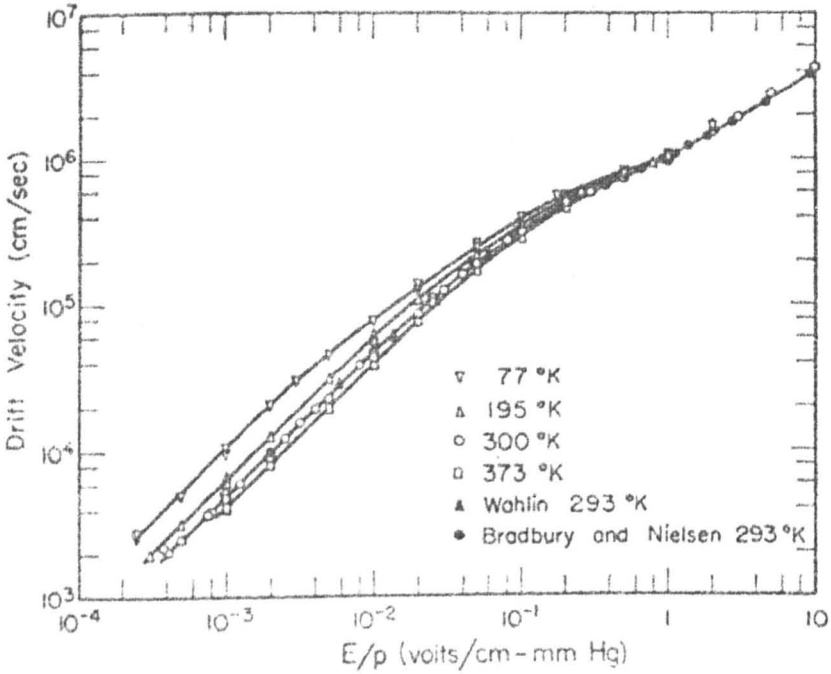

Fig. 3.5

Temperature dependence of v_- (Pack and Phelps).

low electron energies of 0.003 to 0.05eV. The technique differed from that of Bradbury and Nielsen in that photo-electrons were released from the cathode using a pulsed ultra-violet source synchronised with square shutter pulses. This permitted two separate values of v_- to be determined for a given electron swarm by measurement of the transit time to each of the grids from the cathode, so that end effects due to the shutters and initial non-equilibrium of the photo-electrons could be eliminated. Also, the voltage pulses applied to the grids were usually kept below 40% of the applied voltage, when it was found that no end-effects were apparent. Measurements were also made in which the shutters were normally open, with zero voltage applied, and were closed briefly by short voltage pulses so that the applied field was perturbed for the minimum fraction of the total time, which apparantly eliminated end-effects under all conditions. A number of other minor improvements were also made, and the values for v_- for hydrogen are in close agreement with these of Bradbury and Nielsen, and also Wahlin [3.16]. It was shown that $v_- \propto E/p$ for He, H_2, Ar, and N_2 at low E/p ($< 3 \times 10^{-3}$ for H_2), and also that v_- depends on temperature (fig. 3.5), the electrons being in thermal equilibrium with the gas ($T_e = T_g$) and having a Maxwellian velocity distribution. Pack and Phelps calculated momentum transfer cross-sections for this thermal equilibrium region, using the theory due to W.P. Allis [3.17], and for hydrogen obtained the relationship $\sigma^{-1} = (1.28 - 2.17u) \times 10^{15} cm^{-2}$, where u is the electron energy in eV,

valid for the energy range 0.003 - 0.05eV; $\sigma \approx 8 \times 10^{-16}$ cm^2 in this range.

Prasad and Smeaton have most recently applied the Bradbury and Nielson technique to achieve E/p values from 4 up to 40 volts.cm^{-1}.$torr^{-1}$, by employing faster gating pulses than Pack and Phelps (100nsec wide, 10nsec rise and decay times), and applying voltages of up to 10kV across the drift space. They used a thermionic electron source to initiate the avalanches, and made measurements in cylinder grade nitrogen to obtain good agreement with Lowke's [3.18] values; preliminary values were also obtained in hydrogen.

3.4. Measurement of Exponential Growth of Electron Current.

It is shown in Appendix 2 that the current due to the electron component of a pulsed discharge, in the time interval $0 \leq t \leq t_-$, is given by equations A2.1 if $\alpha \neq 0$, that is

$$I_-(t) = \frac{n_0 e v_-}{d} \exp(\alpha v_- t)$$

Determination of the exponential time constant $(1/\alpha v_-)$ permits v_- to be calculated if reliable values for α are available, and it is better if α can be determined concurrently with $(1/\alpha v_-)$ because of its dependence on gas purity. This method has not been widely used,

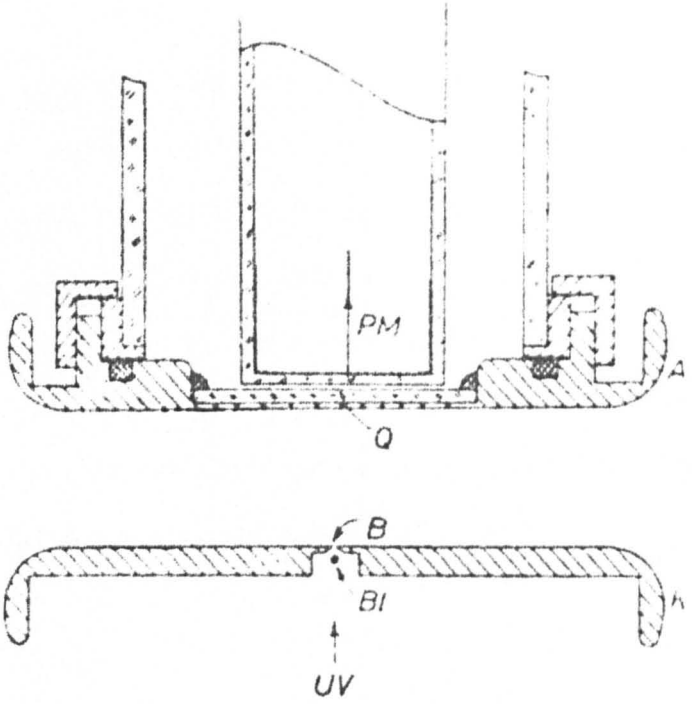

Fig. 3.6

Dibbern's photo-electric determination of $1/\alpha v_-$.

but has been principally employed by the Hamburg group of Raether as a check on v_- values obtained by the pulsed time of flight technique. Its particular shortcoming is that it is necessary to record the current over several orders of magnitude to find the exponential time constant, which means that the final current must be several orders greater than the minimum detectable current, with the consequent possibility of space charge distortion.

The exponential growth rate may also be determined by monitoring the photons from inelastic electron-molecule collisions, if corrections are made for the geometry of the viewing system. The ratio of exciting to ionizing collisions, δ/α, is generally in the region of unity for monatomic and diatomic gases, but depends both on the gas and E/p (e.g. for H_2, $\delta/\alpha = 1.6$ and 10 at E/p = 30 and 15 volts.cm^{-1}.$torr^{-1}$ respectively - Legler (1963)[3.19]), whilst the number of photons detected will depend on p and on the spectral response of the detector. If $\delta/\alpha \sim 1$, the optical method using a high gain photomultiplier is about three orders of magnitude more sensitive than the electrical method, but at high E/p it is necessary to check that the relaxation time of the excited states does not introduce errors. Care must also be taken to avoid false signals due to resonance scattering (section 5.4.3).

The optical method has been used by Dibborn (1961)[3.20] with the experimental arrangement shown in fig. 3.6. The photomultiplier was placed behind a quartz anode, rendered conducting

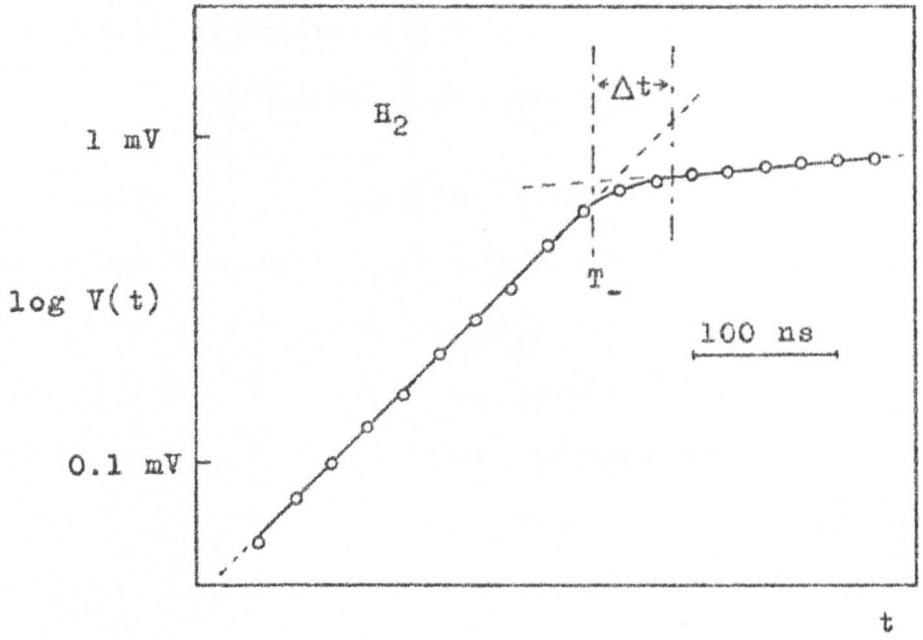

Fig. 3.7

Semi-logarithmic plot of electron current against time (Frommhold).

with a transparent film of $SnCl_2$. A $\frac{1}{2}$μsec pulse of photoelectrons was released through the hole in the cathode by irradiation with a pulsed ultra-violet lamp, the light from which was prevented from reaching the photomultiplier by the disc B1. The geometrical factor g varied according to the position of the avalanche, and had a maximum value of 0.4, and the overall detection efficiency, that is photocathode electrons per "detectable" photon from the avalanche, was about 0.025. After applying the appropriate corrections Dibborn plotted log V, where V was the output signal, against t to obtain a straight line of slope $\tau = 1/\alpha v_-$, to confirm the exponential growth concept. It is stated that the τ values are in agreement with the α and v_- values of other authors, the measurements having been made in N_2 + 20 torr of CO_2, at a total pressure of about 140 torr. Determinations were also made of δ/α , and of v_- by the observation of secondary avalanches in a limited region just below breakdown.

Frommhold (1960)[3.21] has determined $1/\alpha v_-$ by direct measurement of the electron component, in an experiment which combined this technique with time of flight measurements. He observed uniform field electron avalanches below breakdown in H_2, N_2, O_2 and some organic vapours, initiated by a photoelectron pulse of about 10^4 electrons and with a gas amplification of about 10^2. The logarithm of the total current was displayed against time on an oscilloscope (fig. 3.7); the initial straight portion is due to the electron component and $1/\alpha v_-$ is obtained from the slope, and the

plateau is due to the ion component. The section Δt has a finite length because of electron diffusion and the length of the initiating electron pulse, but the electron transit time, from which v_- was calculated, could be obtained by relating the position of this portion to a start-time marker. Ideal curves of this type were obtained with H_2 and N_2, but not with O_2, air and the organic vapours.

Rose's [3.22] values for α in H_2, and Masch's [3.23] for α in N_2 were used to calculate v_- from $1/\alpha v_-$, and these agreed well with the time of flight measurements, indicating that the physical picture of an avalanche described by equation 1.2 is valid in H_2 and N_2 for the E/p range 20-35 and 30-80 respectively. Fig. 3.4 shows that the H_2 values appear to be consistent with those at lower E/p due to Bradbury and Nielsen.

Jager and Otto (1962)[3.24] used a technique that was essentially the same as that of Frommhold, to determine v_- in H_2 and Ar in the E/p range from 15 to 30 volts.cm^{-1}.torr^{-1}, but with residual gas pressures as low as 7×10^{-10}torr. The meticulous vacuum technique necessary to achieve this pressure in a glass system was unfortunately wasted to some extent, since the gases used had an impurity content of 20p.p.m. The purity of these "spectroscopically pure" gases could have been substantially improved by diffusing the hydrogen through a palladium thimble and by cataphoresis of the argon (section 4.2), but they were still more pure than those of Frommhold. For low gas multiplications ($\exp \alpha d < 10$), v_- was

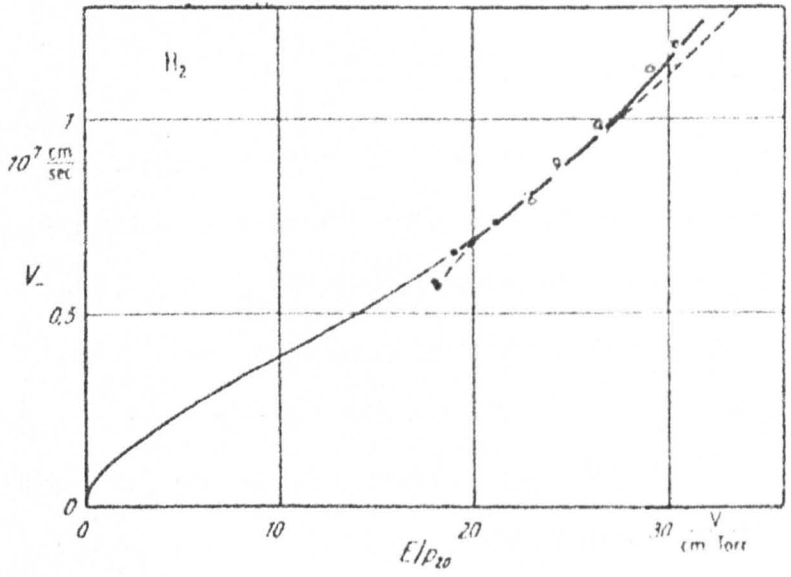

Fig. 3.8

Electron drift velocities in Hydrogen
(• Jager & Otto t.o.f., ○ J.& O. 1/ v_-,
—Bradbury & Nielsen and Frommhold).

determined from transit time measurements, and for higher multiplications from $1/\alpha v_-$, using Rose's values for α. These values agree well with Frommhold's, and likewise are consistent with those of Bradbury and Nielsen (fig. 3.8).

3.5. The Pulsed Time-of-Flight Method.

Prior to 1940, all quantitative investigations of the properties of gas discharges had been made below breakdown, under equilibrium conditions, by relating the total d.c. current (though the ion current is only $\sim 1\%$ of the electron current) to such parameters as p, i_o, d, and E. The only exception to this was the determination of Paschen curves by observation of the catastrophic breakdown which occurred at the sparking potential (e.g. de la Rue and Miller (1880)[3.25], Paschen (1889)[3.26], Carr(1903)[3.27]).

In 1940 Engstrom and Huxford [3.28] initiated the study of current transients when they observed that the time-resolved current from gas-filled phototubes, subjected to a chopped light source took several milliseconds to react fully to the light transients. This they attributed to the action of metastable states as a secondary process.

Von Gugelberg (1947)[3.29] irradiated the cathode of a plane-parallel gap with intense ultra-violet light to release a heavy photoelectron current, and then applied a step-function voltage

across the gap and observed the resultant current transients on an oscilloscope. He applied the theory of Bartholomeyczyk (1940)[3.30] to the results and evaluated the contribution of secondary processes, making the assumption that photon secondary emission at the cathode was neglible. This technique has been refined and exhaustively applied under conditions of high purity and in a number of gases by the groups at Keele and at Swansea (e.g. D.K.Davies et al (1963, 1964)[3.31], Morgan and Williams (1965)[3.32], Betts (1965)[3.33], Willis and Morgan (1969)[3.34]), using the more rigorous analysis due to Davidson (1953)[3.35]. Davidson's treatment of the problem has been criticised because it does not take into account the effects of space charge, but careful experimentation can minimise space charge distortion.

Molnar (1951)[3.36] conducted a study of metastable secondary action in inert gases by applying a d.c. potential to a plane parallel gap and irradiating the cathode with chopped ultra-violet light. By observing the current transients on a oscilloscope Molnar was able to derive values for the diffusion coefficient and the probability for volume destruction of metastables, using his own theory.

Hornbeck (1950)[3.37] conducted a parallel investigation into faster current transients with the initial intention of determining γ_i, the positive ion secondary coefficient, in the inert gases. This experiment will be described in some detail, as it is a good example

of a careful study of current transients and also produced values for positive ion and electron drift velocities, some of which will be used for comparison with the early results obtained in the present investigation.

3.5.1. Hornbeck's time-resolved experiment.

This experiment, conducted in helium, neon and argon in the E/p range 0-800 volts.cm^{-1}.$torr^{-1}$ yielded:

1. confirmation of a theoretical treatment due to Newton (1948)[3.38]
2. some imprecise values of γ_i
3. positive ion drift velocities (E/p = 8 to 800)
4. electron drift velocities (E/p = 0 to 3.6).

The cathode of a plane-parallel gap was illuminated by a 0.1μsec pulse of ultra-violet radiation whilst a d.c. sub-breakdown potential was applied between the electrodes, and the subsequent current transient was observed on an oscilloscope. It was intended that the short u.v. pulse would permit resolution of the faster secondary processes from the effect of slowly diffusing metastable atoms; the time scale was not fast enough to resolve secondary effects due to energetic photons (provided there were no photon delaying processes in the gas), since the u.v. pulse length was of the same magnitude as the electron transit time, so only positive ion effects should have been seen.

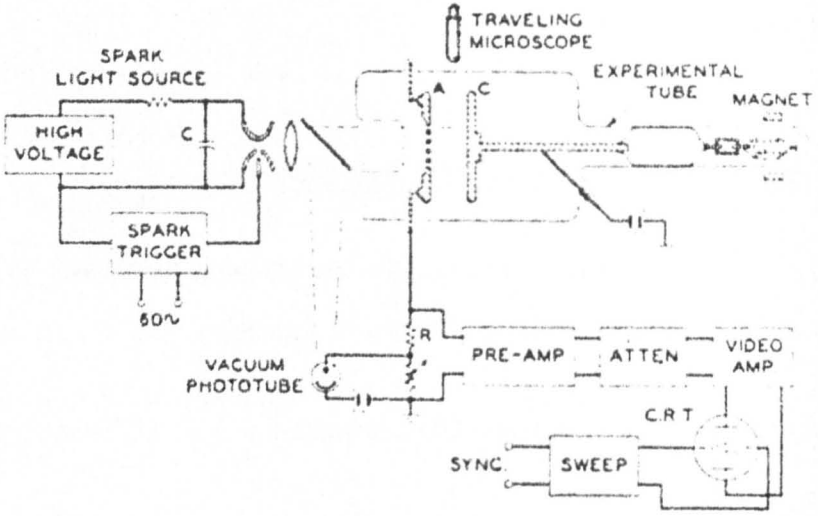

Fig. 3.9

Hornbeck's apparatus for studying current transients.

The experimental arrangement was as shown in fig. 3.9. A glass experimental tube contained a nickel anode and a BaO/SrO coated nickel cathode, both of diameter 5cm, separated by a variable distance $\sim$ 1 cm. Adequate high vacuum techniques were used, though the presence of an oxide-coated cathode almost certainly prevented the attainment of very high gas purity. Mass spectrometry showed the impurity content to be less than 50 p.p.m. The d.c. potential was derived from dry batteries, and the cathode was illuminated through the quartz window and the perforated anode by a u.v. pulse from a spark gap in air, triggered by a third electrode at 60p.p.s. The oscilloscope was triggered by a photocell which monitored the light output from the spark to eliminate the effect of jitter in the timing of the spark, and the voltage developed across R was displayed on the oscilloscope. The variable portion of R was used to offset the high initial current, due to transit of the photo-electrons, by superimposing a signal of opposite polarity from the photocell, thus preventing saturation of the amplifiers.

Hornbeck formulated a theory to calculate values for γ_i from discontinuities in the current transients; in fact, he was not able to do this with any accuracy, and values for γ_i were not obtained until Varney (1954)[3.39] repeated the experiment and applied a modified theory. Instead, he was able to derive values for v_+ and v_- in helium over a limited E/p range. Hornbeck predicted and achieved current transients of the shape shown in fig. 3.10. There

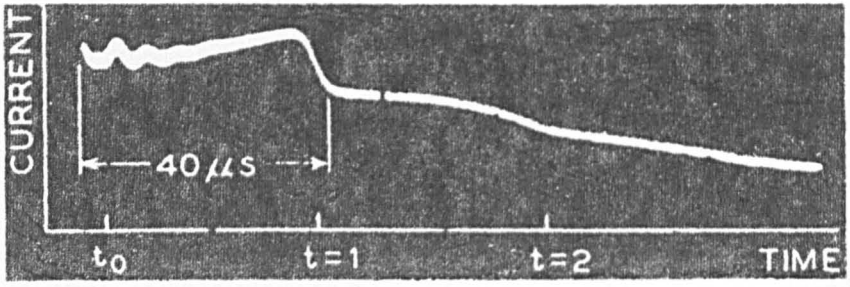

Fig. 3.10

A current transient in Argon (Hornbeck).

was first a very short, large amplitude current, of exponentially increasing magnitude, due to the passage of the primary electron avalanche to the anode, with an abrupt discontinuity as these electrons were collected by the anode. Fig. 3.10 does not show this pulse because of the electronic blocking technique described earlier, but Hornbeck measured its width at low E/p, where ionisation was slight, to obtain values for v_-. Following this pulse, the approximately flat section between t = 0 and t = 1 corresponded to the drift of positive ions from the anode back to the cathode, when there was a second discontinuity as they were collected. The section from t = 1 to t = 2 was explained by the drift of a second generation of positive ions from anode to cathode, these ions having been created by a secondary electron avalanche of smaller amplitude than the primary (since $V < V_s$), initiated by positive ion bombardment of the cathode. This was precisely as would be expected in the below-breakdown conditions prevailing, except that it is difficult to understand why the short current pulse due to the second electron avalanche was not recorded. All the discontinuities are blurred out by diffusion, but Hornbeck determined the point of inflection at t = 1 to calculate values for v_+. Typical positive ion transit times were $\sim$ 50μsec, and electron transit times ½μsec; the width of the u.v. pulse (1/10μsec) would have caused the v_- determinations to be rather imprecise and limited the E/p range to a maximum of 3.6 volts.cm^{-1}.torr^{-1}. The magnitude of the currents flowing in the gap, equivalent to about 10^7

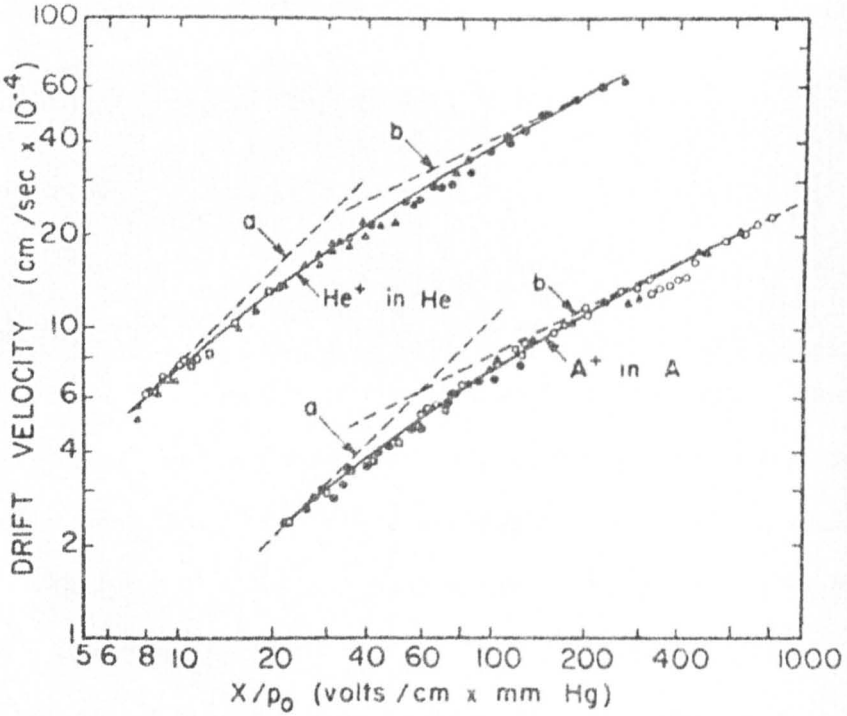

Fig. 3.11

Positive ion drift velocities in Helium and Argon (Hornbeck).

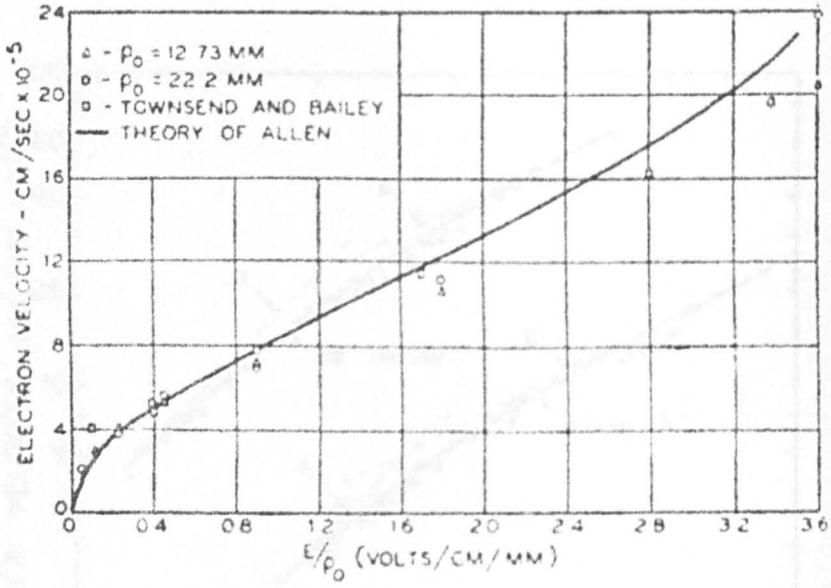

Fig. 3.12

Electron drift velocities in Helium (Hornbeck).

electrons, were not excessively large but would have caused some distortion of the applied electric field (sections 1.6 and 5.4.2).

The technique would not have allowed any discrimination against the effects of delayed photons in its original purpose of measuring γ_i, because of the comparable time scales of these two secondary processes.

The values obtained by Hornbeck for v_+ and v_- in helium are shown in figs.3.11 and 3.12 respectively. The v_- values show fair agreement with those of Townsend and Bailey (magnetic deflection method) and, though not illustrated in fig. 3.12, with those of Bradbury and Nielsen (shutter method), so that some confidence may be placed in the pulsed method, and its extension to higher E/p, where other techniques fail, is justifiable. Loeb (1955)[3.40] remarked that "It is seen that the pulse method without much care yields interesting data on the electron drift velocity, and this technique deserves further exploitation".

In an early variant of the pulsed technique, Raether (1937) [3.41], and subsequently Riemann (1942)[3.42] and Allen and Phillips (1960)[3.43], were able to produce single avalanches in a cloud chamber, by the use of very carefully controlled conditions in gas mixtures (to quench photon secondary processes). This has never been a particularly potent technique for the measurement of v_-, but it illustrates spectacularly the phenomena being studied and a photograph

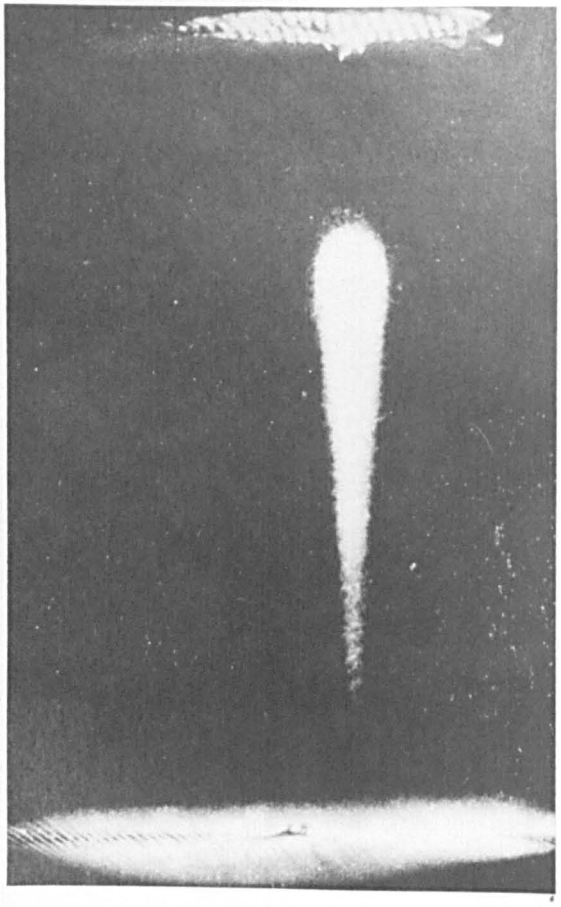

Fig. 3.13

A single electron avalanche
in a cloud chamber (Raether)

by Raether is reproduced in fig. 3.13.

3.5.2. Recent Time of Flight Measurements.

Breare and von Engel (1964)[3.44] developed a technique, first used by Corrigan and von Engel (1958)[3.45] to obtain absolute values for the excitation coefficient, to measure electron drift velocities in hydrogen for E/p in the range 14 to 43 volts.cm^{-1}.$torr^{-1}$. This technique closely resembles the photo-multiplier method of the present investigation, and the experimental arrangement is shown in fig. 3.14. A glow discharge between electrodes S_1 and S_2 produced initiating electrons, which were introduced into the drift space in short pulses by the application of square voltage pulses on the gate electrode G. Two photomultipliers (only one is shown) recorded the progress of the avalanche through their respective viewing regions to permit a drift velocity to be calculated; wavelength conversion by a phosphor at P was thought to increase the sensitivity. The v_- values obtained are shown in fig.3.15, and good agreement with the results of other workers for E/p < 20 volts.cm^{-1}.$torr^{-1}$ is shown. At higher E/p, the values appear to be a little high, and it is suggested that this might be due to the effects of resonance radiation (section 5.4.3) since the pressure was 2 torr, a fairly favourable value for the observation of spurious signals.

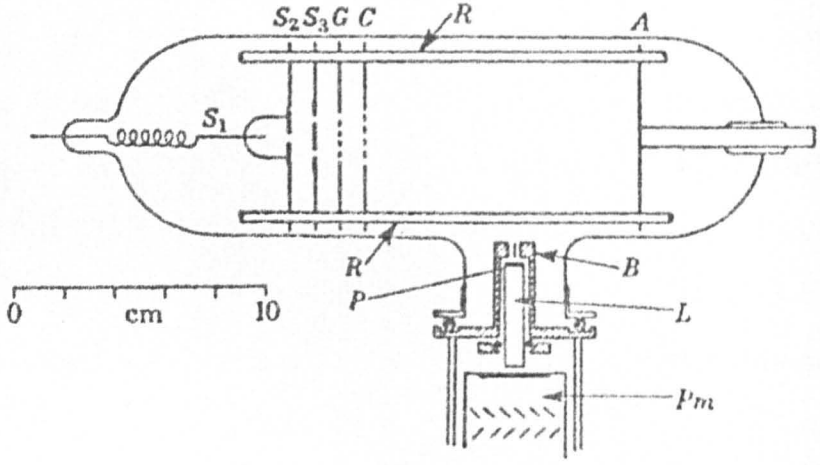

Fig. 3.14

Breare and von Engel's apparatus for the determination of v_-.

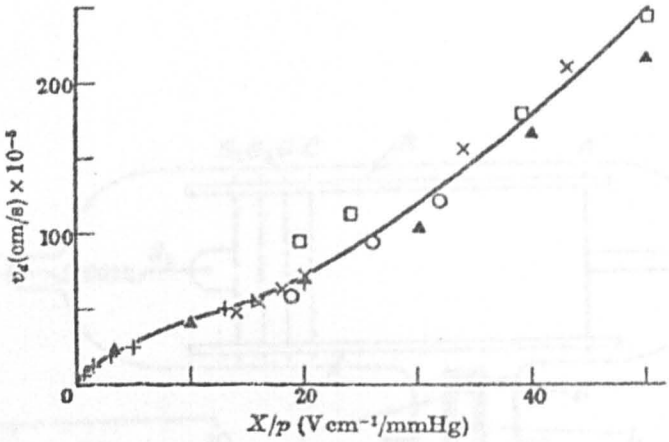

Collected results of electron drift velocities in hydrogen as a function of the reduced field. +, Bradbury & Neilsen (1936); ○, Frommhold (1960); ▲, Townsend & Bailey (1921); □, Gill & von Engel (1948); ×, Present measurements.

Fig. 3.15

Breare and von Engel's values for v_-

in Hydrogen.

Schlumbohm (1965)[3.46] measured values of v_- and v_+ in a number of gases to very high values of E/p, reaching 10^4 volts.cm^{-1}.torr^{-1} in O_2, and 2×10^3 in H_2. The method and apparatus was similar to that of Frommhold (section 3.4), but a linear display of electron and ion currents against time (instead of a semi-logarithmic display) was recorded on a wide-band oscilloscope after amplification, and the measurements were principally time of flight rather than exponential current growth. A 15nsec duration ultra-violet light pulse released between 10^4 and 10^5 photoelectrons, which drifted in a uniform field for a distance of 4.7cm with a gas amplification $\exp(\alpha d)$ of about 10 only, to preserve below breakdown conditions so that a d.c. electric field could be applied. This necessitated gas pressures between 5 torr and 10^{-2} torr, the low values being used at high E/p. It is most unlikely that equilibrium was achieved at the lower pressures in the inter-electrode distance of 4.7cm (this problem is discussed in greater detail in section 5.2), and Schlumbohm's values for v_- at high E/p are open to some doubt, but are the only ones available in this region. His results for H_2 are reproduced in fig. 3.16. Although he does not give details of the vacuum techniques employed, the gas impurity content was 100 p.p.m. before introduction into the experimental tube, and a residual gas pressure of 10^{-6} torr would have contributed an equal amount of contamination at the low pressures, so it would appear that gas purity was only moderate.

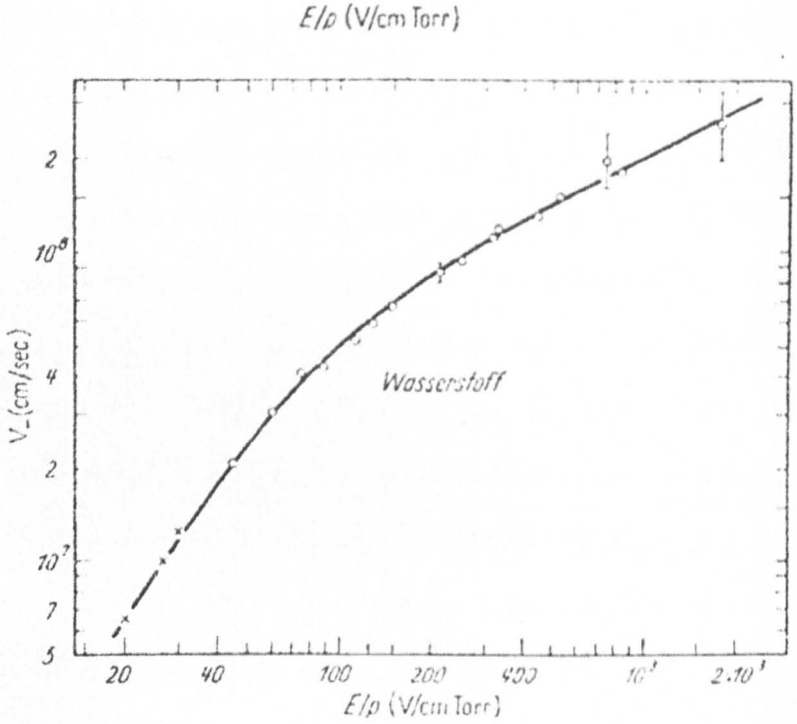

Fig. 3.16

Electron drift velocities in H_2 at high E/p (∘ Schlumbohm, ∧ Jager & Otto).

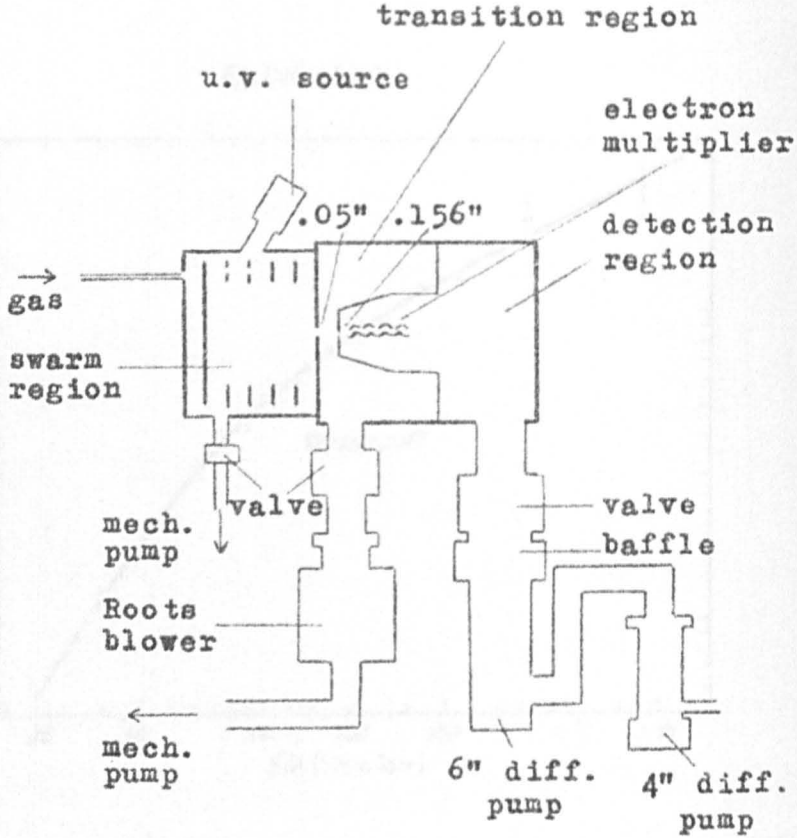

Fig. 3.17

Differentially pumped system using an electron-multiplier for determination of v_- at low E/p (Wagner et al).

A recent investigation by Wagner,Davis and Hurst (1967)[3.47] used a technique of particular interest because of its similarity to that employed by the author, though the measurements they made of v_- and the diffusion coefficient D were at very low E/p (0 to 2.5 volts. $cm^{-1}.torr^{-1}$). This group had previously used a Geiger-Muller counter to detect the arrival of single electrons in time of flight measurements (Hurst et al (1963)[3.48], Hurst and Parks (1966)[3.49]), the counter being an intrinsic part of the experimental tube, which severely limited the types of gas and the pressures that could be used. Their new apparatus is shown in fig. 3.17, and has three sections. Gas was steadily leaked into the swarm region, where a uniform d.c. electric field was applied between the cathode and the earthed anode, in which there was an aperture of 0.050" diameter to the transition region (c.f. the apertures of 0.002" and 0.020" in the present investigation). The transition region was differentially pumped to a pressure of about 10^{-2} torr by a Roots blower with a pumping speed of $75 l.sec^{-1}$. The detection region was linked to the transition region by a 0.156" aperture, and was pumped by a 6" oil diffusion pump to a pressure of less than 10^{-5} torr, which is an adequate vacuum for the operation of an electron multiplier.

A 0.3μsec wide pulse of photo-electrons from the cathode drifted a distance of 24.5cm in the uniform electric field at gas pressures of 1 to 25 torr normally, but up to 200 torr on occasions, and a sample of the swarm passed through the hole in the anode and the transition region into the detection region, for amplification by

the electron multiplier. The data was automatically handled by interfacing the experiment with a multichannel analyser to obtain a time of flight spectrum.

Drift velocities were calculated from the most probable time of flight and diffusion coefficients from the shape of the spectrum for a number of moderately pure gases, including hydrogen. Good agreement with the results of other authors was obtained for the v_- values, but not for the D values, for which the discrepancies ranged between a factor of 2 and of 7 (for argon). This discrepancy may have been attributable to the measurement of D in the field direction in this experiment, whereas it is measured perpendicular to the field in the Townsend method.

3.6. The Investigation of Very Fast Current Transients.

All of the investigations so far described have been confined to the below-breakdown regime, in which there is relatively little gas amplification and secondary processes are of slight importance. The formative time lag (f.t.l.), that is the time from initiation of the discharge to breakdown, has received a great deal of attention, both under conditions of small overvoltages for the evaluation of secondary processes using the Bartholomeyczyk-Davidson theory (section 1.3) which assumes a knowledge of v_-, and in the large overvoltage region where f.t.l's are $\sim 10^{-8}$ sec.

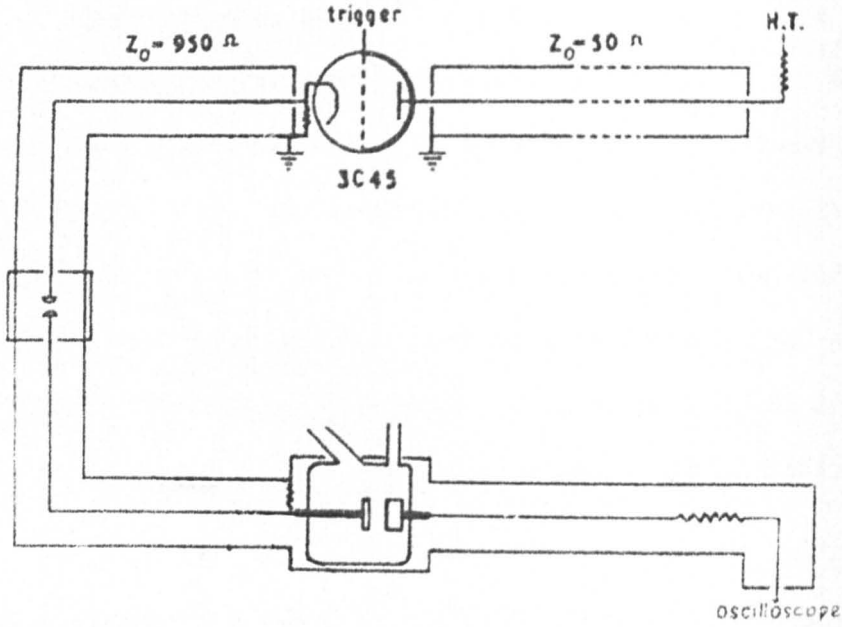

Fig. 3.18

Dawson's apparatus for the determination of v_- at high E/p.

The very early studies of highly overvolted break-down were largely qualitative (Pederson (1923)[3.50], Tam (1928)[3.51], Beams (1928)[3.52]), and these were followed by a series of semi-quantitative and highly ingenious experiments. Wilson (1936)[3.53] polarised the light emitted by a spark and viewed the light through a Kerr cell which closed after application of the voltage to the spark gap, at a time determined by a variable delay line; White (1936)[3.54] performed a similar experiment using pulsed ultra-violet irradiation of the cathode. Newman (1937)[3.55] measured the f.t.l. of a spark in air by using as a timing device a delay line along which were distributed bistable voltage sensitive devices of an unspecified nature. Fletcher (1949)[3.56] used a fast oscillo-scope and coaxial experimental geometry to investigate the time of formation of streamers. These investigations were all concerned, because of their low sensitivity, with an advanced stage of catastrophic breakdown.

Dawson (1963)[3.57], Dawson and Davies (1963)[3.58] and later Betts and Davies (1968)[3.59] performed an experiment in which it was intended to obtain values of v_- by observation of the early stages of this type of breakdown. Their experimental arrangement (fig. 3.18) was designed to form a virtually continuous transmission line. The length of 50ohm cable was discharged by switching on the hydrogen thyratron so that a rectangular voltage pulse, with a rise-time of 20nsec, propagated down the 950hm cable;

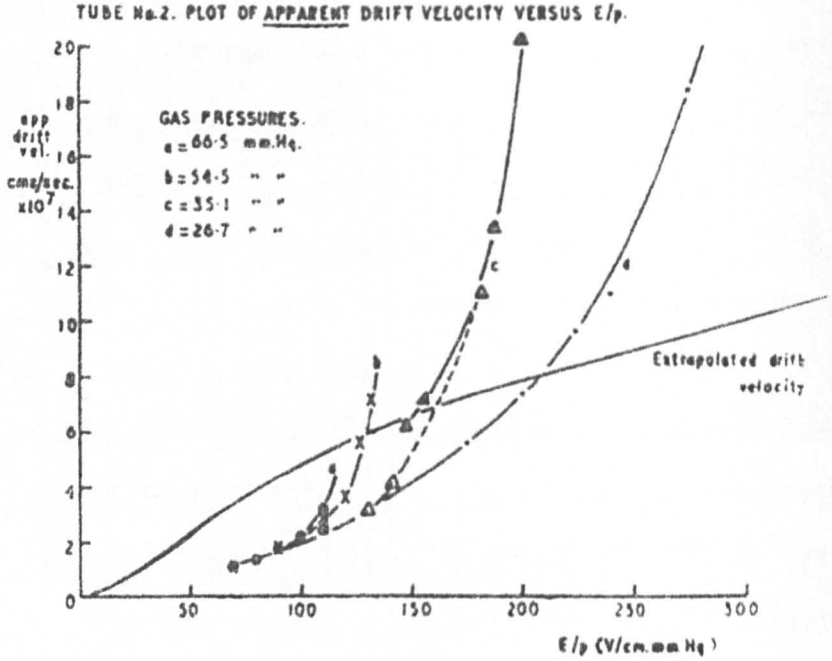

Fig. 3.19

Dawson's values for v_- in Hydrogen

a reduction of the rise-time to 3.5nsec was effected by the pressurised pulse-sharpening spark gap. On reaching the experimental tube, the pulse was totally reflected until the gap started to break down, when the growth of current propagated along a further length of cable which was matched into a Tektronix 519 travelling wave oscilloscope. The displacement current when the voltage pulse first reached the inter-electrode capacitance of the experimental tube provided a timing mark. Constant illumination with ultraviolet radiation ensured that initiating electrons were always available.

Dawson calculated that, if the gas multiplication $\exp(\alpha d)$ was equal to 10^8, the arrival of the primary avalanche at the anode could just be detected on the oscilloscope, and thus v_- could be calculated from the time of flight. However, it was found in practice that the experimental conditions to give a signal of this amplitude required theoretical values of $\exp \alpha d$ (calculated from $\alpha/p = f(E/p)$ and pd) in excess of 10^8 and often as high as 10^{14}, indicating that the simple picture of a single avalanche propagating in a uniform electric field of known magnitude was not applicable. The values obtained for the "apparent" drift velocity are shown in fig. 3.19, together with an extrapolation of the well-known values at low E/p, and it is seen that at lower E/p the experimental values are depressed, but that there is a rapid increase and a marked dependence on pressure as E/p increases above 100 volts $cm^{-1}.torr^{-1}$. There is no doubt that, because of inadequate

sensitivity, this experiment required sufficiently high currents in the gap to cause considerable space charge distortion of the applied electric field, and the anomalous values of exp(ad) substantiate this. Dawson was able to adequately explain, on a qualitative basis, the low v_- values below E/p = 100 volts.cm^{-1}.$torr^{-1}$, but failed to account for the pressure dependent increase at higher E/p. It is possible that this effect could be attributed to a lack of equilibrium between the avalanche and the gas and the field, and this is discussed further in sections 2.5 and 5.4.2.

3.7. The Present Investigation.

The present investigation was initiated as an extension of that of Dawson, and with the same purpose of obtaining values for v_- at moderately high E/p, but with the intention that the factors which made Dawson's results unreliable, in particular the effects of space charge distortion and secondary avalanches, should be minimised.

If (pxd) values are to be high enough to ensure rapid equilibrium of the photo-electrons, it is necessary at high E/p to operate above break-down and so to use a pulsed discharge. The delicate current balancing of the magnetic deflection method makes it particularly unsuitable for pulsed applications, whilst the intrinsically pulsed exponential current growth technique is unsatisfactory because of the magnitudes of the currents required. The

shutter method is attractive but is technically more difficult above break-down because of the need to synchronise, with variable delays, the shutter pulses with the applied voltage pulse and the u.v. lamp pulse. Also, the problem of resonance location, with the slow data acquisition rate of the present experimental design, would be formidable. In consequence, the approach adopted was the time of flight technique, the details of which are described in Chapter 4.

CHAPTER 4

EXPERIMENTAL APPARATUS AND TECHNIQUES

4.1. Design Criteria for the Experiment.

The principal purpose of this investigation was to measure electron drift velocities in hydrogen at moderate E/p and above the range in which v_- is well known, that is for E/p > 30 volts.cm^{-1}.$torr^{-1}$. The reasons for the selection of the pulsed time-of-flight technique are outlined in section 3.7, and the experimental philosophy was that the greatest confidence could be placed in the data if the conditions were arranged to ensure that a simple and well understood model was reproduced experimentally. The model was that of a single electron avalanche drifting in a uniform electric field, completely described by $n = n_o \exp(\alpha v_- t)$, and free of the effects of secondary processes and space charge distortion of the applied field. The investigation is conveniently divided into two phases, a preliminary assessment of the problem with tubes A and B, followed by the main experiment with tube C.

The design criteria, some of which were not formulated or applied until the second phase, were as follows -

1. Uniform field geometry. If values for v_- at precisely known E/p are to be obtained, field uniformity is essential, and it is also desirable that $\alpha/p = f(E/p)$ should be known. Implicit in this condition is the requirement that the number of electrons in the avalanche should be kept below 10^6 to minimise space charge disturbance of the applied field (section 1.6). This necessitated the use of a detection technique of high sensitivity.

2. Generation of single, discrete avalanches, which requires initiation of the avalanche by a single electron or by a pulse of electrons of width very much less than the electron transit time, and that the secondary avalanches are suppressed or separated from the primary avalanches.

3. Electron transit times > 5×10^{-8} sec to permit the use of a high sensitivity oscilloscope, and to obviate the need for very fast pulse techniques, with their attendant limitations. The problem of generating very short initiating electron pulses also imposed this condition.

4. Rapid attainment of equilibrium by the initiating electrons (sections 2.5 and 5.4.2), for which it was necessary that the (pxd) product should be adequately large. At E/p = 100 volts.cm^{-1}.$torr^{-1}$ for instance, (pxd) > 14.5 for equilibrium to be achieved within 5% of the total drift distance. $\alpha/p = 1.29$ at E/p = 100 (5.26), so that $\exp(\alpha/p.pd) = 1.4 \times 10^{8}$ for (pxd) = 14.5, which exceeds the condition that the number of electrons in the avalanche should be less than 10^{6}. An $\exp(\alpha d)$ value of 10^{4} was adopted as a compromise between these incompatible requirements, and also for reasons detailed in section 4.2. This gives a (pxd) value of 7.1, and equilibrium will be attained within about 10% of the drift distance. Now the sparking criterion is that

$$\exp(\alpha d) \geq (1/\gamma + 1),$$

and for hydrogen $\gamma = 2.0\times10^{-2}$ to 6.0×10^{-2}, to give $(1/\gamma + 1) \simeq 2.5\times10^{1}$; thus the value adopted for $\exp(\alpha d)$, 10^{4}, greatly exceeds the breakdown threshold of 2.5×10^{1}, and all measurements had to be taken in the above-breakdown regime.

5. The use of two different techniques to determine electron drift velocities, to enable the consistency of the data to be checked. It will be shown in Chapter 5 that one of the techniques, the photomultiplier method, proved unreliable when the data was analysed.

6. The application of ultra-high vacuum techniques to ensure that the impurity level was reduced to the minimum practical level. It is concluded in section 1.7 that gas purity is not of paramount importance in the determination of electron drift velocities, but it seemed preferable that the data should have been obtained in clean gas samples. However, in retrospect, it is thought that the techniques for this investigation could have been developed with greater facility if preliminary measurements had been taken in a system offering a poorer vacuum but affording ready access to the electrode and detection regions.

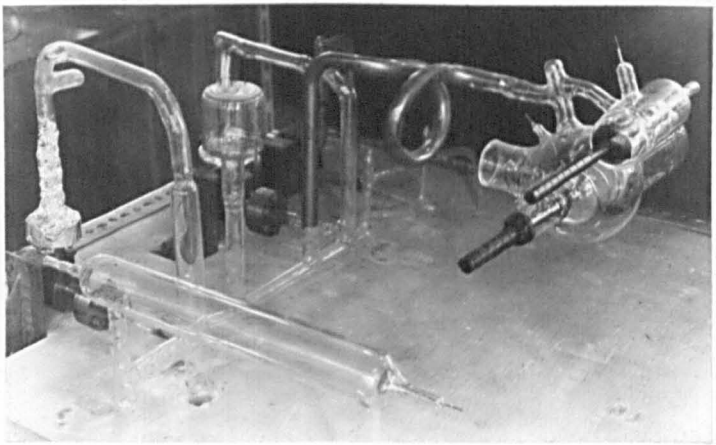

Fig. 4.1

Tubes A and B, and the bakeable section of the vacuum system (tube A is the larger).

4.2. The Experimental Tubes and Vacuum Systems.

4.2.1. Tubes A and B, for the Preliminary Investigation in Helium.

Tube A is shown in fig. 4.1. The anode and cathode were pressed from sheet nickel to have a flat surface over a diameter of 4.5 cm, curving at the edges with a radius of about 0.5 cm to avoid local high field regions; the overall diameter was 5.0 cm and the anode-cathode separation was 4.64 $\pm$ 0.05 cm to give a D/d ratio of a little under 1.1. Two guard rings of diameter 5.0 cm, made from 0.15 cm thick nickel wire, were equispaced between the anode and cathode. The uniformity of the field for this tube was not determined, but the similar electrode configuration of tube C implies that the field was adequately uniform (fig. 4.6). To permit accurate alignment, the assembly was held in a jig whilst being mounted on a glass frame, and was sealed into the tube as a unit. No conducting coating was applied to the inner walls of the vessel to eliminate charge build-up, as the walls were fairly remote from the electrodes and a degree of screening was provided by the guard-rings.

A step voltage was applied across the electrodes by a manually operated mercury switch in series with the output of a precision potentiometric divider, which was powered by a stack of dry batteries. The rise-time of the mercury switch was 3 μsec, but at an earlier stage, when it was hoped that electron drift velocities could be measured, a hydrogen switch with a rise-time of 30 nsec was built. The

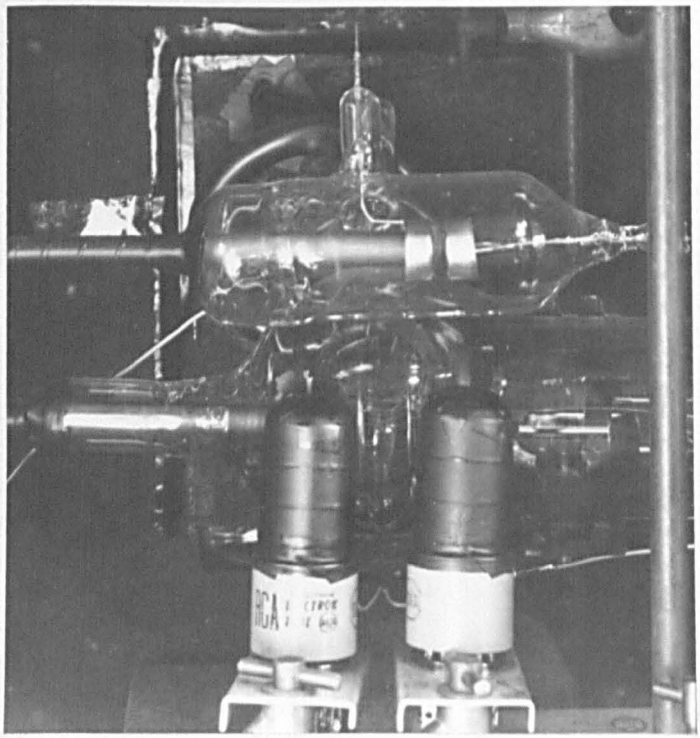

Fig. 4.2

Tubes A and B, with the photomultipliers positioned to monitor tube A.

breakdown current was limited to a maximum of 4 mA by a series resistance, the signal across part of which was used to monitor the discharge current; the time constant of the resistance in parallel with oscilloscope and electrode capacitances was 200 nsec. The zero-current applied potential (200 to 1400 volts) was measured with negligible error using a precision potentiometer. The guard-ring potentials were maintained by a resistance chain, selected to match the separations to within 1%, and the time-constant was sufficiently short for the guard-rings to follow the potential variations.

Initiating electrons were released from the cathode by continuous ultra-violet irradiation from a high pressure mercury lamp. The development of the discharge was monitored by two photomultipliers which viewed regions near the anode and cathode through collimating slits. The experimental tube was enclosed in a light-proof box (fig. 4.2), and was pumped through a length of tubing shaped to have an optical path involving a minimum of four internal reflections and coated internally with colloidal graphite (Aquadag). This arrangement gave a background count of about 10^4 photons per second from the photomultipliers. The ultra-violet irradiation was introduced by a light-guide projecting through the side of the box, and passed through a quartz window and the perforated anode (20 x $\frac{1}{2}$ mm holes) onto the cathode. Inside the tube the light-guide was coated with Aquadag, outside with opaque black tape, and the stray ultra-violet signal was reduced to an acceptable level by the collimating slits of the photmultipliers.

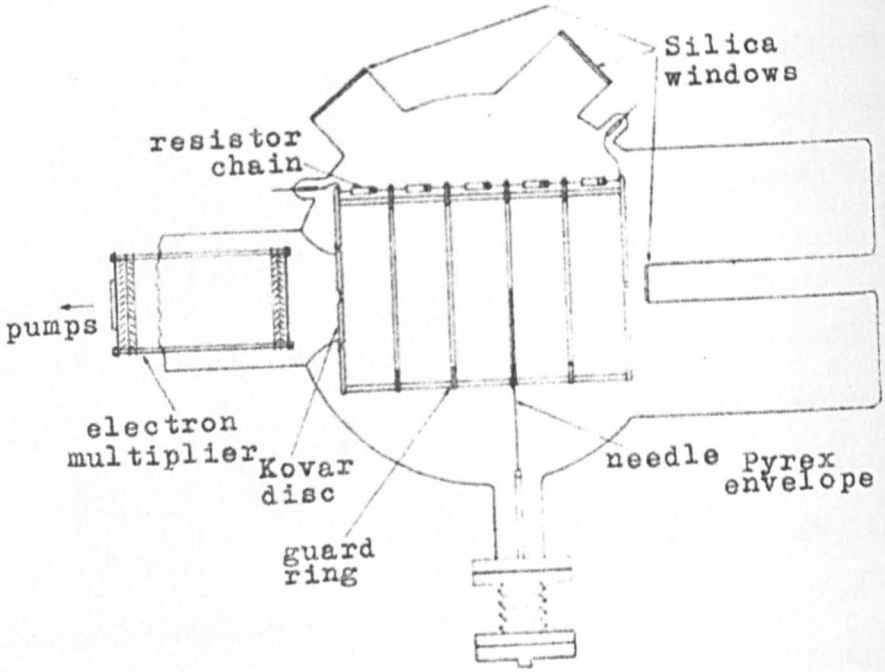
Silica
windows
resistor
chain
pumps
electron
multiplier
Kovar
disc
guard
ring
needle
Pyrex
envelope

Fig. 4.3

Tube C.

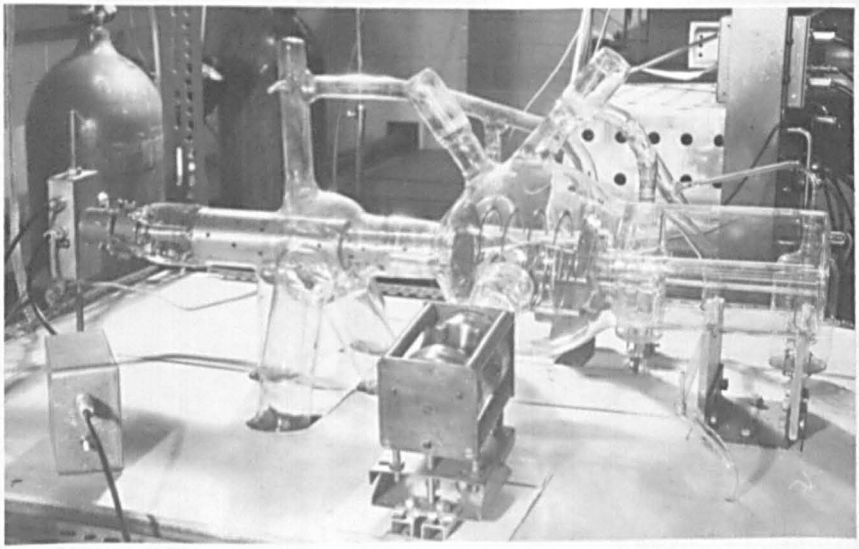

Fig. 4.4a

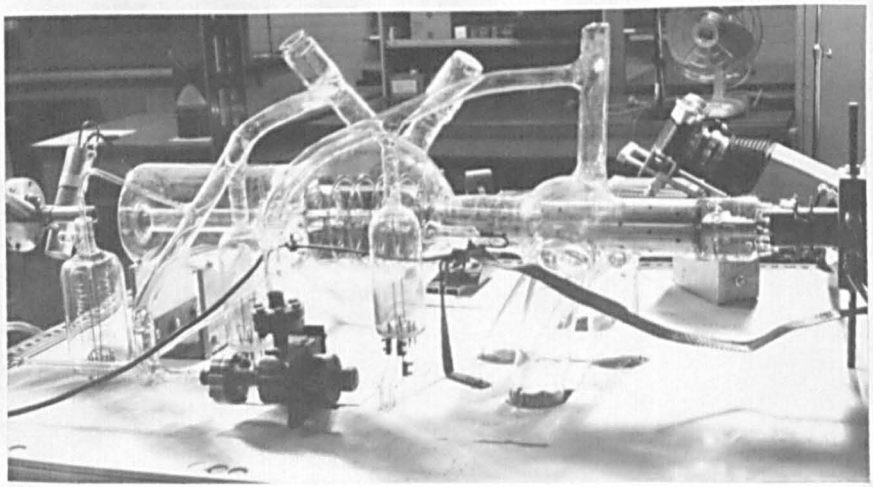

Fig. 4.4b

Tube C and the bakeable section

of the vacuum system.

Tube B is shown in fig. 4.1. The sheet nickel anode and cathode had a flat surface over the whole diameter of 2.0 cm, with a slight bevel at the edge, and the fixed separation was 0.37 $\pm$ 0.05 cm to give a D/d ratio of 5.4. This ratio is sufficiently favourable to make the use of guard-rings unnecessary. Tube B did not differ from tube A in any other respect.

4.2.2. Tube C, for the Principal Investigation in Hydrogen.

Tube C is shown in figs. 4.3,4.4a and 4.4b. The machined and polished stainless-steel electrodes (fig. 4.5) had a diameter of 10.0 cm, the anode-cathode separation was 11.88 cm, and the four guard-rings were separated by glass spacers which were ground to the same length to within a tolerance of 0.01 cm, so that the anode and cathode were parallel to within 0.05 cm. The assembly was clamped together by tightening the nuts at the ends of the three glass rods, which passed through the electrodes and spacers and had threaded steel studs attached to tungsten seals at each end. There were no differential expansion problems as both spacers and rods were glass. A 5.0 cm diameter nickel-iron (Kovar) disc completed the anode, and made an electrical pressure contact to the outer annulus of the anode. A hole of diameter 5×10^{-3} cm was punched at the centre of the Kovar disc, but this was later enlarged to 3.5×10^{-2} cm for what will be called the 'large hole data' (Chapter 5). The anode was earthed and a pulsed negative voltage was applied to the cathode (section 4.3), the correct

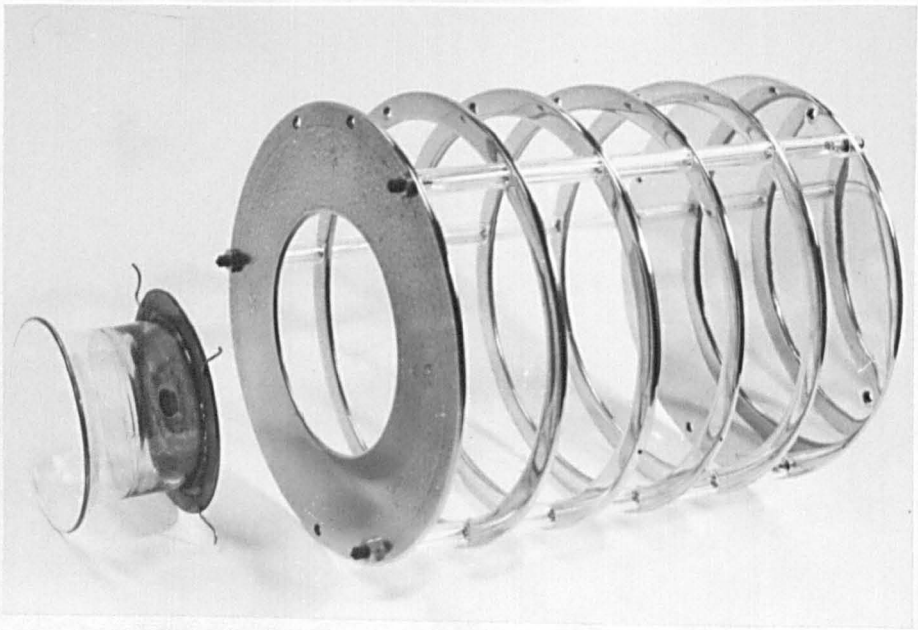

Fig. 4.5

The electrode system for tube C.

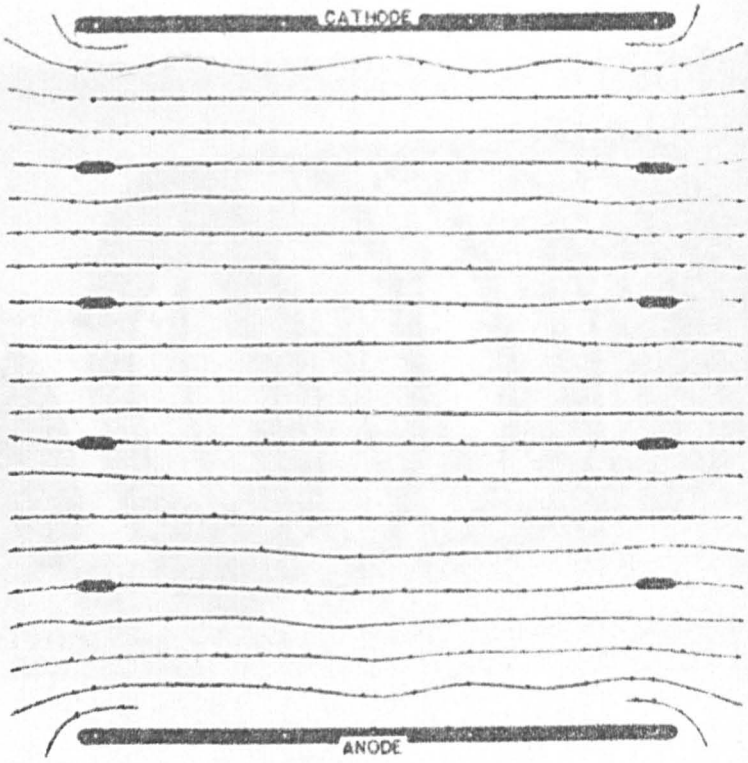

Fig. 4.6

The electric field distribution for Tube C.

potentials being established on the guard-rings by the chain of vacuum resistors (Pyrofilm), which had a tolerance of $\pm 1\%$. The maximum voltage rating of these resistors proved to be the limiting factor for the greatest potential that could be applied across the drift space (1250 volts). The field uniformity was determined by an electrolytic tank method, and was found to be satisfactory (fig. 4.6).

A fine needle, of diameter 7.5×10^{-2} cm, passed through and made contact with the second guard-ring from the cathode, and the position of its tip could be varied in three dimensions over a small region on the axis of the electrode system by adjustment of the stainless-steel bellows. Ultra-violet irradiation of the tip by the pulsed light source (Bedford (1970)[4.1] - Appendix 4) initiated an avalanche, and the area of the needle was sufficiently small for the probability of initiation of secondary avalanches at the needle to be slight. Secondary avalanches originating at the cathode were spatially separated from the primary avalanche, which could thus be clearly resolved, and the secondary avalanches had achieved only a small degree of development at the time that the primary reached the anode, and so were unlikely to contribute to space charge distortion. Provision was also made for ultra-violet irradiation of the anode for calibration purposes, and for initiation of avalanches at the cathode.

Calculations made from diffusion considerations (section 1.6) showed that, for typical experimental conditions, an average of

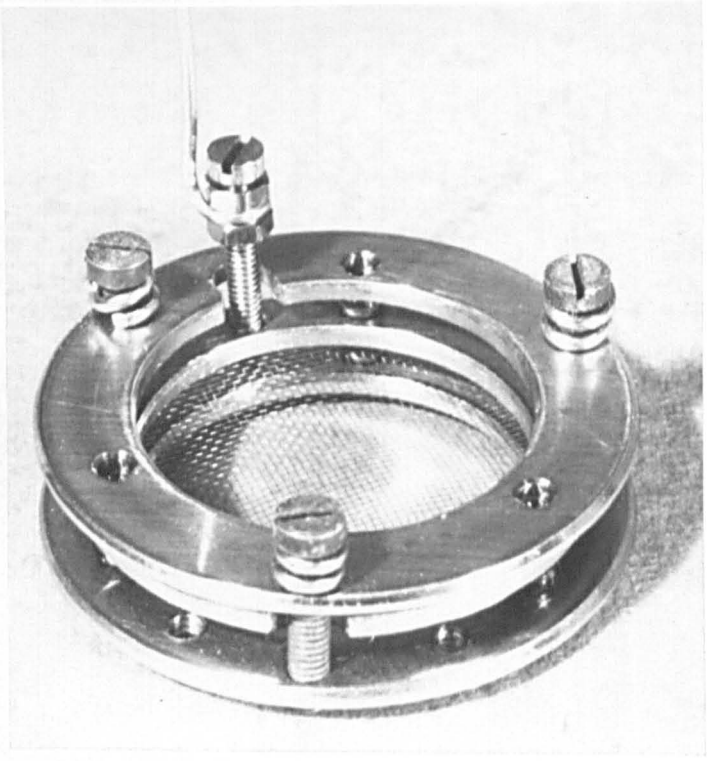

Fig. 4.7

The electron energy analyser.

one electron from an avalanche of 10^4 would pass through the anode orifice for detection by the electron-multiplier. It has been mentioned that, if space charge distortion is to be unimportant, n must be less than 10^6, whilst the requirement for an adequate number of free paths in the drift space requires that n should be large ($> 10^8$), and the minimum detectable value of 10^4 was adopted as a reasonable compromise. A simple retarding-potential energy analyser (fig.4.7) could be interposed between the anode and the electron-multiplier to assess the electron energy distribution. A plane-parallel analyser geometry is unsatisfactory for the analysis of electrons which may be incident over a range of angles, and an improved version is described in section 5.8. A secondary measuring technique was provided by a pair of photomultipliers which monitored the radiation emitted from sections of the drift space close to the anode and cathode; the viewing angle of the photomultiplier collimating slits was about 1°, so that the sections had a width in the field direction of approximately 0.6 cm on the axis of the electrode system, or about 5% of the total drift space.

4.2.3. The Vacuum Systems.

Two vacuum systems were used in the course of this investigation, both being constructed principally of borosilicate glass and capable of attaining ultimate vacua $\sim 10^{-7}$ torr. The first system, which served tubes A and B, was entirely conventional in design and

was evacuated by a 30 litre.sec^{-1} mercury diffusion pump backed by a two-stage rotary oil pump. The standard procedures of liquid nitrogen trapping, eddy-current heating of metal components, periods of baking at 350°C, and firing of getters achieved ultimate vacua of 3×10^{-8} torr, which rose to 1×10^{-7} torr after the system had been isolated from the pumps by a bakeable metal valve for 24 hours. Intermediate and residual pressures were measured with a Penning and an Alpert gauge, and gas pressures were determined to within ± 0.1 torr by an oil manometer which was isolated from the experimental volume by a glass spiral gauge; the pressure range investigated was 1 to 40 torr.

Spectroscopically pure helium, supplied by B.O.C. in pyrex flasks, was admitted through a bakeable metal valve. The manufacturer's figures for the gas composition are He = 99.9995%, Ne < 3 v.p.m., N_2 < 1 v.p.m., O_2 < 1 v.p.m., Ar < 1 v.p.m., H_2 < 0.5 v.p.m., CO_2 < 0.5 v.p.m., and the gas was further cleaned to an unknown extent by cataphoresis. The mechanism of cataphoresis has been discussed by a number of authors, including Baly (1893)[4.2], Druyvesteyn (1935)[4.3], Riesz and Dieke (1954)[4.4], Loeb (1958)[4.5], Mittelstadt and Oskam (1961)[4.6], Miller (1964)[4.7] and Schmeltekopf (1964)[4.8]. Schmeltekopf's work was directed to establishing empirically the optimum conditions for cataphoretic separation of He-Ne mixtures containing more than 1% of the minority constituent, and showed that the theoretical predictions of Druyvesteyn are valid, except at pressures above 40 torr and at currents above 20 mA. It is necessary that the vehicular gas should be

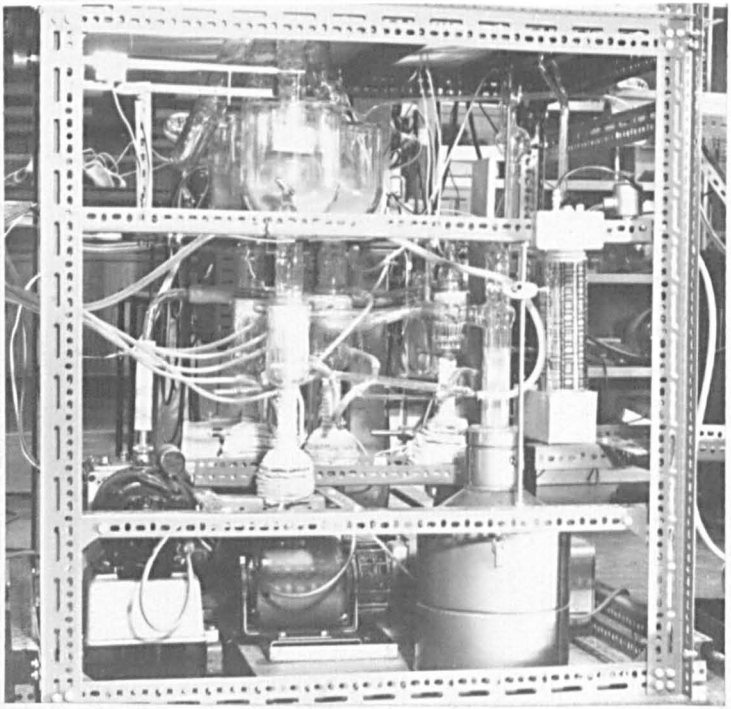

Fig. 4.8

The differential pumping system for tube C.

capable of completely ionising the minority impurity gas, either by virtue of a higher ionisation potential or by the formation of complex ions such as $NeHe^+$, so that the impurity is trapped in the cathode region, which is located at the "blind" end of the cataphoresis tube. Separation is enhanced by high pressures and by high current densities, whilst high atomic weight is unfavourable. Ricaz and Dieke give the following experimental figures for Ne impurity in He: for 2 litres of gas at 20 torr in a 20 cm long tube with a current of 20 mA, the time for equilibrium to be established was 2 hours,when there was an exponential distribution of Neon along the tube, with a concentration ratio of 100:1 between the ends. Smith [4.9] reports a reduction in the impurity content of B.O.C. spectroscopically pure helium from several v.p.m. to an estimated 0.1 v.p.m., measured with a mass spectrometer.

In this investigation, cataphoretic cleaning was applied before and during all readings at a current of 10 mA, the tube length being 30 cm, and it would be reasonable to assume a reduction in impurity level by a factor of at least 10 to give an impurity content of less than 0.5 v.p.m. Contamination due to vacuum technique should be negligible, equal to about 0.01 v.p.m.

The second vacuum system (figs. 4.8 and 4.9) for tube C was differentially pumped to allow the electron-multiplier to be operated at a pressure of about 10^{-5} torr whilst the drift space was filled with hydrogen at a pressure of several torr. The rate of diffusion of a

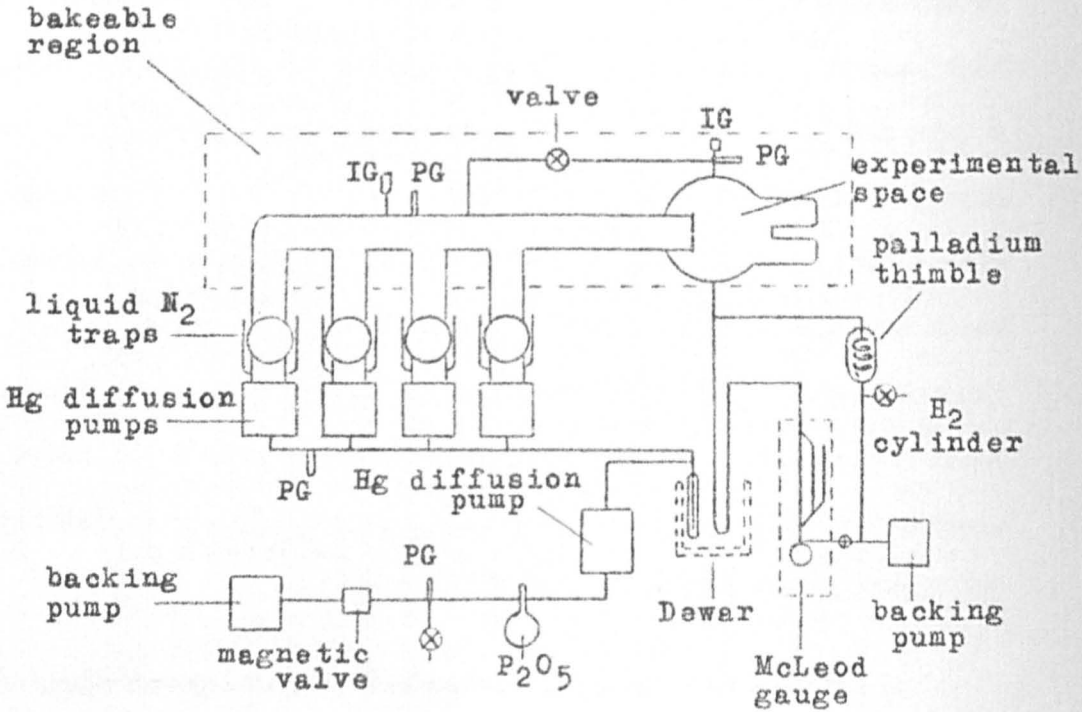

Fig. 4.9

The vacuum system for tube C.

gas through a small aperture is given by [4.10]

$$\frac{dV_2}{dt} = A \cdot \frac{p_1}{p_2} \left[\frac{13T}{M}\right]^{\frac{1}{2}} \quad \text{litre.sec}^{-1} ,$$

where A is the area in cm^2 , p_1 and p_2 are the pressures in torr, T is the temperature in $^{\circ}K$, and M is the molecular weight. Thus for hydrogen at room temperature and a pressure of 5 torr, to maintain 10^{-4} torr in the electron-multiplier region requires pumping speeds of 40 and 2200 litre.sec^{-1} for the small and large orifices respectively. Sufficient pumping speed for the small orifice was obtained by four parallel 30 litre.sec^{-1} mercury diffusion pumps with straight-through liquid nitrogen traps, backed by a fifth diffusion pump and a two-stage rotary oil pump, and this arrangement could maintain a pressure of 1.5×10^{-6} torr in the electron multiplier section with 10 torr of hydrogen in the drift section. When the sampling orifice was enlarged to 3.5×10^{-2} cm, the pumping speed was inadequate for the higher pressures and operation was restricted to $p < 1$ torr. Baking to $350^{\circ}C$ was necessary before every experimental run as the high vacuum section could not be isolated and the liquid nitrogen traps required refilling every three hours, which necessitated shutting down the pumps overnight. Cylinder grade argon at about $\frac{1}{2}$ atmosphere pressure was admitted during shutdown to protect the electron multiplier and to inhibit mercury diffusion. Ultimate vacua after bakeout were $\sim 1.0 \times 10^{-7}$ torr. Residual pressures were measured by an Alpert gauge, and the gas pressure was monitored by a Pirani gauge and measured with a McLeod gauge,

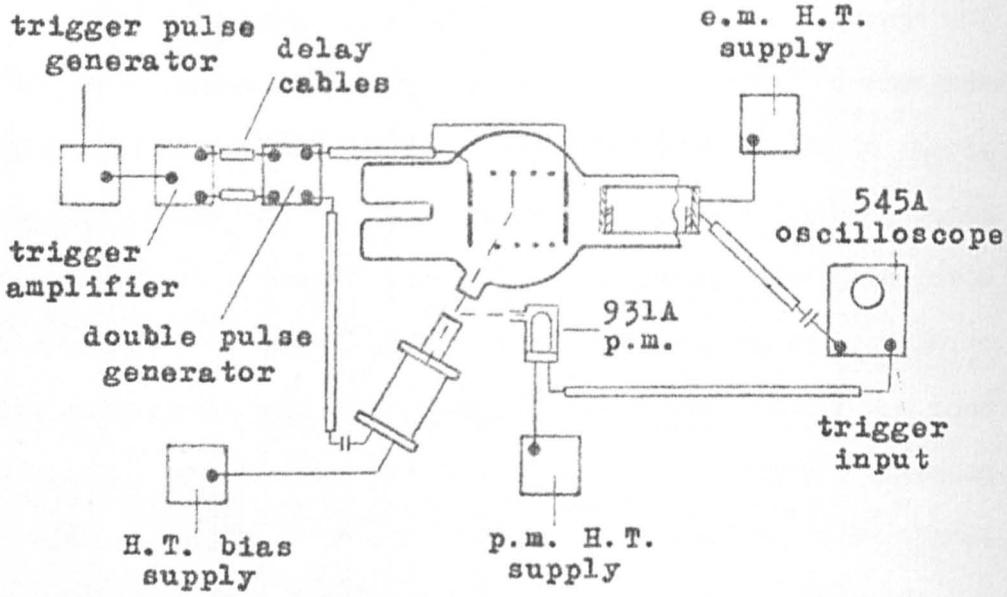

Fig. 4.10

The electronic arrangements for Tube C.

which was isolated from the experimental volume by a liquid nitrogen trap. (The Ishii-Nakayama effect [4.11] is not important at pressures in the region of 1 torr.) Cylinder grade hydrogen was purified by admitting it to the system through a heated palladium thimble, which also served as a controlled leak to balance the egress of gas through the anode orifice. The extent of the purification by this method is not known, but it assumed that the impurity level was determined by the residual gas pressure to be 0.1 v.p.m.

4.3. The Ancillary Electronics.

The simple electronics system for tubes A and B has been described in section 4.2. The output from the photomultipliers (RCA type 931A, side window, S4 spectral response with the peak in the green at 5000 Å) was displayed directly on a Tektronix 545A oscilloscope, the signal voltage being developed across 10^4 ohms. The time-constant was 5×10^{-7} sec, and the oscilloscope and photomultiplier rise-times were 1.4×10^{-8} and 2.0×10^{-9} sec respectively, so that the overall bandwidth was well within the requirements of the experiment. The photomultiplier gain was typically 10^6, but was occasionally increased to 10^8. The oscilloscope was triggered by the displacement current generated when the potential was applied across the electrodes.

For tube C it was required to generate discrete single avalanches for conditions above breakdown, which necessitated the

application of a step voltage across the electrodes shortly before the release of a pulse of initiating electrons. Fig. 4.10 shows schematically the arrangements for measurements with the electron-multiplier; for the photomultiplier data, the oscilloscope was connected to the photomultipliers (not shown) instead of the electron-multiplier output.

The double-pulse generator (fig. 4.11) had three sections. The triggering stage generated a step waveform of amplitude 300 volts, rise-time 2.3×10^{-7} sec, which was amplified to 800 volts and sharpened to 4.0×10^{-8} sec rise-time by the pulse amplifier, and then divided and fed through delay cables to the trigger inputs of the high voltage double-pulse generator. The pulse repetition frequency was variable from single shot to 50 p.p.s. The double-pulse generator produced two almost simultaneous pulses for application to the drift space and to the pulsed ultra-violet light source (Appendix 4). The rise-time of the drift space pulse (fig. 4.12) needed to be very much shorter than the shortest electron transit time ($\sim$ 100 nsec), and the amplitude had to remain constant for at least the duration of the longest transit ($\sim$ 1 μsec). Charged transmission lines are the ideal source of such pulses and a certain amount of effort was directed to the development of a circuit using distributed lines in the form of coaxial cables. However, the considerable length of cable required (about 300 metres), the non-ideal behaviour of practical cables and the problems of high voltage operation frustrated this approach, and a simple, long time-constant RC network, discharging through an XH3-045 hydrogen thyratron,

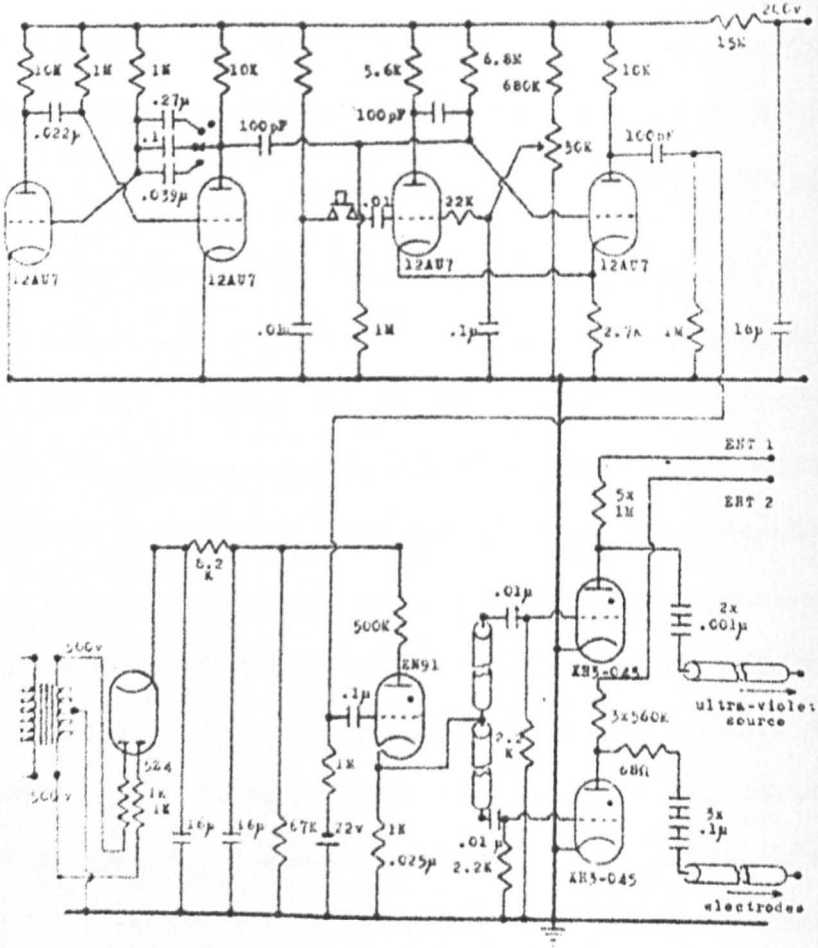

Fig. 4.11

The double pulse generator.

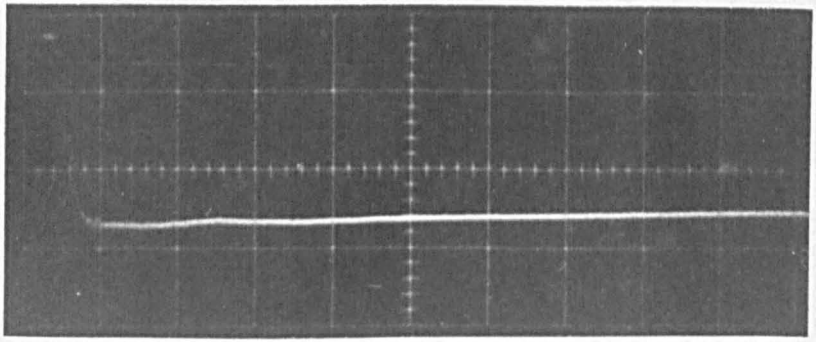

Fig. 4.12

The voltage pulse applied across the electrodes of tube C.

(100 nsec/division)

was eventually adopted. After testing a large number of different types of capacitor, it was found that the most satisfactory performance was obtained with inexpensive paper capacitors rather than with non-inductive types, and a rise-time of 20 nsec was achieved for amplitudes between 400 and 3000 volts. The optimum compromise between rise-time and over-shoot was obtained with a damping resistor of 68 ohms. The time-constant of 3.9×10^{-4} sec gave 0.2% fall in amplitude in 1 μsec. The inverted configuration generates negative pulses, and has the advantage of avoiding the problems associated with a floating heater transformer. The pulse to fire the ultra-violet light source discharged into a predominantly capacitative load, but it was found that the temporal requirements were not very stringent and could be satisfied by the same basic circuit used for the drift space pulse, with the addition of a matched termination at the input end of the cable to absorb reflections. The light source fired approximately 40 nsec after application of the voltage pulse, and was synchronised with the drift space pulse by the delay cables between the trigger pulse amplifier and the double pulse generator.

The output signal from the electron-multiplier (E.M.I. type 9603/B), which was operated at a gain of approximately 10^6, was developed across a resistance of 10^4 ohms and applied through a decoupling capacitor to the input of the 545A oscilloscope, enabling the arrival of single electrons to be detected. The rise-time of the detection circuit was 25 nsec, and the time-constant 60 nsec. The photomultiplier signal was similarly treated. The oscilloscope

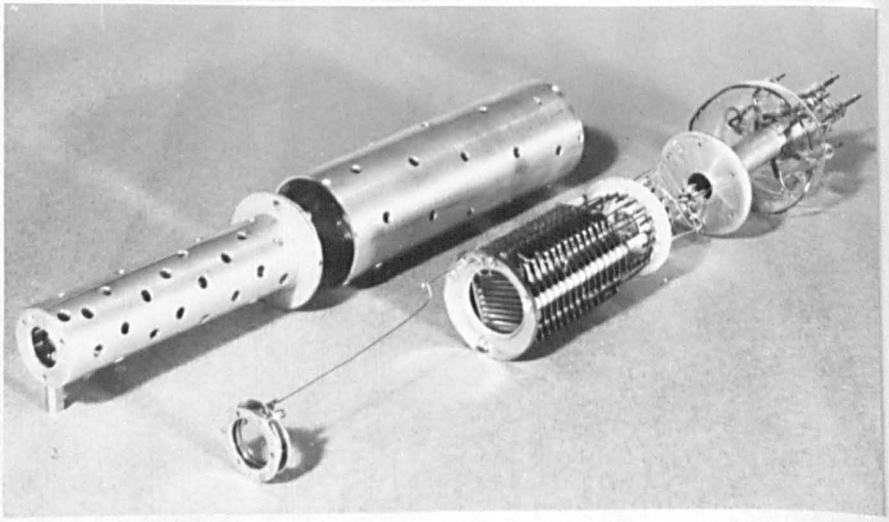

Fig. 4.13

The electron multiplier and its screening container.

was triggered externally by the signal from the photomultiplier that monitored the pulsed light source.

The elimination of pick-up by the electronmultiplier of the high voltage pulses caused considerable difficulty, and was accomplished by extensive and rather arbitrary earthing arrangements, and by enclosing the multiplier in a screening container within the vacuum system (fig. 4.13).

4.4. Experimental Procedure.

The methods used to introduce the gases into the experimental tubes have been described in section 4.2. For tubes A and B the gas was contained in a space which could be isolated from the pumps, so that the pressure was not subject to fluctuations and could be determined to within $\pm 2.5\%$ to $\pm 10\%$, depending on the pressure (section 4.2.3). The dynamic conditions of tube C made precise pressure measurements more difficult. The inflow of gas was regulated by variation of the potential across the heater of the palladium thimble until the required pressure was indicated by the L.K.B. Autovac Pirani gauge (which had previously been calibrated against the McLeod gauge, but was liable to drift). A McLeod reading was taken at the beginning and end of each pressure setting (typically separated by 10 minutes), and the mean of these two readings was taken as the pressure. The Pirani gauge was monitored during this period in case of excessive fluctuations.

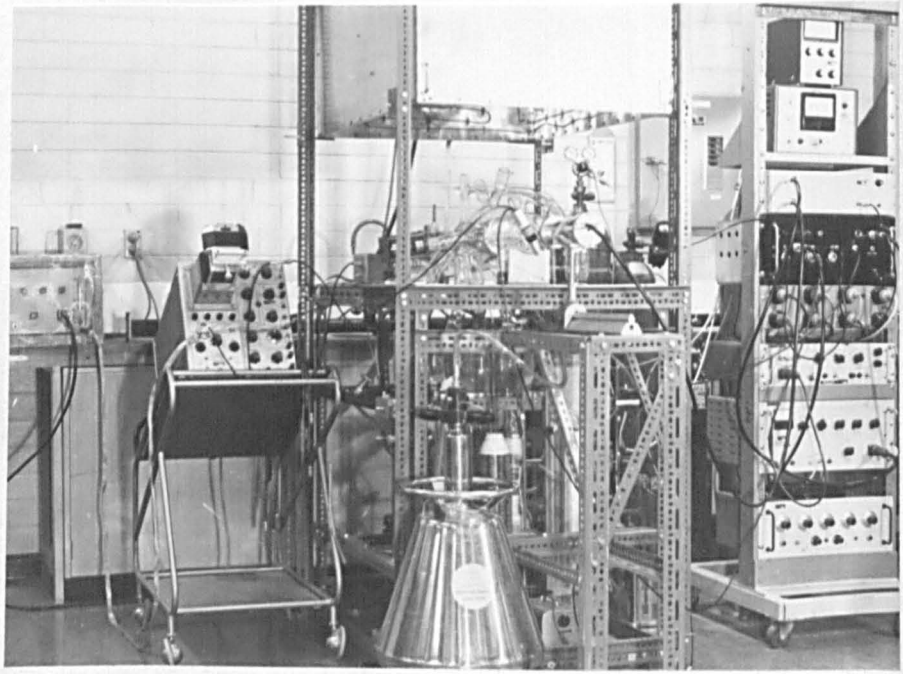

Fig. 4.14

The experimental apparatus.

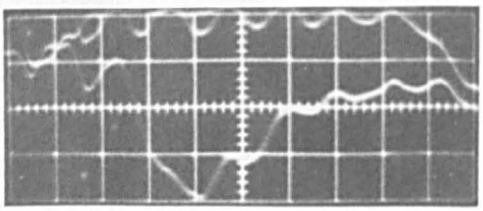

a. photomultiplier trace, cathode upper, anode lower. 40 nsec/div.

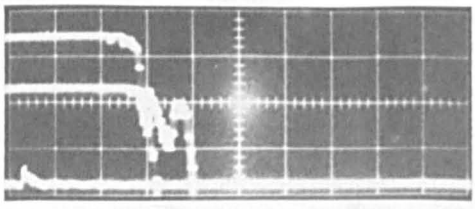

b. anomalous p.m. trace, cathode signal before anode. 400 nsec/div.

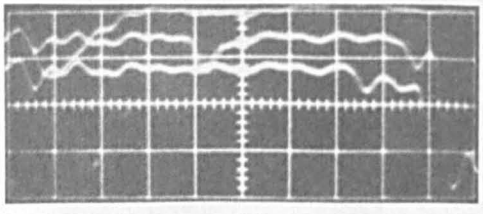

c. anomalous p.m. trace, early cathode signal. 40 nsec/div.

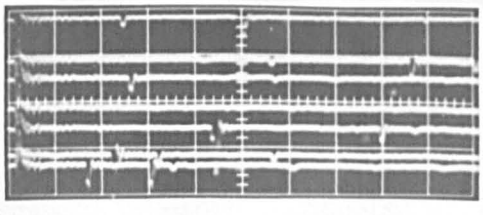

d. small hole electron-multiplier trace. 200 nsec/div.

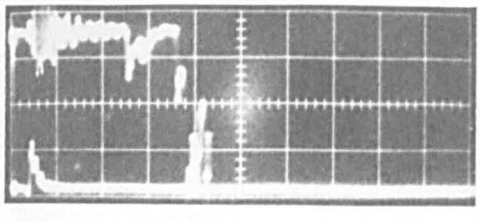

e. large hole electron-multiplier trace. 400 nsec/div.

Fig. 4.15

Typical experimental records.

The nonavailability of a suitable double-beam oscilloscope made it necessary to record consecutively the signals from the anode and cathode region photomultipliers, an unsatisfactory procedure because of the statistical variations between avalanches. Because of this, a temporal comparison between the anode and cathode signals was not attempted, and only the time between initiation and detection of an avalanche on a single trace was identified with an electron transit time. A typical pair of photomultiplier traces for tube C is shown in fig. 4.15a, with a monitor trace of the ultra-violet pulse added. The zero time-mark was derived from electrical pick-up from the ultra-violet spark, which was established to occur simultaneously with the light output. Anomalous photomultiplier records of the type shown in fig. 4.15b where the cathode signal precedes and greatly exceeds the anode signal, and fig. 4.15c where a very early signal is recorded, may be attributed to resonance radiation effects (section 5.5). Typical electron-multiplier traces are shown in figs. 4.15d and 4.15e. The individual electron signals in fig. 4.15d were obtained by sampling the avalanche through the small orifice, and it was found that very few electrons were detected that could be associated with the first avalanche. This was attributed to the unfavourable shape of the orifice, which was cylindrical with a depth/diameter ratio of about 7, and also to the build up of charge on a thick oxide layer, formed when the Kovar disc was sealed to the glass, which could not be cleaned from the walls of the orifice. The orifice was later enlarged by drilling, in situ, to a

diameter of 3.5×10^{-2} cm, increasing the sampling area by a factor of 50, removing the oxide layer, and reducing the depth/diameter ratio to 1. The signal (fig. 4.15e) increased very much more than would be expected from the geometrical effect alone, and permitted the electron transit time to be determined from about 10 pulses at a given value of E/p, compared with the 200 to 400 pulses with the small hole, greatly reducing the uncertainty in the value of the pressure by decreasing the period of time over which the readings were spread.

The voltage applied across the drift space was determined by setting the voltage applied to the anode of the thyratron by a calibration curve, relating this voltage to the mean pulse voltage during the first microsecond. This calibration curve was obtained by potential division of the pulse with a resistor chain (of suitable time-constant when associated with the input capacitance of the oscilloscope) and measurement of the pulse amplitude on the oscilloscope, the vertical deflection system of which was calibrated against a precision potentiometer. The horizontal time-base was calibrated against a Hewlett-Packard 5245 L crystal oscillator to within $\pm 0.5\%$ (limited by the width of the cathode ray trace). For the electron-multiplier measurements, the time between the arrival of the avalanche at the anode of the drift tube and the detection of a pulse at the anode of the multiplier was determined by firing the ultra-violet source at the anode orifice.

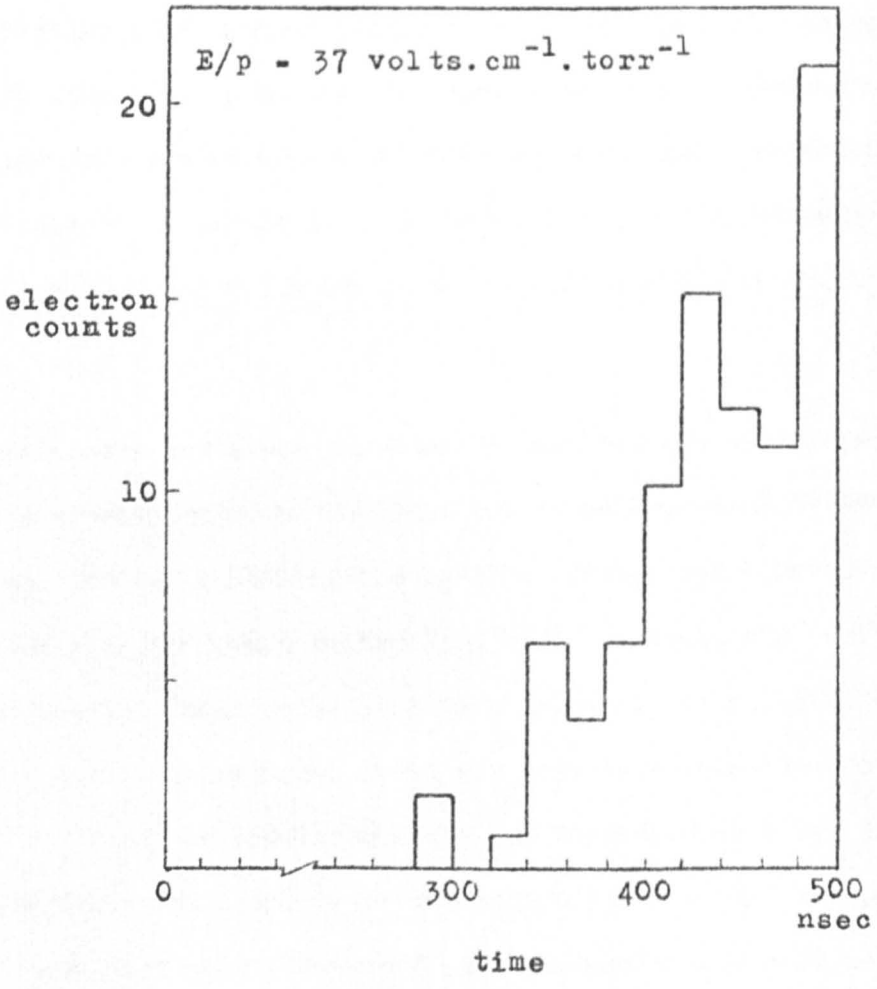

Fig. 4.16

Histogram of electron counts per 20 nsec channel against time.

It was not possible to determine directly the number of initiating electrons released by the ultra-violet pulse, and the procedure used was to attenuate the light pulse until the formative time lag of the discharge started to show statistical scatter, when it was assumed that about one photo-electron was being released. The attenuation was then reduced by a factor of 10 to release approximately 10 initiating electrons.

All the oscilloscope traces were recorded on high speed film (Kodak 2485, 16000 ASA). The signals obtained with the photo - multipliers, and with the electron-multiplier sampling through the large hole, had sufficient amplitude to permit direct determination of the electron transit times but, with the small hole, single electron pulses were counted into time channels to produce histograms of the type shown in fig. 4.16, from which it is seen that only 2 electrons from 300 shots could be associated with the first avalanche. To obtain a barely adequate sample of only 10 electrons at each of the E/p values would have required about 12,000 avalanches, which was not attempted with the manual data acquisition and handling techniques that were available. The electron energy measurements were obtained by interposing the analyser between the large hole and the electron-multiplier, and incrementing the potential on the retarding grid with each avalanche.

4.5. Assessment of Observational Errors for Tube C

The experimental variables which reflect directly on the relationship between v_- and E/p are the applied voltage V_a, the anode-cathode and the drift distances d (not necessarily having the same value), the pressure p, and the electron transit time t_-.

For V_a the droop of the "square" pulse during the electron transit time was very small, contributing a maximum error of $\pm$ 0.1%. All other errors in this parameter were estimated to be less than $\pm$1%.

The values of d were determined with negligible error by a cathetometer. The anode and cathode were parallel to within $\pm$0.25%, and field uniformity due to edge-effects was shown to be slight (fig. 4.6). The sampling orifice was small and is expected to contribute negligible field distortion. Thus the maximum error in E = V_a/d is estimated to be $\pm$1.5%.

McLeod gauge errors are systematic, occurring almost entirely during calibration of the gauge, and are estimated to be less than $\pm$1%. The principal errors in pressure measurement arise from fluctuations due to the dynamic pumping arrangements, and the greatest fluctuation observed was $\pm$3.5%.

The error in measuring t_- from the photographic records ranged between $\pm$1% and $\pm$5%, and the linearity and calibration of the oscilloscope time-base was better than $\pm$0.5%, to give a maximum estimated

error in t_- of $\pm 5.5\%$.

Thus the maximum errors in the two basic parameters are estimated to be -

$$v_- = d/t_- \rightarrow \pm 5.5\% \quad ; \quad E/p \rightarrow \pm 6.0\%.$$

The errors for the photomultiplier data are not assessed, since it will be shown in Chapter 5 that reliable v_- values could not be derived from these results.

CHAPTER 5

A DISCUSSION OF THE RESULTS

Part 1

5.1. Preliminary Photomultiplier Measurements in Helium

Part 2

5.2. An Appraisal of Schlumbohm's and Dawson's Experiments.

5.3. Introduction to the Work in Hydrogen.

Part 3

5.4. The Data in Relation to Models for Possible Unconventional Behaviour

- 5.4.1. Fundamental Processes
- 5.4.2. The Effects of Non-Ideal Experimental Conditions

5.5. Sources of Spurious Signals

Part 4

5.6. Interpretation of the Final Electron Drift Velocity Values, Obtained by the Electron Multiplier Technique.

- 5.6.1. Large Hole Data
- 5.6.2. Small Hole Data
- 5.6.3. The Entire Electron Multiplier Data

5.7. Electron Energy Measurements

5.8. Conclusions and Suggestions for Further Work.

This chapter is subdivided into four parts to assist in the identification of the discussion with either the photomultiplier or the electron-multiplier data, or with a combination of both. Each part is labelled appropriately, and is introduced by a very brief abstract of the contents.

PART 1

Photomultiplier Data

Crude measurements in helium yielded transit times which, in one case, can be identified with positive ion crossing times. In other cases, evidence for the predominant secondary process is adduced.

5.1. Preliminary Photomultiplier Measurements in Helium.

A preliminary investigation of current transients in helium was performed with two experimental tubes, A and B, to evaluate the possibility of determining electron drift velocities by monitoring with photomultipliers the light emitted from a Townsend discharge. The experimental tubes and the technique are described in section 4.2. The time intervals between peaks, either on the same trace or on a pair of anode and cathode traces, were measured, and "drift velocities" were calculated using a knowledge of the electrode separation and the positions of the photomultiplier slits.

Tube A. The results from tube A showed that two distinct groups of velocities emerged, one in the region of 10^5cm.sec^{-1} and one in the region of 10^3cm.sec^{-1}. The latter group corresponds to transit times which exceed the time taken to reach breakdown, and therefore is influenced by the collapse of the applied potential and by space charge distortion, and will not be considered. These velocities probably correspond to the propagation of space charge disturbances across the gap, though they are also consistent with the time taken

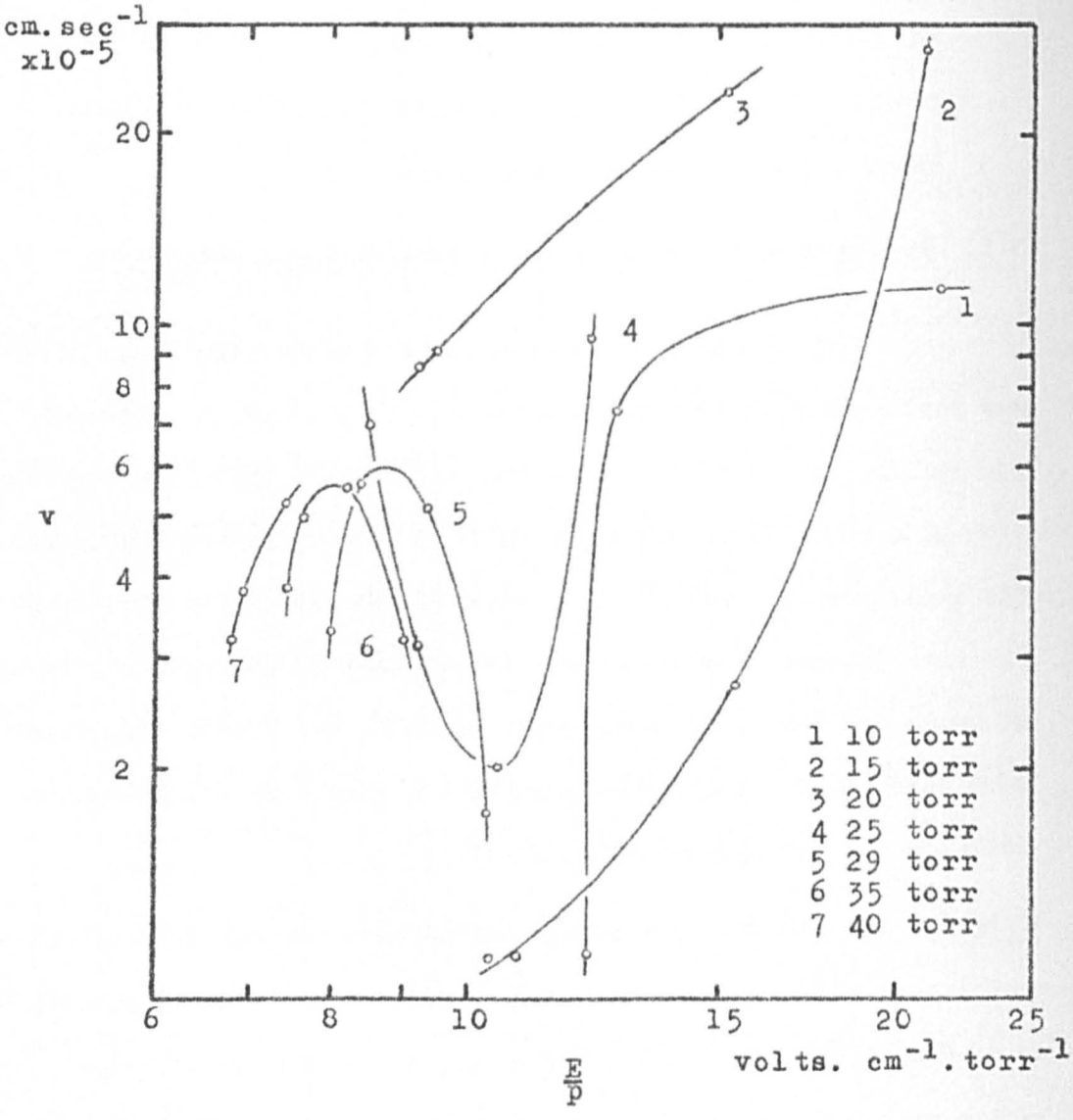

Fig. 5.1

Tube A (Helium) : log(v) - log(E/p) at constant p.

for metastable atoms to diffuse from the anode to the cathode.

The 10^5 cm.sec^{-1} group of velocities clearly cannot be associated with electron transits, and may be attributed to the initiation at the cathode of secondary avalanches by delayed photons, positive ions or diffusing metastables. This group was inspected in three ways:

1. A dependence of v on p was sought, but was not found. Both metastable and delayed photon effects are expected to show a pressure dependence.

2. log(v) was plotted against log(E/p) for fixed p (fig.5.1), to search for a power relationship. It is not considered that any valid inferences can be made from these curves because of the large range of discharge currents and conditions over which the points were taken, nor is there any indication of a change in the predominant secondary process from positive ion action at the cathode for p < 19 torr (curves 1 and 2), to photon release by volume destruction of metastable atoms

$$He_m^{2^1S} + He \rightarrow 2\ He + photon \quad \text{for } p > 19 \text{ torr (curves 3 to 7)},$$

as reported by Davies, Llewellyn Jones and Morgan (1963)[1.12]. The exact pressure at which this transition will occur depends on the electrode geometry, since both metastable diffusion and photon effects are field independent. An apparent "drift velocity" can be estimated for the metastable process by making the reasonable assumption of thermal equilibrium between the metastable and the

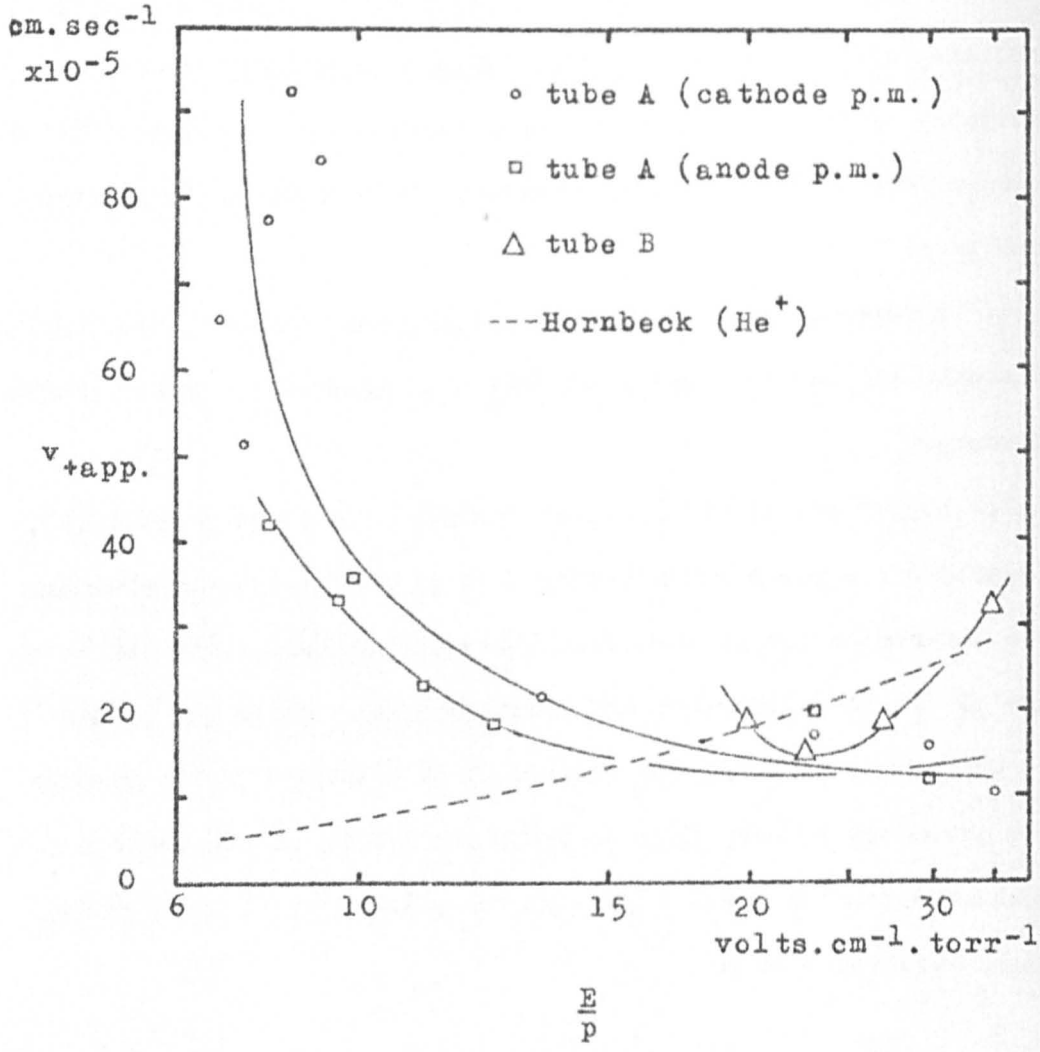

Fig. 5.2

Tubes A and B (Helium) : $\log(v_{+app}) - \log(E/p)$ with Hornbeck's values for v_+.

neutral gas atoms and taking the cross-section for the process $\sigma = 3 \times 10^{-20} cm^2$ given in (1.12) to calculate the metastable lifetime, and is found to be $1.3 \times 10^4 cm.sec^{-1}$ for tube A and $1.1 \times 10^4 cm.sec^{-1}$ for tube B, interposed between the two observed velocity groups.

3. Only the v values derived from the first peak on the cathode and anode traces were used to plot (v) against log(E/p) in fig.5.2.

Tube B. Tube B produced similar results, except that another group of velocities emerged in the $10^4 cm.sec^{-1}$ region. This group is plotted as v against p for approximately constant E/p in fig.5.3, and shows evidence of a change of process between 17 and 20 torr, in accordance with the findings of (1.12), whose conclusions are further supported by the absence of any values in the $10^5 cm.sec^{-1}$ group above a pressure of 19 torr (indicating that positive ion secondary action was not predominant for p > 19 torr). The D/d ratio for tube B is greater than for tube A, and the loss of metastables from the gap would be less severe, so it is more likely that this process would have been observed with tube B. But, the metastable photon process would exhibit a v α p dependence , and the positive ion process would be independent of p at fixed E/p, whereas fig.5.3 shows the opposite to be the case in this experiment and also that the observed v values are too low to be associated with positive ions. It is probable that the inflection in fig. 5.3 is due to some process that reflects the change of secondary agency, rather than a direct observation of the agency.

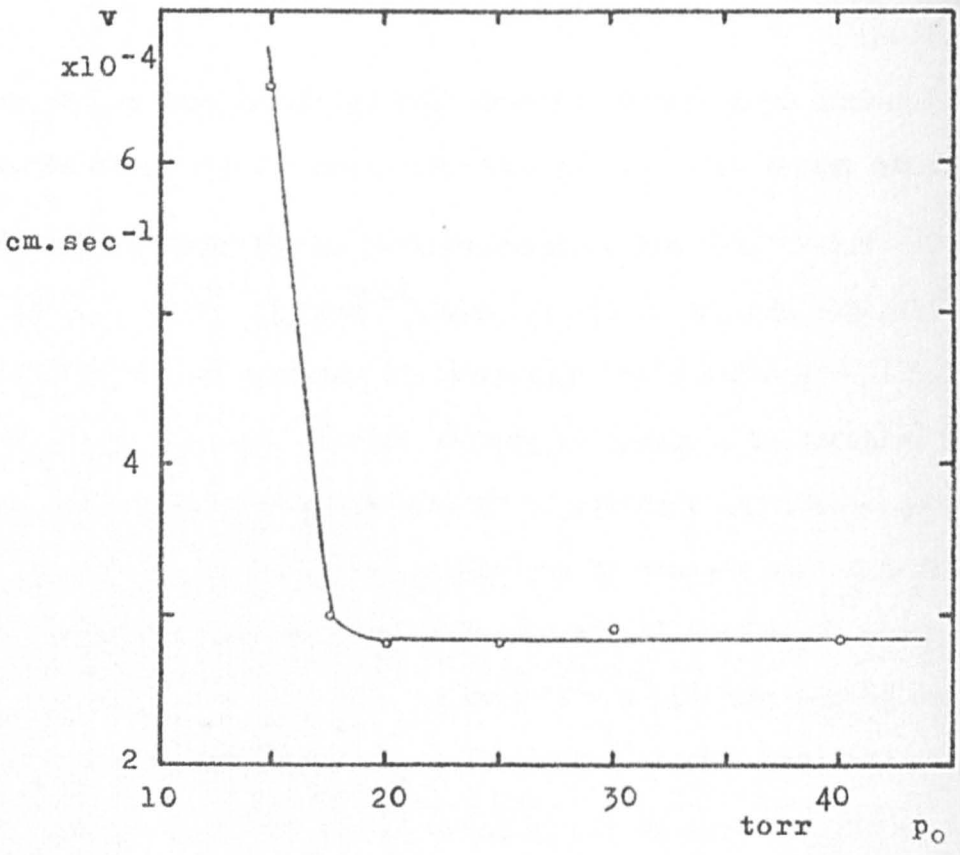

Fig. 5.3

Tube B (Helium) : (v) - (p_o) at constant E/p.

The $10^5 cm.sec^{-1}$ group of velocity values is shown for tubes A and B in fig. 5.2, together with Hornbeck's (1950)[5.1] values for He^+ drift velocities, in a $\log(v_+)$ - log (E/p) plot. The range within which these velocities fall makes it reasonable to identify them tentatively as positive ion drift velocities, though at the lower E/p values they are very much too high and v_+ decreases with increasing E/p instead of increasing (c.f. fig. 5.4 and section 5.4.3). There is very rough agreement with the values of (5.1) above E/p = 20 volts.cm^{-1}.$torr^{-1}$ for tube A, whilst tube B shows fair agreement over the entire range of E/p = 30 to 60.

The abnormally high values at lower E/p cannot be explained by invoking other secondary processes. The time scale is too long for direct photon action, and delayed photon effects have not been reported in the formative time lag studies of (1.12) and Evans (1967)[5.2]; the process is too fast for diffusion of metastables to the cathode, and also for the reported metastable/photon effect (1.12). Space charge distortion of the applied field is likely to be a contributory factor, but it is probable that the "velocities" are associated with resonant scatter of photons directly into the photomultipliers (section 5.4.3), and are only loosely related to the motion of positive ions in the gap.

This part of the investigation was conducted to establish the feasibility of determining electron drift velocities by a photomultiplier technique, and the "positive ion drift velocities"

obtained were entirely incidental. Conditions were not set to favour such measurements, nor was great care exercised in taking the readings, so it is not intended that the data presented should be considered reliable. All attempts to observe the first electron avalanche were unsuccessful, almost certainly because insufficient attention was paid to protecting the photomultipliers from electrical pickup and background light, so that their effective sensitivity was greatly reduced. The photomultiplier technique was relegated to the role of supporting the electron multiplier technique in the work that follows, partly because of the above problems, but principally because of the remoteness of the effect observed from the effect to be measured, involving firstly the collision of an electron with a neutral atom to produce an excited state, followed by relaxation of the excited state after a time $\sim 10^{-8}$ sec with emission of a photon, which is then detected virtually instantaneously by the photomultiplier. If the excited state is metastable, or if photon trapping can occur, the delay can be very much longer. Unless corrections are applied, a lower limit is put on the electron transit times that can be observed without serious error, and it is interesting to note that apparently no allowance has been made for this in photomultiplier investigations of streamer processes (e.g. Amin (1954)[5.3], Hudson and Loeb (1961)[5.4], Dawson (1965)[5.5]).

PART 2

Photomultiplier and Electron-Multiplier Data

To provide a basis for a comparison of the results obtained in this investigation, the experiments of Dawson and Schlumbohm are first assessed in detail. All the drift velocity data for hydrogen is then introduced, and the general features are discussed.

5.2. An Appraisal of Schlumbohm's and Dawson's Experiments.

Schlumbohm's Experiment.

A description of this method of determining electron drift velocities is given in section 3.5.3. To briefly summarise, a short pulse of 10^4 to 10^5 photo-electrons was released from the cathode, and the time taken to drift to the anode was determined by displaying the current on a fast oscilloscope. The anode-cathode separation d was variable up to a maximum of 4.7cm, and the diameter of the electrodes was 21cm, so the D/d ratio was greater than 4 and field uniformity would have been moderately good. Also, for single avalanches initiated on the axis and having short transit times, so that lateral diffusion broadening is slight, field uniformity is not of great importance. Pressures were in the range 0.01 to 5.0 torr, and gas purity was 100 v.p.m. All measurements were made with an applied voltage less than the sparking potential, which simplified the experimental technique but restricted the available range of exp(ad) to low values of less than 10. This investigation showed

E/p	α/p	(pxd)	V_a	v'_-	v_-	v'_-/v_-
$v.cm^{-1}.torr^{-1}$	$cm^{-1}.torr^{-1}$	torr. cm.	volts.	$cm.sec^{-1}$ $x10^{-8}$	$x10^{-7}$	-
50	0.32	5.03	252	4.7	1.25	37.6
70	0.71	2.27	159	4.1	3.50	11.7
100	1.29	1.25	125	3.3	5.05	6.5
200	2.36	0.68	136	3.5	8.40	4.2
400	2.56	0.63	252	4.7	13.00	3.6
1000	1.40	1.15	1150	10.0	19.50	5.1

Table 5.1

Inferred values of experimental parameters for Schlumbohm's determination of v_- in Hydrogen (v'_- is the maximum possible velocity).

that for oxygen and nitrogen, in the range E/p = 100 to 400 volts. $cm^{-1}.torr^{-1}$, $v_- \propto (E/p)^{\frac{1}{2}}$ in accordance with the predictions of existing theory (section 2.2), but that for hydrogen

$$v_- \propto (E/p)^{\nu(E/p)}$$

where inspection of fig. 3.14 shows that the function $\nu(E/p)$ has the values 1.6 for E/p = 20 to 60 volts.$cm^{-1}.torr^{-1}$ and 0.5 for E/p = 320 to 2000, with a transition region between; extrapolation of the linear portions yields a transition point at E/p ≈ 97 (reduced to $0^{\circ}C$).

The individual values of the experimental variables p, V_a, d, exp(αd) at each value of E/p were not indicated, but it is inferred that they were set to keep exp(αd) approximately constant, between 1 and 10, so that between 10^5 and 10^6 electrons would have arrived at the anode in an interval of 50 nsec, and the maximum instantaneous current would have been 10^{-6} amps, under which conditions space charge distortion of the applied field would have started to become important (sections 1.6 and 5.4.2). To maintain the low level of gas amplification, the pressure must have been varied between 5 torr at E/p = 40 to only 0.01 torr at E/p = 2000, and d may also have been reduced below the maximum of 4.7 cm to assist in the attainment of small (pxd) products. For example, at E/p = 500 volts. $cm^{-1}.torr^{-1}$, for exp(αd) = 10, the product (pxd) is 0.9, requiring p ∿ 0.2 for d = 5 cm. Table 5.1 gives values of (pxd) which have been calculated on the assumptions mentioned, and these values are

substantially lower, by a factor that ranges between 3 and 30, than the values in the present investigation, which were selected as the minimum permissible if the in itial energy distribution of the photo-electrons is to have an insignificant effect on the measured drift velocity (sections 2.5 and 5.4.2). Thus there is reason to suspect that Schlumbohm's values may be subject to distortion by initial non-equilibrium. Furthermore, at the quoted minimum pressure of 0.01 torr, the electron mean free path is about 30 cm (using the maximum σ for ionisation = 0.95×10^{-16} cm^2 at 65eV, from Englander-Golden and Rapp (1964)[2.8]), in which case the majority of the photo-electrons would reach the anode without suffering any collisions, and the "drift velocity" would depend only on V_a, according to equation (A5.2) (provided the initial photo-electron energy $eV_{pe} << eV_a$). In the extreme case of E/p = 2000 volts.cm^{-1}.$torr^{-1}$, v'_- under freely accelerating conditions is calculated by inference to be 1.3×10^9 cm.sec^{-1}, compared with the measured value of 2.3×10^8. Table 5.1 shows calculated values v'_- for collisionless conditions to be greater than the measured values by a factor of between 3 and 40. It is improbable that equilibrium was achieved for the smaller factors - if it is assumed that all the momentum in the field direction is lost on collision, the factor of 3 implies only 9 collisions, the factor of 4 only 16.

It would appear that Schlumbohm did not appreciate that "runaway" conditions might appear as E/p was increased, nor that it

was necessary to ensure that the avalanche comes rapidly to equilibrium at all values of E/p. It is not stated whether the value of v_- at a particular value of E/p was derived from measurements with a fixed set of values for p, d and V_a, or whether these parameters were varied to investigate possible dependences, but it would appear that the former was the case. (An investigation by the author of the relationship between the measured values of v_- and inferred values of V_a has not yielded a dependence). For the reasons stated, and because these omissions do not permit a more thorough evaluation of the data, the experimental values obtained in this investigation, though not discredited, must be treated with caution.

Dawson's Experiment.

This is described in some detail in section 3.6. The important points are that the pressures were moderately high, in the range 26 to 66 torr, to give (pxd) products that were adequately large (9 to 23 torr.cm) to ensure negligible effects from initial non-equilibrium although d was only equal to 0.35 cm, and that the sensitivity of the detector was only sufficient to detect an avalanche containing a minimum of 10^8 electrons. Field uniformity was poor since the D/d ratio was ≈ 2, and the initiating photoelectron (a single electron was assumed) was released from any point on the cathode; however, the scatter that might be expected between the transit times of avalanches originating at the centre and on the edge of the cathode, was not reported, so this may not have been a serious problem.

Discrimination between the primary and secondary avalanches was not possible, and the small physical dimensions of the drift space resulted in electron transit times in the 3 to 100 nsec region, and necessitated the use of the fast, low sensitivity detector.

The values of v_- that were obtained were described as "apparent" and no claim was made for their authenticity, so they will not be used for comparison with the data of the present investigation, nor will they be examined in detail. These values are reproduced in fig. 3.19, where the extrapolated drift velocity lies close to Schlumbohm's curve for $E/p < 100$ volts.cm^{-1}.torr^{-1}, but is about 10% lower for $E/p = 100$ to 300. The low experimental values were explained qualitatively in terms of space charge retardation of the avalanche, but the enhanced values could not be accounted for, although the contribution of secondary avalanches to the growth of the discharge current was investigated as a possible mechanism. Inspection of fig. 3.19 shows a rapid enhancement of v_- above $E/p = 100$ volts.cm^{-1}.torr^{-1}, which suggests possible avalanche "runaway" (discussed further in section 5.4.1), and also that the shape of the family of curves appears to be parabolic (see section 5.6).

5.3. Introduction to the Work in Hydrogen.

It has been described in Chapter 4 how time of flight measurements were made in molecular hydrogen using two different techniques for detection of the avalanche. The electron multiplier

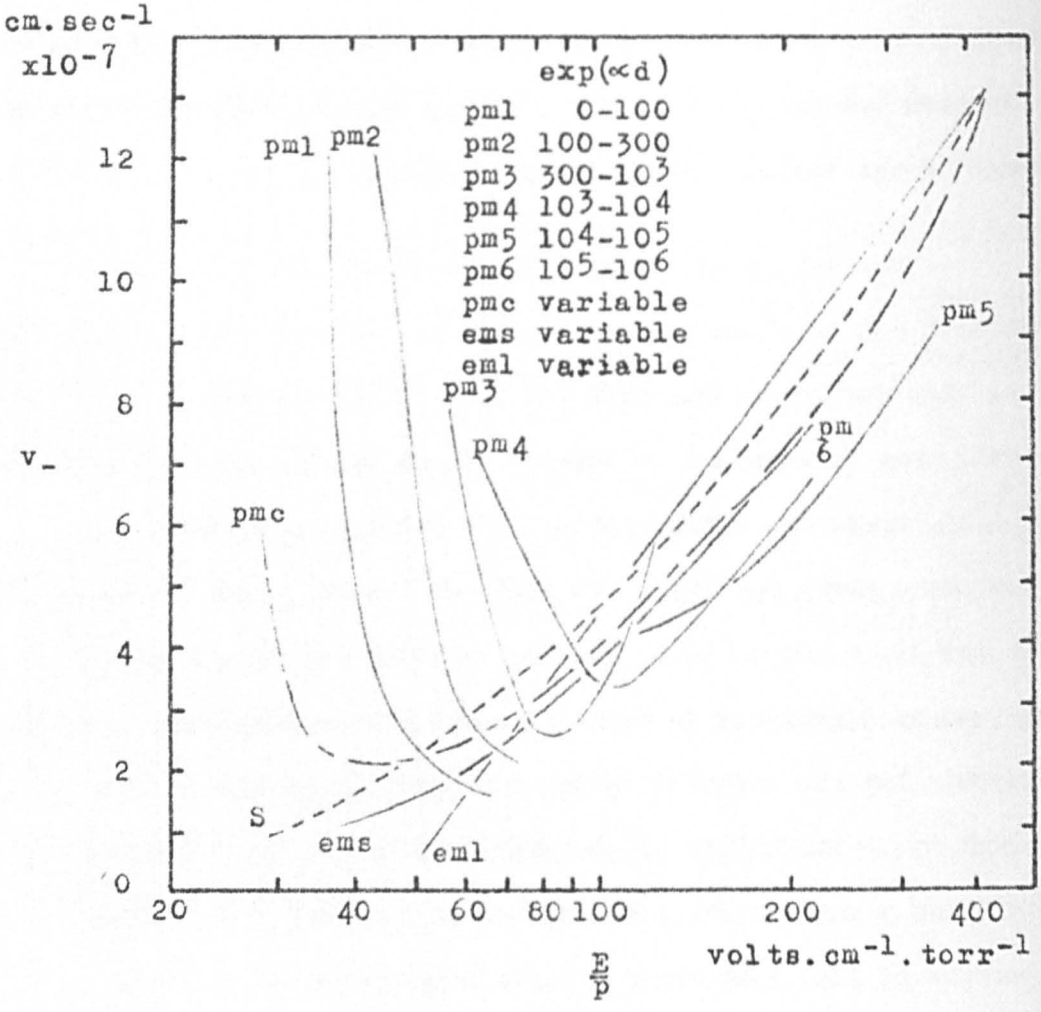

Fig. 5.4

Tube C (Hydrogen) : (v_-) - log(E/p) for the electron-multiplier data (ems and eml, small and large holes) and the photomultiplier data (pm1-pm6 and pmc, end and centre released), with Schlumbohm's results (S) for comparison.

method was intended to constitute the principal approach, and it was hoped that the ancillary photomultiplier measurements would support the data obtained by the former technique, in spite of the shortcomings of the latter delineated in section 5.1. Some of the results were obtained with initiating electrons released at the cathode, others at the tip of the central needle, and these are referred to as "end-released" and "centre-released" respectively.

Fig. 5.4 shows a plot of (v_-) against log(E/p) for the following cases (the terms pml, pm6, etc., are explained in the figure)

1. Photo-multiplier data (end-released) for a range of fixed exp(αd) in curves pml to pm6.
2. Photo-multiplier data (centre-released) with variable exp(αd) in curve pmc.
3. Electron-multiplier data (centre-released) with variable exp(αd) for the small and the large sampling holes in curves ems and eml.
4. The data presented by Schlumbohm[3.46], which consists of his own points above E/p = 40 volts.cm^{-1}.torr^{-1}, and points due to Jager and Otto [3.24] at E/p less than 40.

For clarity, only the curves are presented, but the same curves, together with the points from which they are derived are plotted in figs. 5.5 and 5.11.

A very important feature of fig. 5.4 is that there is a considerable discrepancy between the values obtained by the two

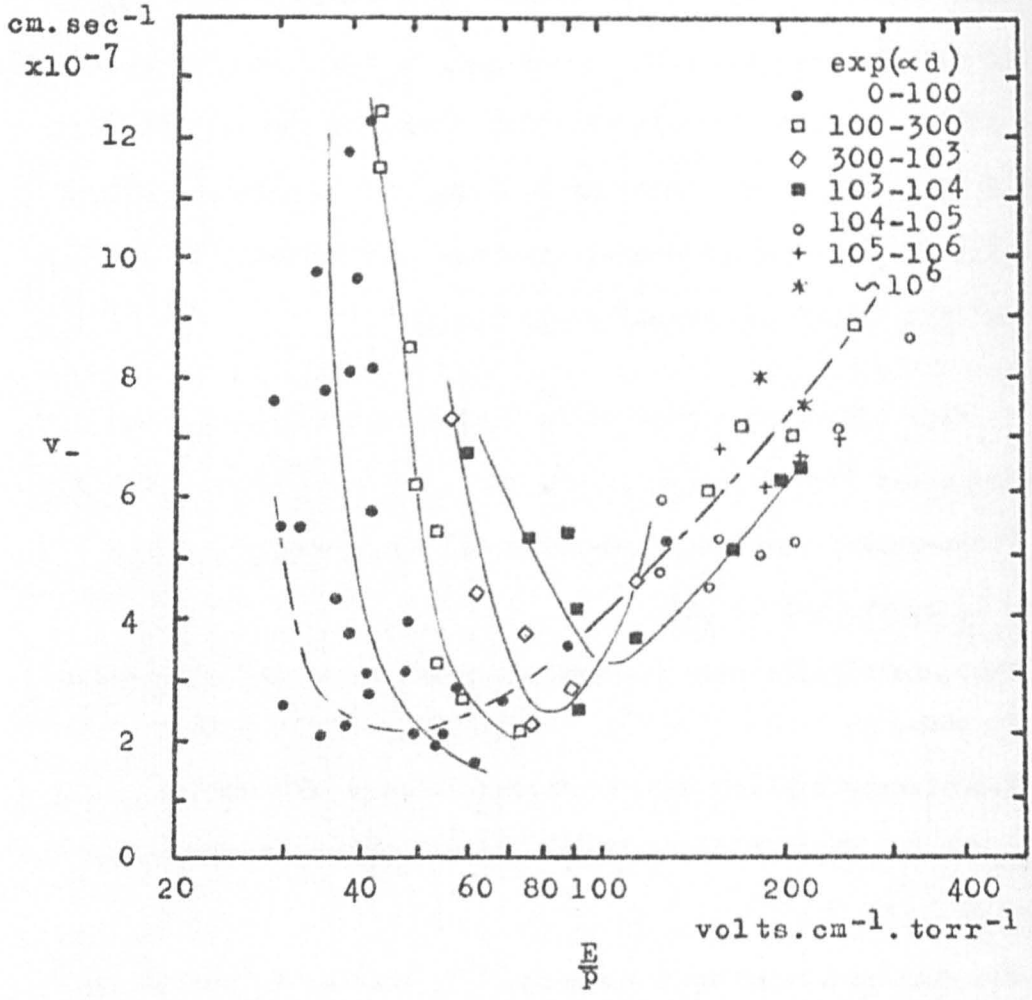

Fig. 5.5

Tube C (Hydrogen) : (v_-) - log(E/p) at constant exp(∝d) for the photomultiplier data.

techniques, particularly at E/p < 70 volts.cm^{-1}.torr^{-1}. It is possible to attribute this deviation from the anticipated behaviour to two types of effect, namely -

1. Failure of the conventional model under the conditions of this experiment so that v_- does not depend on E/p alone, but also on other parameters in such a way that the two sets of data are compatible. Such a failure could be due either to inexpertise in the arrangement of the experimental conditions to satisfy the conditions of the model, or to a fundamental breakdown of the model.

2. Detection of spurious signals by one or possibly both of the techniques, the variation of these signals with time not reflecting the true motion of electrons in the drift space.

Because of the uncertain reliability of the only values of v_- in hydrogen at higher E/p known to the author, due to Schlumbohm [3.46] and to Dawson [3.58], the present data is first allowed to stand on its own merits and is subjected to a search for a number of features which fall into the two previously mentioned categories. In particular, it was suspected that avalanche "runaway" might be occurring, a situation in which the velocity of the electrons never reaches equilibrium, but continues to increase until the anode is reached, and this is discussed in section 5.4.1. Although the models assumed for investigation of the various possible processes are superficial, evidence is found that the scattering of resonance-radiation into the photo-multipliers was an important source of spurious signals, and that none of the models proposed for "unconven-

-tional" processes, namely photo-ionisation, resonant scatter of electrons, and runaway can be supported. On this basis, the photo-multiplier data is discounted as unreliable, and a comparison of the electron-multiplier data only is made with the v_- values of (3.46).

A number of the graphs that follow plot two variables whilst keeping a third constant (for instance, fig. 5.4 shows (v_-) plotted against log(E/p) for several values of constant p). The available experimental data is insufficient for it to be possible to keep any variable precisely constant for such a plot, and in these cases the "constant" parameter has a value within certain limits, and a family of curves for constant values of a parameter is in fact a family of contiguous channels.

PART 3

Photomultiplier and Electron Multiplier Data

All the hydrogen drift velocity data is inspected for a number of possible "unconventional" processes, so that the discrepancies between the photomultiplier and electronmultiplier results may be explained or reconciled.

5.4. The Data in Relation to Models for Possible Unconventional Behaviour.

5.4.1. Fundamental Processes.

Photo-ionisation.

If, by the process of ionising collisions between electrons and hydrogen molecules, and subsequent recombination of an ion and a free electron, the avalanche produces continuum radiation of frequency $\nu > eV_i/h$ (where V_i is the ionisation potential, equal to 15.6 eV for molecular hydrogen), photo-ionisation can occur in the gas by absorption of this radiation. Further, if there is an impurity content having a higher ionisation potential than hydrogen, such as helium (V_i = 24.5 volts), impurity atoms may be collisionally excited to produce intense ionising radiation from persistent lines of frequency $\nu > eV_i/h$; the impurity level of the gas in this investigation (0.01 v.p.m. - section 4.2) is believed to be too small for this latter process to be important. The process of self-ionisation is potentially an important secondary process, especially since its speed is limited

only by the time for a recombination reaction to occur plus the negligibly short transit time of the photons. It is faster than photon secondary processes at the cathode, which are limited by electron transit times, because of its ability to act ahead of the avalanche. In the present investigation it is possible that spurious avalanches, initiated ahead of the original avalanche by photo-ionisation, might be detected to cause abnormally high electron drift velocities to be recorded by both the photomultiplier and electron multiplier techniques. The amplitude of the spurious avalanche would depend both on σ, the appropriate absorption cross-section, and on δ/α , the number of ionising photons produced per ionising collision. If δ/α is less than unity, there is no possibility of producing spurious avalanches with an amplitude comparable with that of the primary avalanche. σ must be large enough for appreciable absorption to occur in the available gas volume, but not so large that the ionising radiation is absorbed within a very small fraction of the drift space, or the spurious avalanche will not be discrete from the primary avalanche. Also, except under very favourable conditions, the spurious avalanche would not be discrete, but would be an exponentially increasing (with time) electron flux. Thus, to summarise, the conditions for anomalous v_- values due to photo-ionisation are

1. photons with $\nu > eV_i/h$,
2. $\delta/\alpha > 1$,
3. $\beta \sim (pd/760)^{-1}$, where β is the absorption coefficient at N.T.P. ($\beta = \sigma N$, where N is Loschmidt's number).

The production of recombination photons in a discharge in a pure gas is a well established process, so condition (1) is satisfied. Qualitatively, it is expected that some recombination will occur between quasi-stationary hydrogen ions, produced by the leading edge of the avalanche, and electrons in the tail of the avalanche, but only if the avalanche is dispersed spatially along the field direction by diffusion or by a broad pulse of initiating photo-electrons. At high E/p, even if dispersion is present, the effects of the applied field and the high energies of the incident electrons make recombination unlikely. There is, therefore, a finite possibility that ionising photons will be produced, but it is not expected that δ/α will be large. Przybylski (1962)[5.6] has measured δ/α for ionising photons (as well as absorption coefficients) in oxygen, nitrogen and air, and gives values for $\delta/\alpha \sim 10^{-3}$, virtually independent of E/p for oxygen, but not for nitrogen and for air. Geballe (1944)[5.7] obtained the value $\delta/\alpha \simeq 1$ in hydrogen for E/p = 100 to 150 volts.cm^{-1}.torr^{-1}, for photons with sufficient energy to release electrons from a brass surface (work function $\sim$ 3-4 eV). Legler (1963)[5.8] showed that δ/α (for visible photons) $\simeq 2$ for hydrogen at E/p = 50, p = 10 torr. Although the hydrogen line spectrum is predominantly in the ultra-violet, there is no justification for extrapolating the δ/α values from (5.7) and (5.8) to the recombination continuum, and it will be assumed that in this region the values from (5.6) of $\delta/\alpha \sim 10^{-3}$ also apply to hydrogen. Thus condition (2) that $\delta/\alpha > 1$ appears not to be satisfied.

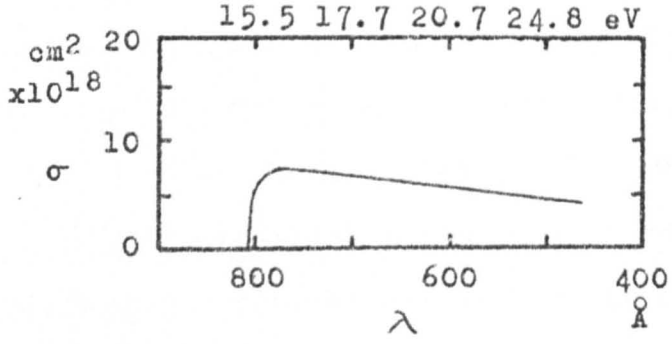

Fig. 5.6

Photo-absorption cross-section of H_2 (McDaniel).

Values of β and σ for condition (3) are taken from Bhalla, Craggs and Meek (1961)[5.9], Raju, Harrison and Meek (1965)[5.10], and from McDaniel's collation of σ values due to Po Lee and Weissler (1952), Wainfan, Walker and Weissler (1955), Bunch et al (1958), and Schonheit (1960)[5.11]. Bhalla et al measured absorption by a gaseous target of photons produced by a discharge in the same gas, in a number of gases including hydrogen, for which a β value $\simeq 200\ cm^{-1}$ was obtained, referred to a platinum plated detector (work function $\simeq$ 4-6 eV). Po Lee and Weissler used an external radiation source and an ultra-violet spectrophotometer to obtain absorption cross-sections (fig. 5.6), principally for photons of $\nu > eV_i/h$, in the region of $7 \times 10^{-18} cm^2$ ($\beta = 190\ cm^{-1}$), which were in general agreement with the later work of (5.9). Raju et al, using a self-maintained discharge as a source, obtained β values ranging from 1.5 cm^{-1} at $E/p = 40$ volts.cm^{-1}.$torr^{-1}$ to $76 cm^{-1}$ at $E/p = 120$. At a pressure typically used in this experiment, 1 torr, $(pd/760)^{-1} = 65\ cm^{-1}$, which is close to the β value at higher E/p from (5.10) and is comparable with the values from the earlier work, so condition (3) is satisfied. 50% absorption would occur in a distance of 6.9 cm for these typical values.

It is concluded that this mechanism could not be a source of spurious avalanches of detectable magnitude because of the small value of δ/α, although the value of σ is favourable for "leapfrogging" of the electron swarm. If the mechanism was important, the observed

drift velocities would be expected to depend both on E/p, because of the dependence of δ/α and of the true drift velocity on E/p, and on 1/p, in the limited pressure range which satisfies condition (3), since a decrease in pressure would permit the absorbed radiation to produce ionisation further ahead of the avalanche. At fixed E/p, a dependence on 1/p only is expected. In a graph which is not reproduced here, v_- has been plotted against 1/p for approximately fixed E/p for all the data, and no clear dependence was apparent. For E/p < 70 volts.cm^{-1}. torr^{-1} there was an indication of a negative linear dependence of the form

$$v_- \propto -\frac{1}{p} \quad \text{for } p = 0.25 \text{ to } 1.25 \text{ torr},$$

but for E/p > 70 no dependence could be found. The general trend of the points for all E/p showed a minimum v_- of between 2×10^7 and 5×10^7 cm.sec^{-1} at a pressure of approximately 0.9 torr (at 0°C). These features are not consistent with the semi-quantitative predictions which have been formulated for a photo-ionisation mechanism.

Resonance Scatter Electrons.

If the interaction time in an electron-molecule collision is not negligible compared with the time between collisions, the electron drift velocity will be pressure dependent. Rotational resonance is described by Kouri (1966)[5.12] and two other types of resonance scatter, namely core-excited resonance and single-particle resonance, are described by Taylor, Nazaroff and Golebiewski (1966)[5.13] and Eliezer,

Taylor and Williams (1967)[5.14]. Core-excited resonance involves the collisional raising to an excited state of a bound electron by an incident electron, which then temporarily attaches to the slightly positively charged nucleus and inner shells until auto-ionisation occurs. Golden and Bandel (1965)[5.15] have observed resonances in hydrogen in the 10 to 13 eV region, and the dissociative attachment reaction described by Rapp, Sharp and Briglia (1965)[5.16]

$$H_2 + e \rightarrow (H_2^{-*}) \rightarrow H + H$$

has a broad peak between 8 and 12 eV, and another peak at 14.2 eV. Single particle resonance involves the temporary trapping of an electron by polarisation attraction, and has been observed in hydrogen by Schulz and Asundi (1965)[5.17]. Frommhold (1968)[5.18] invoked single-particle and rotational resonances to explain a linear pressure dependence of v_- in H_2 at low E/p (0.03 to 4.0 volts. $cm^{-1}.torr^{-1}$) and high pressures (500 to 30,000 torr), and this is discussed further by Kouri, Sams and Frommhold (1969)[5.19], where it is deduced that the electron trapping time is less than $4x10^{-9}$ sec.

In the present investigation the mechanism of resonance scatter is not considered to be important, since there is no evidence of a linear pressure dependence. The probability of attachment is less at moderate and high E/p than at very low E/p, and also the high pressures that enabled the effect to be observed in Frommhold's experiment imply that the cross-section is very small.

Avalanche "Runaway".

Conventionally, electron drift velocities are expected to be stationary functions of time, provided the parameters defining the experimental conditions are also stationary when viewed from the frame of reference of the electron. Further, considerations of the type outlined in Chapter 2 predict that v_- will be a function of E/p only, though it is possible to envisage situations in which there may also be a dependence on p; for example, the pressure dependent effects of diffusion will alter the shape of the avalanche and possibly therefore the observed drift velocity, depending on the precise manner in which the apparent value for v_- is derived from the experimental observations. It would not be expected to depend on any other parameter, except where this parameter might modify E/p, such as distortion of the applied field by large values of n_o or $\exp(\alpha d)$. In particular, it would not be expected to depend on the length d of the drift space, a dependence which could only be observed in a situation where $dv_-/dt \neq 0$. This non-equilibrium situation will occur if, on the average, the rate of gain of energy by the electrons from the applied field exceeds the rate of energy loss by all possible processes. Usually the most important loss process is by collision with neutral gas molecules, but radiative losses and interaction with space charge fields can be important.

The evidence in the literature for the existence of non-equilibrium situations of this type is slight. Ecker and Muller

(1961)[5.20] and Muller (1962)[5.21] have predicted that runaway will occur at E/p > 500 volts.cm^{-1}.torr^{-1}, and Muller and Wahle (1964) [5.22] have demonstrated its existence experimentally at E/p as low as 100 under special conditions where the initial electrons are injected into the drift space with energies in excess of the mean equilibrium energy at the ambient value of E/p - i.e. an electron will continue to gain energy once it has acquired a certain threshold energy. The measurements were taken at low (pxd), in the range 0.2 to 0.8 torr.cm, where the findings may not be meaningful (see section 5.4.2). Fletcher and Haydon (1966)[5.23] found it necessary to invoke the concept of non-equilibrium to account for observations in hydrogen in (ExB)fields at E/p = 200 volts.cm^{-1}.torr^{-1}. Bagnall (1964)[5.24] observed a (pxd) dependence of α/p in nitrogen at high E/p, and Chanin and Rork (1963)[5.25] observed a similar dependence in hydrogen for E/p > 150. Conversely, Haydon and Stock (1966)[5.26] failed to find evidence of runaway when measuring α/p in hydrogen for E/p in the range 300 to 1000 volts.cm^{-1}.torr^{-1}, with (pxd) = 0.04 to 1.25 torr.cm. Schlumbohm [3.46] also gives no indication that such a process might exist in his measurements of v_-, either in hydrogen (section 5.2) or in nitrogen (c.f. Bagnall). Dawson [3.58] obtained v_- values which he was unable to explain in terms of a conventional drift velocity model, and his results are discussed in section 5.2.

Comparison of the Experimental Data with the Predictions of the Runaway Model.

In Appendix 5 a simple model for electron runaway is used to derive expressions for the apparent drift velocity under such conditions. Case (3) in Appendix 5 assumes that $eV_o << eV$, where eV_o is the energy of the initiating electrons and eV is the total energy available from the applied field. The most energetic photons available to release initiating photo-electrons from the cathode have an energy of about 7 eV and the cathode work function is about 4 eV, so the energy of the photo-electrons should not exceed 3 eV. Under runaway conditions, the electrons will acquire at least an appreciable fraction of the total energy available from the applied potential, which is between 500 and 1250 volts in this investigation, so $V_o << V$ is a reasonable approximation. The predictions of the model for this case are that -

$$\begin{cases} v_{-app} \propto (V)^{\frac{1}{2}}, & \text{for fixed p,d,f} \\ v_{-app} \text{ is a function of p,} & \text{for fixed V,d,f} \\ v_{-app} \text{ is a function of d,} & \text{for fixed V,p,f} \\ v_{-app} \text{ is a function of (pxd),} & \text{for fixed V,f} \end{cases}$$

where f is the fractional energy loss on collision.

It will be assumed that f has a constant value over the range of electron energies in this experiment, as it appears that values are not available for this region. In fact, it might be

expected that, above a threshold energy approximately equal to the ionisation energy (15.4 eV for hydrogen), f would diminish with increasing electron energy because of the decreasing interaction time.

The effects of electron runaway would be apparent in both the photo-multiplier and the electron-multiplier data, and an investigation of the relationship between $\log(v_-)$ and $\log(V_a)$, for approximately constant (pxd), showed the following features -

1. for (pxd) ≈ 4 torr.cm : slight correspondence between electron- and photo-multiplier data, to give a straight line of slope 2.7 from badly scattered points.
2. for (pxd) ≈ 9 torr.cm : fair correspondence between electron- and photo-multiplier data, to give a slope of 2.2.
3. for (pxd) ≈ 17 torr.cm : poor correspondence, but the photo-multiplier data alone gives a line with a slope of 2.7.
4. for (pxd) ≈ 29 torr.cm : no electron-multiplier data available, but the photo-multiplier data has a slope of 2.7.

Thus it was found that there exists for the photo-multiplier data a relationship of the type

$$v_{-app} \propto V_a^{\nu}$$

where ν is in the range 2.2 to 2.7, whereas it was predicted that $\nu = \frac{1}{2}$. The result ν = 2.2 to 2.7 may be compared with Dawson's parabolic curves (section 5.2), and is discussed further in section 5.6.

A graph plotting $\log(v_-)$ against $\log(pxd)$ for all the data, for approximately constant V_a, is not reproduced (because of the confusion, on a single graph, between points of differing V_a), but showed the following features -

1. no correspondence between the electron- and photo-multiplier data

2. widely scattered points but, overall, a minimum in $\log(v_-)$ at $(pxd) \simeq 10$, and

$$\text{for } (pxd) < 10, \quad \text{gradient} \simeq -1,$$

$$\text{for } (pxd) > 10, \quad \text{gradient} \simeq +1.$$

There is qualitative agreement, therefore, with the model for $(pxd) > 10$, but the points in this region are exclusively from the photo-multiplier data (whereas runaway effects would be evident in both detection techniques) and correspond to the elevated values of v_- at low E/p shown in fig. 5.4. The disagreement of the data with the model for runaway at $(pxd) < 10$ (i.e. higher E/p), where such a mechanism might most reasonably be expected, invalidates any interpretation of the (pxd) data as evidence of runaway, especially in the perspective of the well established v_- values at low E/p and the complete absence of any evidence of non-equilibrium effects in the previous work performed in this region.

This, together with the failure to obtain correspondence between the electron-multiplier and photo-multiplier results, and the failure to demonstrate a $v_- \alpha (V_a)^{\frac{1}{2}}$ dependence, indicates with some

certainty that a mechanism of electron runaway cannct be invoked in the E/p range of 30 to 350 volts.cm^{-1}.torr^{-1}.

5.4.2. The Effects of Non-Ideal Experimental Conditions.

The criteria adopted in the design of the experiment are detailed in section 4.1, and particular attention was paid to the following points -

1. the (pxd) product,
2. secondary avalanches,
3. space charge density,

all of which could affect the observed values of v_-, and lead to dependences on parameters other than E/p.

The (pxd) product.

If the (pxd) product, which determines the number of collisions that an electron experiences in traversing the drift space, is not sufficiently large, the number of collisions before an initial electron comes to equilibrium may represent an appreciable fraction of the total number, and so lead to a dependence of v_- on p, for fixed E/p and d. Von Engel[2.3] calculates that, for elastic collisions in helium at E/p = 3 volts.cm^{-1}.torr^{-1} and p = 1 torr, 3600 collisions are required to acquire 94% of the terminal velocity, involving the traversal of a distance of about 1 cm in the field direction. This problem is discussed in section 2.5, and taking the electron-neutral ionisation cross-section $\sigma = 0.78 \times 10^{-16}$ cm^2 at 35 eV

for hydrogen from (2.8), λ = 0.36 cm at 1 torr, so that at E/p = 100 volts.cm^{-1}.torr^{-1} the average electron energy gain between collisions is 36 volts. Since the ionisation potential for hydrogen = 15.4 volts, it is reasonable to assume that the fractional energy f is $\sim$ 0.5. Then substitution in equations (2.17) and (2.19) gives the time to reach equilibrium t_o = 0.15 and 1.01 nsec respectively for the low and high E/p cases, involving only 1.75×10^{-2} and 5.0×10^{-2} cm travel in the field direction. This is clearly an underestimate, and with f $\sim$ 0.5 it is more realistic to suggest a distance of several mean free paths - i.e. 0.5 to 1.0 cm, or approximately 5% to 10% of the total drift distance. This is therefore a source of error which is likely to lead to measured drift velocities that are too low by up to 10%.

Secondary Processes.

Secondary processes, with the exception of photo-ionisation ahead of the avalanche (section 5.4.1), cannot lead to incorrect values for v_- with the methods of detection employed in this experiment, since these respond to the actual arrival of electrons at a given point, rather than the motion of electrons in the drift space. However, primary avalanches initiated at the cathode (end-released) will not be resolved from secondary avalanches, so that v_- will not be determined with precision, if the δ'/α coefficient (the number of secondary photo-electrons released from the cathode per ionising collision) is greater than $\exp(\alpha v_- \tau)$, where τ is the half-width of the avalanche as it arrives at the anode (see Appendix 7). Amongst

the determinations of δ'/α in pure hydrogen are those due to Llewellyn Jones and Davies (1951)[5.27], Davies, Dawson and Gozna (1961)[5.28] and Morgan and Williams (1965)[5.29]; from 5.29 $\delta'/\alpha \simeq 10^{-3}$ for E/p = 56 to 110 volts.cm^{-1}.torr^{-1}, referred to gold electrodes. For an initiating pulse half-width τ of 25 nsec, $1/\exp(\alpha v_- \tau) = 1.9\times10^{-1}$ and, in the absence of diffusion broadening, primary and secondary avalanches should be resolved.

Space charge.

A possible indirect effect of secondary processes is their contribution to the total space charge between the avalanche and the anode. The effects of space charge are briefly discussed in section 1.6, where it is shown that excessive space charge may lead either to a decrease or an increase in the electron crossing time. A decrease can only occur under conditions conducive to the propagation of streamers, that is a low applied field, usually in a non-uniform geometry, a concentration of at least 10^8 positive ions within a sphere of radius $\sim 10^{-3}$ cm, and a high pressure (200 to 1000 torr) to minimise diffusion; none of these conditions is appropriate to the present experiment. Increased transit times will be observed in the present experimental regime if $\exp(\alpha d)$ becomes greater than 10^6 (Tholl[1.24]) but, with the exception of two readings taken at $\exp(\alpha d) \sim 10^6$, this figure was never exceeded (see Appendix 8). Figs. 5.4 and 5.5 show plots of (v_-) against log(E/p) for various fixed $\exp(\alpha d)$, for a combination of both the electron-multiplier and the photomultiplier data. The left

hand side of the graph shows gross increases in the apparent electron drift velocity, for relatively small values of exp (αd) of less than 10^4, and it is not reasonable to associate this effect in any way with space charge. The right hand side shows a small increase in measured drift velocities with increasing exp(αd) whereas the opposite effect is expected for space charge retardation but, because of the inter-dependence between exp(∝d) and the other experimental variables, the interpretation of these curves is difficult. The two points for exp(αd) ≈ 10^6 are marked * in fig. 5.5, and show no evidence of space charge retardation.

5.5. Sources of Spurious Signals.

Detection of Scattered Photons by the Photo-multipliers.

The photons from inelastic electron-molecule collisions, occurring outside the field of view of one of the photo-multipliers, could produce spurious signals from the photo-multiplier if it is possible for these photons to be deflected into the multiplier, either by reflections from surfaces in the experimental vessel or by a scattering mechanism in the gas. Some care was taken to prevent specular reflections into the photomultipliers and, if such a mechanism were present, it is expected that the "velocities" observed would be virtually independent of the experimental variables V_a and p, in contradiction to the data obtained.

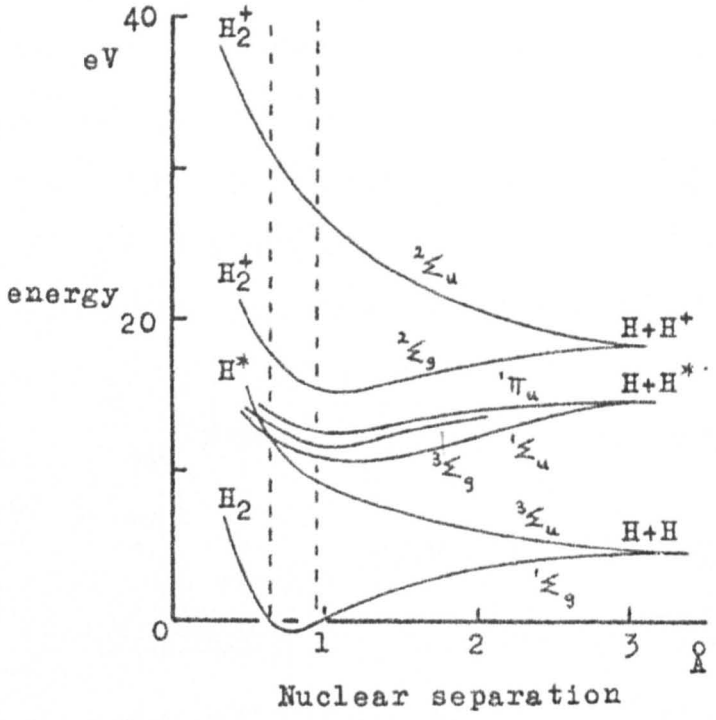

Fig. 5.7

Potential energy diagram for the electronic states of molecular hydrogen.

The process of scattering within the gas volume requires more detailed attention, the possible types being Rayleigh scattering, resonance scattering and fluorescence. The cross-section for Rayleigh scattering is very small ($\backsim 10^{-28} cm^2$) so that this process can be discounted. Resonance scattering involves the absorption of a photon by a ground state molecule to produce an excited state, followed by spontaneous isotropic emission of a photon of the same wavelength; clearly, radiation produced by a discharge in a particular gas is highly susceptible to resonance scattering by neutral gas molecules of the same species. If, instead of decaying directly to the ground state, the excited molecule decays stepwise to emit a photon of longer wavelength than that absorbed, the mechanism is termed resonance fluorescence.

The potential energy diagram for the hydrogen molecule (fig. 5.7) is that given by Breare and von Engel[3.44] and is a simplified version of the diagram due to Massey and Burhop (1952)[5.30]. The lowest triplet state $^3\Sigma_u$ is a repulsive state resulting in dissociation without excitation, the excess energy being carried away as kinetic energy. The singlet states $^1\Sigma_u$ and $^1\pi_u$ decay directly to the ground state $^1\Sigma_g$ to produce the Lyman and Werner bands in the vacuum ultra-violet at about 1000Å; the $^1\pi_u$ can decay first to the $^1\Sigma_u$ state to produce visible radiation. Decay from the $^3\Sigma_g$ triplet cannot proceed directly to the ground state, but goes to the $^3\Sigma_u$ state to produce continuum radiation between 2000Å and 4000Å. The electron energies

required for excitation to these levels, > 12 eV, are readily available in the E/p range investigated in this experiment. The photomultipliers will only detect quanta of wavelength lying within the transmission window of borosilicate glass, that is 3300Å to 7000Å, a region where relatively little emission occurs in the hydrogen spectrum, so that a resonance fluorescence mechanism would be especially favourable to the detection of spurious photons. The $^3\Sigma_g \rightarrow {}^3\Sigma_u$ and $^1\pi_u \rightarrow {}^1\Sigma_u$ transitions provide appropriate wavelength conversion. It is also possible that fluorescence could occur in the glass walls of the experimental vessel.

A qualitative appraisal of the problem predicts a dependence of v_- on pressure because of the linear dependence of the total scattering cross-section per unit volume on pressure, complicated by the inter-relationships between p and α/p, E/p and $\exp(\alpha d)$ in the avalanching process. A simple model for the process (Appendix 6) leads to the relationship (equation A6.2) for fixed E/p, d, σ

$$v_{-app}/v_- \quad \alpha \quad p/\ln(1/p),$$

where v_{-app} is the apparent electron drift velocity that would be observed. Since p varies more strongly than $1/\ln(1/p)$, it is expected the v_{-app}/v_- ratio will depend approximately linearly on p when the other variables are held constant. The model used does not take into account the effect of pressure on the "mean free path" of

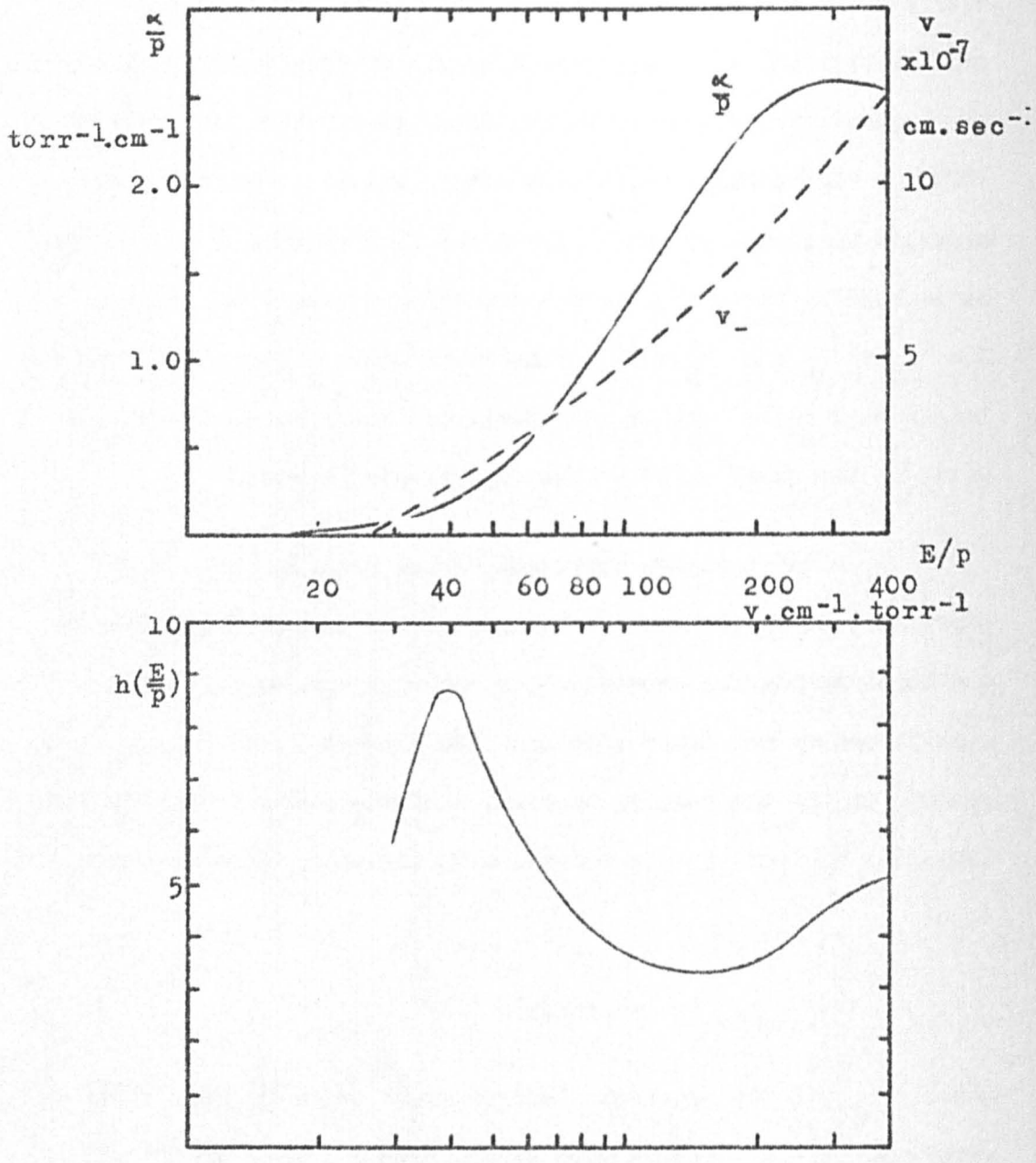

Fig. 5.8

The variation with E/p of $\alpha/p = f(E/p)$, $v_- = g(E/p)$ and $h(E/p) = g(E/p)/f(E/p)$.

the photons; this is discussed in section 5.4.1, and it is apparent that there will be an optimum pressure, such that about 50% of the photons will have been absorbed when they enter the field of view of the photomultiplier. Using the cross-sections quoted in section 5.4.1, 50% absorption would occur in a distance of 6.9cm if the pressure is 0.5 torr, to give a v_{-app}/v_{-} ratio of about 2.

Variation of d, the anode-cathode separation, is also inter-related with other gas discharge parameters in a complex fashion. From equation (A6.3), for fixed E/p, p, σ,

$$v_{-app}/v_{-} \quad \alpha \quad d.$$

A dependence of the v_{-app}/v_{-} ratio, and also of v_{-app} on E/p, assuming equilibrium conditions, is to be expected because of the appearance of v_{-} and α/p, both functions of E/p, in the derivation of the expression for the ratio. In equation (A6.5) where for fixed p,d,σ,

$$v_{-app} = h(E/p),$$

h(E/p) = g(E/p)/f(E/p) - see fig. 5.8 - is not expected to be a simple function because of the complexity of f(E/p) at moderate E/p (for instance, f(E/p) = C.exp(-Dp/E).(E/p)/(1+FE/p), Kantaratos (1965)[5.31]). But from inspection of fig. 5.8, which shows the forms of f(E/p),g(E/p), and h(E/p), the general shape of h(E/p) can be ascertained in the range E/p = 0 to 350 volts.cm^{-1}.$torr^{-1}$.

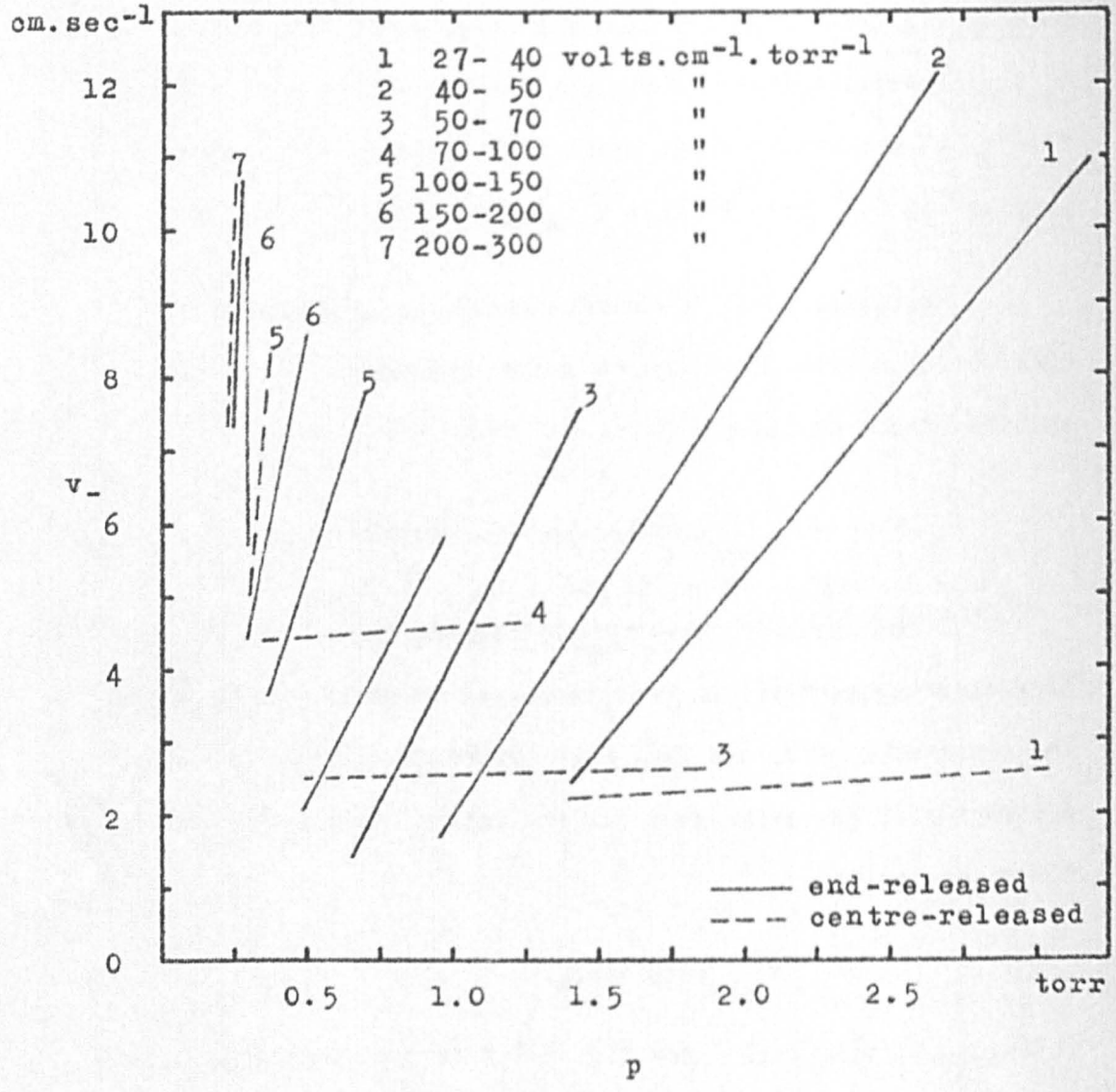

Fig. 5.9

Tube C (Hydrogen) : (v_) - (p) at constant E/p for the photomultiplier data.

The parameter V_a has not been isolated in equation (A6.1), but it is not expected that there would be any dependence of v_- on V_a alone in an equilibrium situation.

Comparison of the photomultiplier data with scattering predictions.

To summarise, the following predictions are to be tested -

1. $v_{-app}/v_- \propto p$, for E/p, d, σ constant
   $v_{-app}/v_- \simeq 2$, for p = 0.5 torr.
2. $v_{-app}/v_- \propto d$, for E/p, p, σ constant.
3. $v_{-app} = h(E/p)$, for p, d, σ constant.

1. Pressure dependence : fig 5.9 shows a family of straight lines in a (v_-) - (p) plot of the photomultiplier data at fixed E/p, with slopes that range from about unity at E/p = 40 to infinity at E/p = 250 volts.cm^{-1}.$torr^{-1}$. The points from which these curves are derived are scattered and are not shown in fig. 5.9 for clarity, but it is evident that there is a marked disagreement between end-released and centre-released avalanches for E/p = 27 to 100, where the centre-released values are virtually independent of p. This discrepancy is not inconsistent with resonance scattering because of the predicted dependence on d. A plot of (v_-) - (p) for fixed V_a revealed no dependence, as is expected in an equilibrium situation.

Inspection of the data showed that at p = 0.5 torr the v_- values obtained are in fair agreement with Schlumbohm's results, and that $v_{-app}/v_- \simeq 2$ for p in the range 1 to 3 torr; however, the abosrption cross-section assumed (section 5.4.1) is not strictly applicable to the wavelengths which can be detected by the photo-multipliers, so this pressure is sufficiently close to 0.5 torr to be interpreted tentatively as evidence of resonance scatter.

2. d dependence : adjustment of the end-released and the centre-released data according to the appropriate value of d failed to demonstrate any equivalence between the two sets of data.

3. E/p dependence : a plot for the photomultiplier data of (v_-) - log(E/p) for fixed p (not reproduced here) did not yield discrete curves for each value of p, but viewed overall, although there was a great deal of scatter, it was evident that the general variation was consistent with the predicted shape of the function h(E/p) in fig. 5.8, though the minimum occured at E/p ≃ 60 volts. $cm^{-1}.torr^{-1}$ instead of 150. Fig. 5.4, which plots (v_-) - log(E/p) for fixed exp(ad), shows similar features.

It is concluded from this semi-quantitative treatment that, within the limitations of the model assumed, there is sufficient agreement between the predicted and the actual behaviour for resonance scattering to be a source of spurious signals from the photo-multipliers, and therefore to render the

photo-multiplier data unreliable.

Detection of u.v. Photons by the Electron Multiplier.

Another possible source of spurious signals is the arrival at the first dynode of the electron-multiplier of ultra-violet photons from the discharge. It is shown in section 5.4.1 that the absorption cross-section is sufficiently low to give only 50% absorption of photons from an avalanche at a distance of 6.9 cm from the anode. However, the solid angles subtended at this distance are only 3×10^{-6} and 3×10^{-8} sterads respectively for the large and small orifices, and only the case where the avalanche has reached the anode, to give about 0.02 sterad collection angle at the first dynode, need be considered. If δ/α is ~ 1 (section 5.4.1) then, for the large hole, photon signals can easily be discriminated from electron signals by noting the amplitude, and for the small hole there is a $\frac{0.02}{4\pi} \simeq 2\times10^{-3}$ chance of detecting a photon instead of an electron. This effect would have given an apparent drift velocity that was high by about 10% at E/p = 30 volts.cm^{-1}.torr^{-1} and 45% at E/p = 350, and is discussed in relation to the electron-multiplier data in section 5.6.1.

Pick-up by the electron-multiplier of electrical interference from the pulsing circuits was difficult to eliminate (section 4.3), but was reduced to a satisfactory level and was not detectable at the time that the avalanche reached the anode.

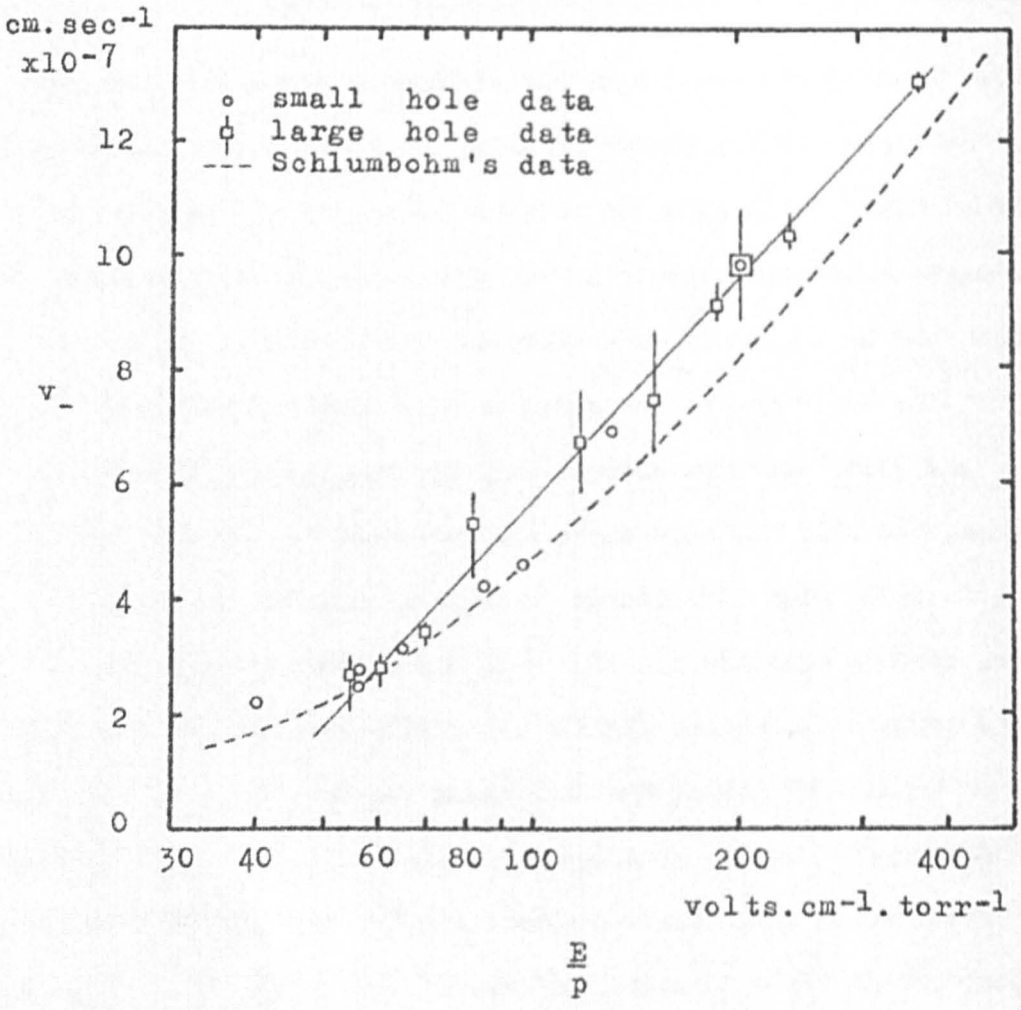

Fig. 5.10

Tube C (Hydrogen) : (v_-) - log(E/p) for the electron-multiplier data.

PART 4

Electron Multiplier Data

The electron-multiplier data, which appears to be reliable, is evaluated and compared with Schlumbohm's values for v_-, and the electron energy analyser results are also discussed briefly. The possibilities for further work with the electron-multiplier technique are explored.

5.6. Interpretation of the Final Electron Drift Velocity Values, Obtained by the Electron Multiplier Technique.

5.6.1. Large Hole Data.

The data obtained by using the electron-multiplier to sample the centre-released avalanche through the larger hole is presented in fig. 5.10 in the form of a plot of (v_-) against log(E/p), the points being marked □ . The only experimental variable held constant in the graph is d, equal in this case to 7.12 cm, the distance from the central needle to the hole in the anode. Both p and exp(αd) increase monotonically with increasing E/p, whilst V_a goes through a minimum at E/p = 82 volts.cm^{-1}.torr^{-1}. Each point is derived from up to 10 individual readings, and the bars indicate the extent of the scatter that was found between these readings; the point is the arithmetic mean of the individual values.

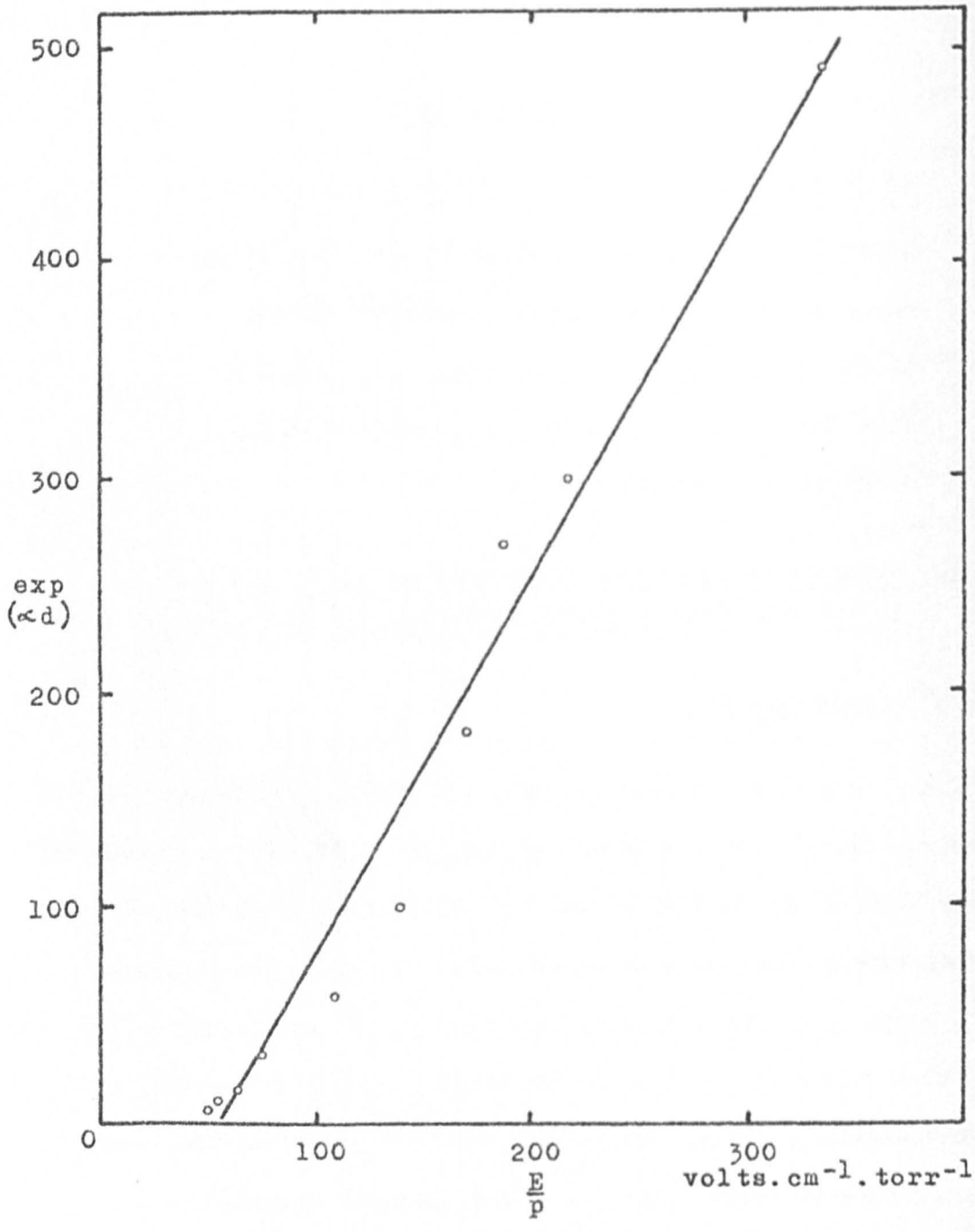

Fig. 5.11

Tube C (Hydrogen) : exp(∝d) - (E/p) for the large hole electron-multiplier data.

A straight line fits the points better than a monotonic curve, and the line drawn is a least squares fit with a correlation coefficient of 0.99. This line can be represented by

$$\frac{E}{p} \propto \exp \frac{v_-}{5.5\times10^7} \qquad (5.1)$$

which resembles $n = n_o \exp(\alpha v_- t)$ (equation 1.2). In general, n/n_o is not proportional to E/p, but a plot of $\exp(\alpha d) = n/n_o$ against E/p (fig. 5.11) shows that, fortuitously, $\exp(\alpha d) \propto E/p$ for this particular experimental run. Thus it seems that the unexpected relationship (5.1) can be explained on this basis, and is not of any fundamental significance.

A $\log(v_-)$ - $\log(E/p)$ plot of the large hole data (marked ◻) is shown in fig. 5.12, and here there is little justification for drawing a straight line through the points. However, the least squares fitted line to all the points (correlation coefficient = 0.85) gives the relationship

$$v_- \propto (E/p)^{0.85} \qquad (5.2)$$

If the points above and below E/p = 82 volts.cm^{-1}.torr^{-1} are considered separately, straight lines (correlation coefficients = 0.95 and 0.39) are obtained, to give

$$v_- \propto (E/p)^{0.60} \quad \text{for } E/p = 80 \text{ to } 360, \qquad (5.3)$$

$$v_- \propto (E/p)^{1.27} \quad \text{for } E/p = 50 \text{ to } 80. \qquad (5.4)$$

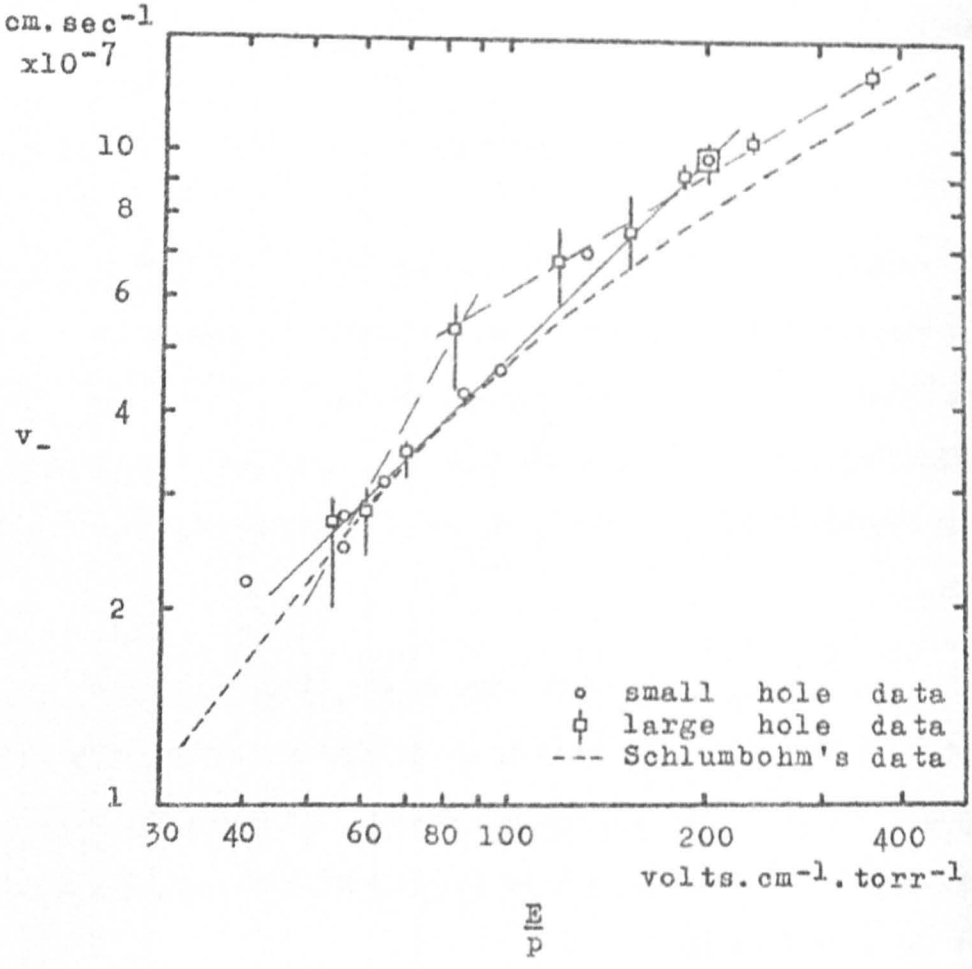

Fig. 5.12

Tube C (Hydrogen) : log(v_) - log(E/p)

for the electron-multiplier data.

In all cases the index ν is greater than the simple theoretical value of 0.5, but is within the range of values measured from Schlumbohm's [3.46] curve, namely $\nu = 1.65$ at $E/p = 30$ to $\nu = 0.5$ at $E/p = 1500$.

The curve from (3.46) is also plotted in both figs. 5.10 and 5.12, and it is seen that the agreement is fairly good at $E/p < 70$ volts.cm^{-1}.torr^{-1}, but that the values are up to 17% lower than those obtained in the present investigation at $E/p > 70$. The principal criticism levelled at the earlier investigation (section 5.2) was that the (pxd) range was too low for it to be certain that equilibrium with the gas and the applied electric field was achieved in a distance that was small compared with the drift distance. The effects of such non-equilibrium are discussed in sections 2.5 and 5.4.2, and whether a depressed or an elevated velocity will result depends on the injection energy of the initiating electrons. In (3.46) it is likely that the injection energy was less than the equilibrium energy, which would yield values for v_- that were erroneously low, in qualitative agreement with the observed discrepancy. The increasing magnitude of the discrepancy with increasing E/p is consistent with possible effects of initial non-equilibrium at the very low pressures thought to have been used at higher E/p in the earlier work. Another possible mechanism, the retarding effect of space charge distortion, may also have caused low v_- values to be recorded in the earlier work (section 5.2). The detection by

the electron-multiplier of ultra-violet photons generated by the avalanche could lead to v_- values in the present investigation that were too high by +10% at E/p = 30 volts.cm^{-1}.torr^{-1} to +45% at E/p = 350 (section 5.5), but it was concluded that the amplitude of such a spurious signal would be too small to be important. Also, although the v_- values from the present investigation are greater than those from 3.46 (figs. 5.10 and 5.12), a quantitative comparison does not support this as a possible source of error.

The reason for the scatter of up to 15% between the individual values at any given E/p is not fully understood. Statistical variations between avalanches are expected to be slight, since a moderate number of electrons ($\sim$ 10) was used to initiate an avalanche, the gas amplification was never very low (10 to 500), and an adequately large sample of electrons was detected (10 to 100). It was difficult with the larger sampling orifice, to balance the gas inflow against effusion through the orifice, so that there may have been pressure variations of up to 7% (section 4.5), with an accompanying uncertainty in the value of E/p, which could have contributed to this scatter.

5.6.2. Small hole data.

The data obtained by using the electron-multiplier to sample the avalanche through the small hole is presented in fig. 5.10 in the

form of a plot of (v_-) against log(E/p), where there is no evidence of the exponential relationship found for the large hole data, and in fig. 5.12 in a log(v_-) - log(E/p) plot, the points being marked o. It is seen that there is a close correspondence between this data and that from (3.46) in the E/p range 50 to 100 volts.cm^{-1}.$torr^{-1}$, and moderate agreement above and below this range. The least squares fit through the log - log plot has a correlation coefficient of 0.99, and a gradient of 1.01 to give

$$v_- \quad \alpha \quad (E/p)^{1.01} \quad \text{for } E/p = 40 \text{ to } 200. \quad (5.5)$$

Because of the poor statistical sampling (section 4.4), it is not proposed to attach significance to the discrepancies and correspondences between this data and that of Schlumbohm. It may be remarked, however, that the fair self-correlation of these statistically unsound points, and their reasonable agreement with the large hole data, would seem to indicate that ambipolar and kinetic diffusion broadening in the field direction was slight, and also that confidence may be placed in a technique that relies on single electron samples retaining the characteristics of the distribution from which they are drawn.

5.6.3. The entire electron-multiplier data.

The foregoing may be summarised thus -

1. $v_- \propto (E/p)^{\nu}$, where

$\nu = 1.01$ small hole data, $E/p = 40 - 200$,

$\nu = 1.27$ large hole data, $E/p = 50 - 80$,

$\nu = 0.60$ large hole data, $E/p = 80 - 360$,

$\nu = 0.85$ large hole data, $E/p = 50 - 360$,

$\nu = 0.92$ all data , $E/p = 40 - 360$,

which may be compared with

$\nu = 1.65$ to 0.5 , from (3.46), $E/p = 30 - 1500$,

$\nu = 0.5$ from theory (Chapter 2).

2. Agreement with (3.46) to better than 17%.

A comparison of the data with that from (3.46) has already been presented in section 5.6.1. It might be added that the $\log(v_-) - \log(E/p)$ plot of the earlier data (figs. 3.16 and 5.12) shows a change of gradient at $E/p = 97$ volts.cm^{-1}.torr^{-1}, which suggests a change of process in this region, and that the large hole data shows a change of slope at $E/p = 82$. Those who invoke non-equilibrium conditions quote rather higher onset values of $E/p = 150$ to 200 (e.g. Fletcher and Haydon[5.23] and Chanin and Rork [5.25]), and the examination of the present data for such a process has not been fruitful.

Some of the theories of electron drift velocities have been discussed in Chapter 2. The mean values approach led to a

relationship in which $\nu = 0.5$ (equation 2.8), except in the case of the Langevin-Thomson polarisation model, which gave the relationship $v_- \propto E/(p)^{\frac{1}{2}}$ - equation (2.6). These theories are valid at low E/p only, but an extension without rigour to high E/p also gives $\nu = 0.5$ (equation 2.19). Huxley's method for low E/p yields an intractable expression (equation 2.18), inspection of which suggests that $\nu = \nu(E/p)$. Qualitatively, on the basis of the simple equation of kinetic and potential energy with p held constant, it is difficult to envisage a situation in which $\nu \neq 0.5$. The polarisation model, where $v_- \propto E/(p)^{\frac{1}{2}}$ is not supported by experiment. It is reasonable to suppose that the fractional energy loss factor f will be a function of E/p, and this would lead to $\nu > 0.5$ and is consistent with the small hole data, the large hole data for $E/p < 82$, and the data from (3.46) for $E/p < 97$. At high E/p it is expected that f would become independent of E/p to give $\nu = 0.5$ again, in agreement with the large hole data for $E/p > 82$, and the data from (3.46) for $E/p > 97$. It is also expected that $f = f(E/p)$ would exhibit resonances corresponding to excitation and ionisation levels, and that these would be reflected in the variation of v_- with E/p. Such resonances have not been observed here or reported elsewhere, but probably have not been sought and therefore may have been missed.

If the applied field is held constant, a model in which the interaction time is greater than the time between collisions

would lead to a 1/p dependence, and ν would have values between 0.5 and 1.0 in the transition region. However, there has been no evidence for such a mechanism under the conditions of this experiment.

In section 5.4.1 it was found that, for the combined photomultiplier and electron-multiplier data, $v_- \propto V_a^{\nu}$ for fixed p, where ν = 2.2 to 2.7; in section 5.3 it was suggested that Dawson's [3.58] values for v_- (fig. 3.19) showed a parabolic dependence on E/p for fixed p, and a log (v_-) - log(V_a) plot for one of the curves yields a good straight line of slope ν = 1.95. The moderate agreement between the values of ν is almost certainly coincidental, particularly in view of the unreliable nature of the photo-multiplier data. It is not obvious why the space charge dominated processes of (3.58) should exhibit this dependence, nor why the present data should show a strong variation with V_a, unless the f = f(E/p) relationship is again invoked.

5.7. Electron Energy Measurements.

The electron energy analyser was of a preliminary design (section 4.2) and readings could only be obtained when the current in the discharge gap was relatively high, probably corresponding to the early stages of the establishment of a glow discharge. The energies measured are likely to correspond to those in the anode glow region and will bear little resemblance to those present in a

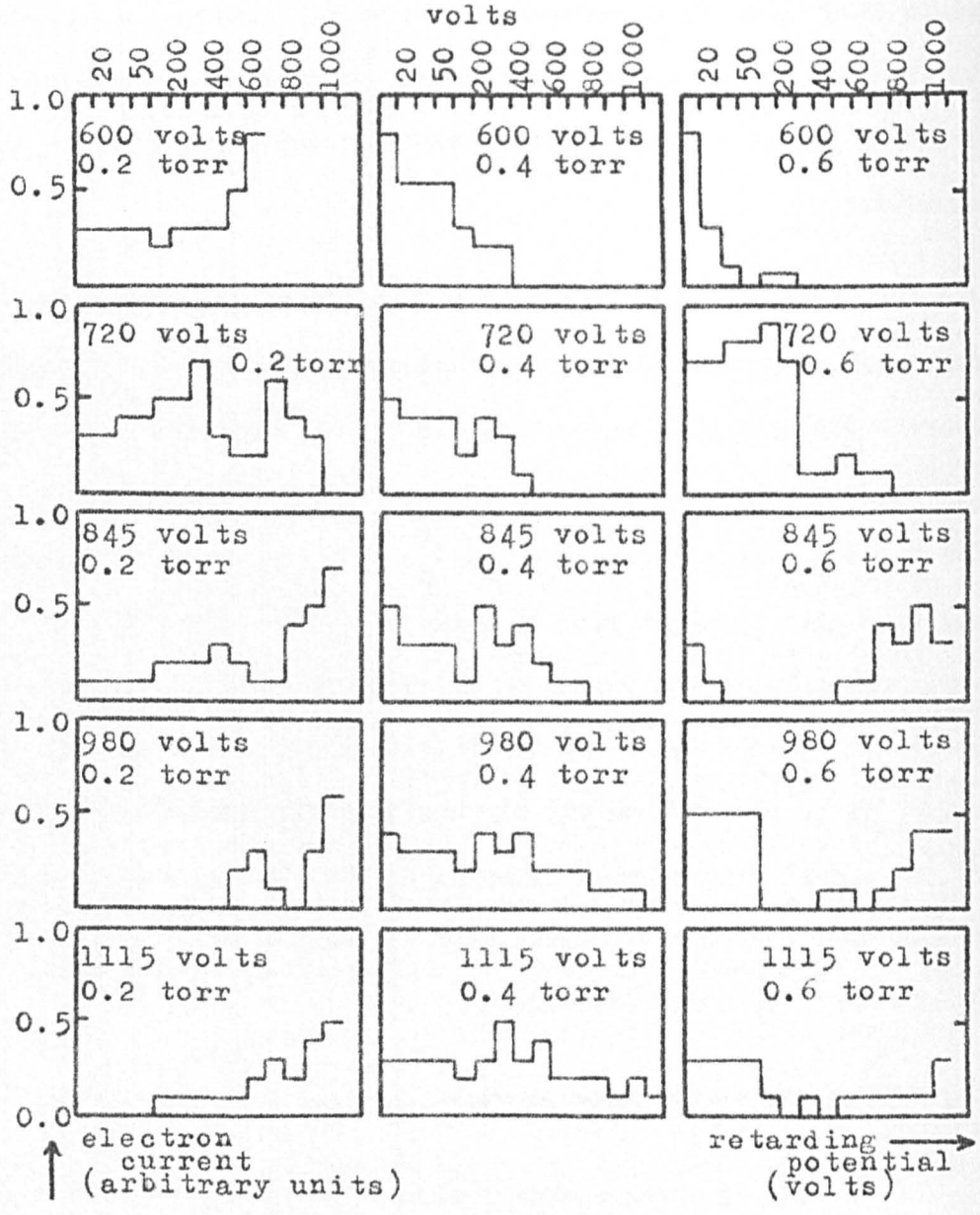

Fig. 5.13

Tube C (Hydrogen) : electron energy histograms.

current Townsend avalanche. The imperfect geometry of the analyser, which permitted electrons to travel in directions other than parallel to the retarding field, allowed energies to be observed which may be lower than the actual energies and also caused poor resolution. Additionally, it will be shown that there were further defects which resulted in the apparent penetration of the analyser by electrons with energies below that corresponding to the retarding potential.

Because of the poor quality of the data and the remoteness of the physical situation from the Townsend regime (the subject of this investigation), the results will be discussed only briefly and superficially. Fig. 5.13 shows histograms of the observed electron energy distributions for five different voltages applied to the drift space, for each of three different pressures. The vertical axes plot the numbers of electrons in arbitrary units, and the horizontal axes electron energies in eV on a non-linear scale. The histograms exhibit the following features -

1. There is no similarity to a Maxwellian or a Druyvesteyn distribution, and many of the histograms show two distinct peaks.

2. At fixed pressure, there is an increasing concentration of high energy electrons as V_a is increased. The peak energy is usually equivalent to at least 50% of V_a, and apparently is sometimes in excess of V_a, which clearly indicates that the observed energies cannot be correct. Nevertheless, the order of magnitude of the measured energies implies that the electrons have acquired an

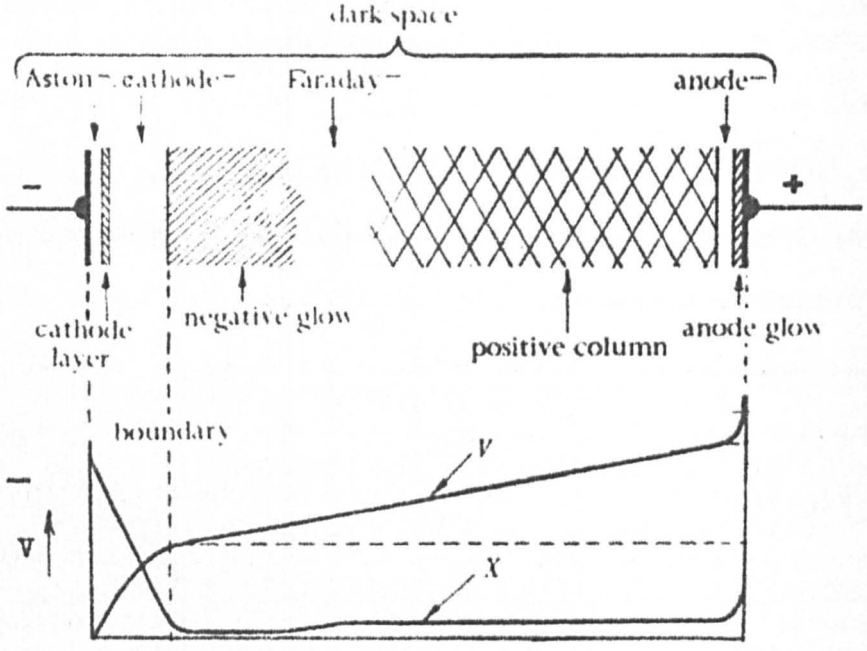

Fig. 5.14

The electric field distribution in a glow discharge.

appreciable fraction of the total available energy, possibly in the interval between the last collision and the anode. This, and the dependence on V_a, is not inconsistent with the potential distribution in a glow discharge, which shows a substantial potential drop across the short anode glow region, after the almost field-free positive column (fig. 5.14).

Penetration of the negatively-biased retarding grid by the field which accelerates electrons onto the first dynode of the electron-multiplier could have caused erroneously high energies to be observed, but it is improbable that this effect would be important. However, detection by the multiplier of ultra-violet photons from the discharge is a more likely source of error, and it has been shown in section 5.5 that the proportion of photons to electrons incident at the first dynode would be about 2×10^{-3}. This did not present problems in the detection of a complete avalanche but, if the electron signal is attenuated by the analyser, the ultra-violet signal becomes comparable or even predominant. It is not possible to adjust the data for this effect since, at a given E/p, the ultra-violet signal varied with the retarding potential, as the transit time of the electrons between the analyser and the multiplier depended on this potential.

3. At fixed V_a, the high energy peak tends to move to lower energies as the pressure increases, and also splits into two peaks at the higher values of V_a. The former feature is again consistent

with the anode glow, where it might be expected that an increase in pressure would be accompanied by a move towards equilibrium conditions. The splitting of the peaks is not understood. The lack of similarity to the Maxwellian and Druyvesteyn distributions is also in accordance with the non-equilibrium conditions of the anode glow.

5.8. Conclusions and Suggestions for Further Work.

It has become apparent that the use of photomultipliers, without spectral discrimination, to make spatio-temporal measurements of discharges in gases at pressures in the region of 1 torr is unreliable. However, if an interference filter or a monochromator were to be used to select a non-resonant line for observation, it is probable that useful data could be obtained, provided the sensitivity would not be too severely reduced. Photomultiplier detection is particularly attractive since there is no uncertainty about possible interference with the development and progress of the avalanche.

The application of electron-multipliers to the determination of electron drift velocities has yielded values with a calculated maximum error of $\pm$ 12% in the E/p range 40 to 360 volts.cm^{-1}.torr^{-1}, for hydrogen. This technique was apparently novel at the time of inception of this investigation, and has emerged as a potentially useful line of attack on the limitations of the (gain x bandwidth)

product that beset investigations of fast, low current processes. Specifically, the electron-multiplier has the ultimate sensitivity in its capability of detection of a single electron, coupled with a risetime that can be as short as 2 nsec. The need for differential pumping sets an upper limit to the gas pressure range that can be investigated, though the sampling orifice can be very small, as long as electrons will pass through sufficiently often to be detectable in multiplier noise, and the pumping speed of the system can be very fast. In addition, the pulsed Townsend discharge becomes amenable to temporally resolved electron energy analysis by sophisticated analysers in a vacuum environment, whereas previously only crude analysers with dimensions less than a mean free path could be employed, immersed in the gas. Diffusion measurements have not been attempted in this work, but would be possible under conditions of low charge concentrations to minimise mutual repulsion.

Many aspects of the present experiment could be improved, and it is not considered that an exhaustive investigation was executed with the techniques that were developed, since the time-consuming methods of data acquisition and reduction, and the unsatisfactory photo-multiplier data, prevented an adequate set of results from being accumulated by the electron-multiplier technique. Thus it still remains for a comprehensive set of data to be acquired, covering the accessible range of E/p, p and (pxd), and exp(αd). An immediate extension would be to modify the pulse generator to enable higher V_a

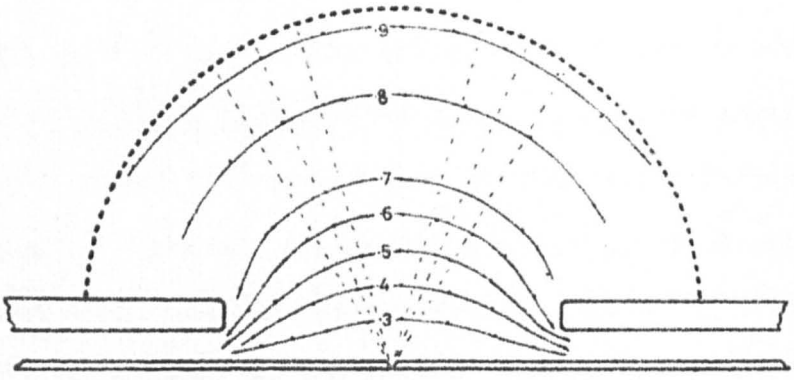

Fig. 5.15

Preliminary design for a retarding-potential electron energy analyser.

to be applied, so that the upper limit for E/p could be extended. Good v_- values, supported by electron energy distributions, in the region E/p = 100 to 2000 volts.cm^{-1}.torr^{-1} would resolve the "runaway" discrepancies between various authors (section 5.4.1). It would therefore be important to develop or adapt a high resolution electron energy analyser to fit the geometrical constraints of the fast pumping system, and a preliminary design for a retarding potential type is shown in fig. 5.15. A determination of the electric field distribution using an electrolytic tank has shown that this geometry has equi-potential lines that are perpendicular to the electron trajectories over a semi-angle of approximately 30°. The problem of detection of ultra-violet photons from the discharge (section 5.7) could be overcome by deflection of the electrons by a magnetic or electric field between the analyser and the electron-multiplier, so that the multiplier could be placed out of sight of the orifice.

There is a clear need for improved data acquisition, and there would be no technical difficulty in arranging for the single electron signals from the smaller sampling orifice to stop a scaler (driven by a 100 MHz oscillator) which had been started simultaneously with the release of the photo-electrons. The output from the scaler could be punched on paper tape, and would set an accuracy limit of 1% and 10% for the lowest and highest velocities that have been measured with the present equipment.

It is evident from Chapter 2 that the existing theories of electron transport at high E/p are inadequate, and the task of analytically determining the electron energy distribution is formidable when a number of types of collision is possible. It is suggested that the use of Monte Carlo methods might provide an alternative approach to the problem; such an approach would be confined to low values of $\exp(\alpha d)$, say < 100, to keep computer usage at an acceptable level, and would require a knowledge of the cross-sections and angular distributions for all the collision processes with a significant probability of occurrence.

APPENDIX 1

The Parameter E/p_o

The parameter E/p is of fundamental importance in the physics of electrons in gases. However, E/p is a function of temperature, and the truly fundamental parameter is E/N, where N is the molecular number density. N is an inconvenient quantity from an experimental point of view since it cannot be directly measured, and the natural consequence was that the early publications in the field used the practical parameter E/p, where p was almost always measured at an unspecified ambient temperature, a practice that was quite adequate for the gas purities and experimental techniques that were then available. As evolving techniques demanded a more precise parameter the majority of workers resorted to the use of E/p_o, where p_o is the pressure reduced to 0^oC, though some used E/N.

Huxley, Crompton and Elford (1966)[A1.1] have suggested that a unit of E/N called the 'Townsend' be used, to honour the remarkable contributions of J.S.Townsend to the field, and that this unit be defined thus -

$$1 \text{ Townsend} = 10^{-17} \text{v.cm}^2.$$

The use of this ratio would make the Townsend a unit of practical magnitude, in that it would be numerically equal to

E/p at a temperature of 96.62°K, whilst multiplication by a factor of 3 would make it approximately equal to E/p at room temperature (± 3% between 9°C and 25°C). The precise relationship is

$$E/N \text{ Townsend} = (1.0354\times10^{-2}T)(E/p_T)\text{v.cm}^{-1}.\text{torr}^{-1}.$$

This proposal would seem to be a compromise between the use of E/N and E/p_o.

Consequent upon this suggestion, the Institute of Physics and the Physical Society[A1.2] stated that it intended to bring to the attention of the 8th International Conference on Ionisation Phenomena in Gases a proposal that a unit called the Townsend be adopted, defined by either

$$1 \text{ Townsend} = 10^{-17}\text{v.cm}^2$$

or

$$1 \text{ Townsend} = 2.8266\times10^{-17}\text{v.cm}^2 .$$

The latter definition would seem to be the more convenient as it is numerically equal to E/p_o; since the principle of the former definition is compromised to give it practical magnitude by the introduction of the factor of 10^{-17}, it would seem sensible to compromise it further to make the unit truly practical.

However, it appears that no decision on this proposal was reached at the conference, and for this reason the author has chosen to use E/p_o in the conventional mixed units of volts.cm^{-1}. torr^{-1}. For brevity, the parameter is written throughout as E/p, and all numerical values quoted are reduced to 0°C unless otherwise stated.

APPENDIX 2

The Currents Due to a Single Avalanche

The Electron Component.

Only the case of a single avalanche, without secondaries, is considered.

Suppose that n electrons, with charge -e, drift with velocity v_- in a uniform field $E = V_a/d$. These electrons, in drifting a distance dx, acquire energy $neE.dx = neE.v_-dt$, which must be equal to $V_a.I_-(t).dt$, the energy put into the circuit in time dt. Hence

$$I_-(t) = \frac{nev_-}{d} ,$$

where $I_-(t)$ is the current due to the electron component. Now, from equation (1.2), n is a function of time such that if the n_o initiating electrons are released instantaneously,

$$n = n_o.\exp(\alpha v_- t),$$

so that

$$I_-(t) = \frac{n_o ev_-}{d} \exp(\alpha v_- t) \qquad (A2.1)$$

(Under conditions of very low α it is not sufficient to consider only the contribution of the electrons in the head of the

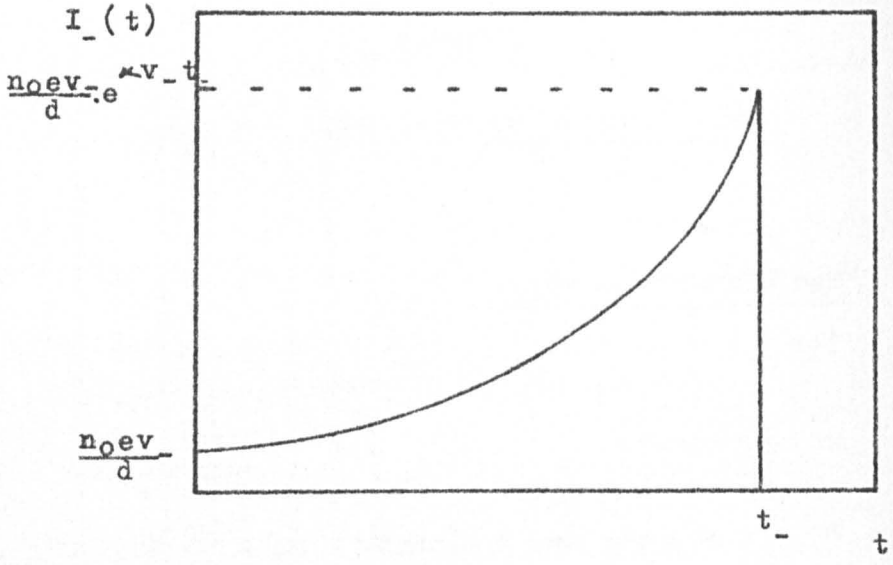

Fig. A2.1

Variation of the electron component with time.

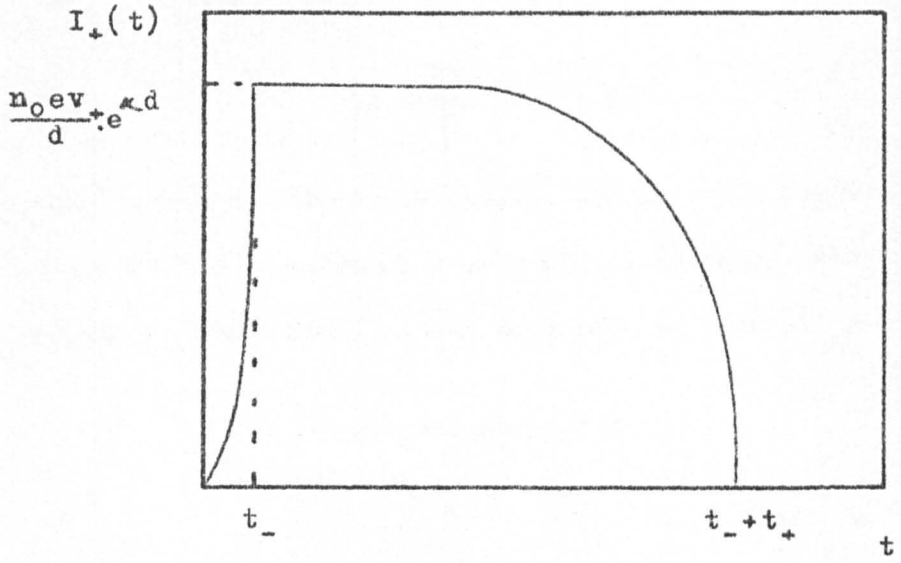

Fig. A2.2

Variation of the positive ion component with time.

avalanche and the expression becomes

$$I_-(t) = \frac{n_o e v_-}{d} \int_0^t \exp(\alpha v_- t).dt \quad .)$$

Equation (A2.1) holds only in the time interval $0 \leqslant t \leqslant t_-$, where t_- is the electron transit time; otherwise $I_-(t) = 0$. From equation (A2.1), it is seen that the electron current increases exponentially with a time constant $1/\alpha v_-$ (fig.A2.1), so that measurement of this time constant and a knowledge of α permits a value for v_- to be obtained.

The Positive Ion Component.

As above, $I_+(t) = n_+ e v_+/d$ for singly charged ions. The number of positive ions in the gap at time t is equal to the number of ionising collisions made up to time t, less the number of positive ions lost to the cathode, so that

$$I_+(t) = \frac{n_o e v_+}{d} \left(\exp(\alpha v_- t) - \exp(\alpha v_+ t)\right) \quad (A2.2)$$

during $0 \leqslant t \leqslant t_-$,

and

$$I_+(t) = \frac{n_o e v_+}{d} \left(\exp(\alpha d) - \exp(\alpha v_+ t)\right)$$

$t_- \leqslant t \leqslant t_+$,

to a good approximation (fig. A2.2).

Now $v_+/v_- \simeq 10^{-2}$, so that it usually sufficient to write equation (A2.2) as

$$I_+(t) = \frac{n_o e v_+}{d} \cdot \exp(\alpha v_- t), \quad 0 \leq t \leq t_- ,$$

which is negligible compared with the electron current flowing during this time interval.

The Negative Ion component.

In electronegative gases, an attachment coefficient η' can be defined as the number of negative ions produced per electron per centimetre path parallel to the field (similarly to α), so that $dn = \eta' n.dx$ ions are produced by n electrons in dx. Thus the number of electrons produced in dx is

$$dn = (\alpha - \eta')n.dx,$$

and thus

$$n = n_o \exp(\alpha - \eta')v_- t.$$

The curve obtained is similar to that in fig.1.3, but now the maximum is $(nev_-/d).\exp(\alpha - \eta')v_- t$ and the time constant is $1/(\alpha - \eta')v_-$.

As hydrogen, the principal subject of this work, does not form negative ions, the derivation of the negative ion current $I'_-(t)$ and the positive ion current $I_+(t)$ for this case will not be given, though the procedure is similar to that for non-attaching gases. The expressions obtained are

$$I_-(t) = \frac{n_o e v_-}{d} \exp((\alpha - \eta')v_- t), \quad 0 \leq t \leq t_-,$$

$$I_+(t) = \frac{n_o e v_+}{d} \frac{\alpha}{(\alpha-\eta')} (\exp(\alpha - \eta')d - \exp(\alpha - \eta')v_+ t),$$

$$t_- \leq t \leq (t_- + t_+),$$

$$I'_-(t) = \frac{n_o e v'_-}{d} \frac{\eta'}{(\alpha-\eta')} (\exp((\alpha - \eta')(d - v'_- t) - 1),$$

$$t_- \leq t \leq (t_- + t'_-).$$

$I_+(t)$ and $I'_-(t)$ are negligible in the time interval $0 \leq t \leq t_-$.

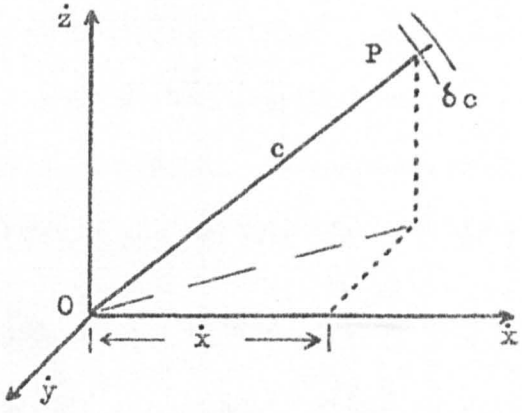

Fig. A3.1a

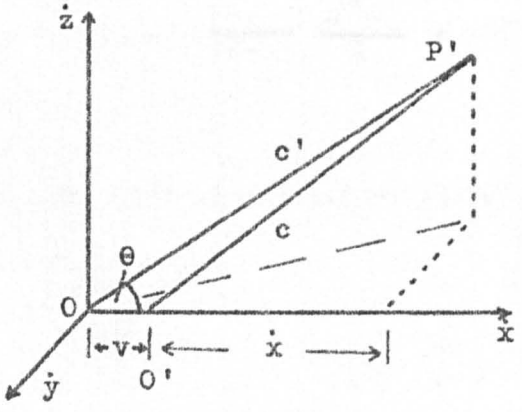

Fig. A3.1b

Velocity-space diagrams.

APPENDIX 3

Boltzmann Transport Theory Applied to Electron Drift Velocities and Distribution Functions.

General Velocity Distribution in a Uniform Field.

In the absence of an applied electric field the isotropic velocity distribution function is f(c). In velocity-space (fig. A3.1a), the number of ions per unit volume with speeds between c and (c+δc), contained in the spherical shell of radius c, thickness δc, is

$$\delta N = N.f(c).4\pi c^2 \delta c$$

and the number in the velocity elementary volume $\delta\dot{x}.\delta\dot{y}.\delta\dot{z}$ is

$$\delta N' = N.f(c).\delta\dot{x}\delta\dot{y}\delta\dot{z}$$

If a drift velocity v = v(c) is superimposed in the x direction, a dependence on c being assumed, all the $\dot{x}$ components will be increased by v to shift the centre of symmetry a distance v from O to O'. c' is chosen to keep the number of ions δN' in the volume $\delta\dot{x}.\delta\dot{y}.\delta\dot{z}$ unaltered (fig. A3.1b).

Assumption 1 : thermal equilibrium, v << c'.

Then $$\cos\theta = (\dot{x} + v)/c' \simeq \dot{x}/c' .$$

It is no longer necessary to differentiate between c and c', so c' is written as c. Then $O'P' = c - v.\cos\theta \simeq c - v\dot{x}/c$.
Let the new distribution function be $F(c,\dot{x})$; then the number of ions in $\delta\dot{x}.\delta\dot{y}.\delta\dot{z}$ becomes

$$\delta N' = N.F(c,\dot{x}).\delta\dot{x}\delta\dot{y}\delta\dot{z} = N.f(c-v\dot{x}/c).\delta\dot{x}\delta\dot{y}\delta\dot{z} \qquad (A3.1)$$

Hence, using Taylor's theorem

$$F(c,\dot{x}) \simeq f(c) - \frac{v\dot{x}}{c} \cdot \frac{df(c)}{dc} \qquad (A3.2)$$

which is a general expression, subject to assumption (1), for the velocity distribution of ions drifting in a force field. It remains to find

1. f(c) the zero field distribution
2. v = v(c) the drift velocity and its variation with c.

Ion Drift Velocities using the General Distribution Function.

If a uniform field E is applied in the x direction, the mean drift velocity is given by

$$\bar{v} = \frac{\int_0^\infty [(\text{mean } \dot{x})_c \times \text{no. with } c]dc}{\text{total no.}}$$

$$\text{where } (\text{mean } \dot{x})_c = \frac{\int_0^{\pi} [(c.\cos\theta)_c \text{ x no.with c},\theta]\, d\theta}{\text{no. with c}}$$

Now
$$\int_0^{\pi} [(c.\cos\theta)_c \text{ x no. with c},\theta]\, d\theta$$

$$= \int_0^{\pi} (c.\cos\theta)_c .\ N\, F(c,\dot{x}).2\pi c \sin\theta\ c\ dc\ d\theta$$

$$= 2\pi N c^3 dc \int_0^{\pi} F(c,\dot{x}) \sin\theta \cos\theta\ d\theta$$

using equation (A3.2), and substituting $\dot{x} = c \cos\theta$

$$= 2\pi N c^3 dc \left[f(c) \int_0^{\pi} \sin\theta \cos\theta\ d\theta - \int_0^{\pi} v \sin\theta \cos\theta \frac{df}{dc}\, d\theta \right]$$

$$= -\frac{4\pi}{3} N c^3 dc\ v \frac{df}{dc} .$$

Hence
$$\bar{v} = \frac{\int_0^{\infty} \left[\frac{-4\pi N c^3 v\ df/3dc}{\text{no. with c}} \text{ x no. with c} \right] dc}{\text{total no. N}}$$

$$= -\frac{4\pi}{3} \int_0^{\infty} v(c) \frac{df}{dc} c^3 dc.$$

Now, from Langevin's approach $\bar{v} = \frac{1}{2} eE\lambda/m\bar{c}$ as given by equation (2.1), and thus $v(c) = \frac{1}{2} eE\lambda/mc$. It is more rigorous to consider the vector momenta between an ion and a molecule, and to equate the mean momentum

lost in a collision with the mean momentum gained from the field between collisions, in which case $v(c) = eE\lambda'/mg$, where g is the mean speed of the ion relative to the molecules, and the equivalent mean free path $\lambda' = \lambda(M+m)/M(1-\overline{\cos\theta})$.

Then
$$\bar{v} = -\frac{4\pi}{3}\int_0^\infty \frac{eE\lambda'}{mg}\frac{df}{dc}c^3dc$$

$$= -\frac{4\pi eE}{3m}\int_c^\infty \frac{\lambda' c^3}{g}\frac{df}{dc}dc.$$

Assumption 2 : λ' is constant, independent of c.

For electrons $g = c$ to give

$$\bar{v}_- = -\frac{4\pi eE\lambda'}{3m}\int_0^\infty c^2\frac{df}{dc}dc \qquad \text{(A3.3)},$$

and it is now necessary to evaluate the zero field distribution f(c).

The Zero Field Distribution Function.

The Boltzmann approach of continuity in phase-space is adopted. From equation (A3.1), the number of ions with velocities between c and (c+δc) is

$$\delta N = N.F(c,\dot{x}).4\pi c^2dc$$

= constant in the steady state.

The mean rate at which energy is supplied to this group of ions by the electric field is

$$NF(c,\dot{x})4\pi c^2 dc.eE.\dot{x} \ ,$$

averaged over all $\dot{x}$, c constant

$$= NeEv4\pi c^2 dc\left[\dot{x}f(c) - \frac{v\dot{x}^2}{c}\frac{df}{dc}\right]$$

by substituting for $F(c,\dot{x})$ from equation (A3.2). As before $v = eE\lambda'/mg$ and $\dot{x} = c\cos\theta$, and the $\dot{x}f(c)$ term $\to 0$ since $f(c)$ is isotropic, so the rate becomes

$$- N\frac{4\pi}{3}\frac{\lambda' c^2 E^2 c^3}{mg}\frac{df}{dc}\,dc \qquad \text{(A3.4)}$$

To maintain a stationary distribution, energy must be lost by collision at the same rate.

Assumption 3 : stationary molecules, $\overline{c^2} = 0$.

Then the energy loss rate is given by

$$Nf(c)^{*}4\pi c^2 dc.\ f\ .\ \tfrac{1}{2}mc^2.\ g/\lambda \qquad \text{(A3.5)}$$

(* It is difficult to justify the use of $f(c)$ here, rather than $F(c,\dot{x})$, though it is necessary to be able to proceed.)

Assumption 4 : elastic collisions, $f = 2mM/(m+M)^2$.

Equating (A3.4) and (A3.5)

$$- N \frac{4\pi}{3} \frac{\lambda' e^2 E^2 c^3}{mg} \frac{df}{dc} dc = N4\pi \frac{m^2 Mg}{(m+M)^2 \lambda} c^4 f(c) dc.$$

Substituting $\lambda = \lambda'.M(1-\overline{\cos\theta})/(m+M)$, where $\overline{\cos\theta} = 0$ for isotropic scatter, and rearranging

$$- \frac{1}{3}\left(\frac{eE\lambda'}{mg}\right)^2 \frac{df}{dc} = - \frac{1}{3}\bar{v}^2 \frac{df}{dc} = \frac{m}{m+M} \; c \; f(c) \qquad (A3.6)$$

subject to

Assumption 5 : the ions are istropically scattered.

Integration gives

$$f(c) = \text{constant} \times \exp\left[- \frac{3m}{m+M} \int \frac{c}{\bar{v}^2} dc\right].$$

If $\overline{C^2} \neq 0$ and $\bar{v} = 0$, f(c) will be Maxwellian, of the form $\exp(-3mc^2/2M\overline{C^2})$, so that $df/dc = (-3mc/M\overline{C^2}).f(c)$. Equation (A3.6), which was derived for $\overline{C^2} = 0$, must be modified so that it will satisfy a Maxwellian distribution when $\bar{v} = 0$; this criterion is satisfied by

$$(\bar{v}^2 + \frac{M}{m+M} \overline{C^2}) \frac{df}{dc} = - \frac{3m}{m+M} c \; f(c).$$

Integration gives

$$f(c) = \text{constant} \times \exp\left[-\frac{3m}{m+M} \int^c \frac{cdc}{\bar{v}^2 + M\overline{C^2}/(m+M)}\right]$$

$$= \text{constant} \times \exp\left[- \int^c \frac{mcdc}{(m+M)\bar{v}^2/3 + kT}\right]$$

and, for electrons, $M \gg m$, $g \approx c \rightarrow \bar{v}_- = \frac{eE\lambda'}{mc}$,

so that $f(c) = \text{constant} \times \exp\left[-\int^{c} \frac{mcdc}{2M(eE\lambda')^2/3(mc)^2+kT}\right]$ (A3.7).

APPENDIX 4

The Pulsed Light Source

A4.1. Introduction.

One of the principal requirements of this experiment was that a short burst of electrons, of maximum duration 20nanoseconds, should be produced in the drift space of the experimental tube, either at the surface of the cathode or, preferably, at any selected position in the drift space. A number of approaches seemed possible -

1. A glow discharge behind a perforated cathode, with a gating electrode to permit short bursts of electrons to pass through the perforations, as used by von Engel, Corrigan and Breare[3.44,3.45]. Careful circuitry should avoid any problems in achieving the necessary pulse length, but this method was not attempted because electron release is limited to a pre-selected area of the cathode, and also because of the dependence of the number of electrons released on the gas pressure, which is a variable parameter in this investigation.

2. Breakdown between the cathode and an auxiliary electrode to which a short pulsed voltage is applied, or between two auxiliary electrodes. A coaxial two-electrode system was constructed and tested under d.c. conditions, when it was found that a sufficient number of initiating electrons was produced to maintain a discharge in the gap, the current in the main gap being dependent on the voltage applied to the auxiliary gap.

However this method was abandoned for the following reasons -

a. To keep the electron swarm dimensions small, the auxiliary gap must be small, $\sim \frac{1}{2}$mm. At the pressures to be used, $\sim$ 1 torr, (pxd) is $\sim$ 0.05 torr.cm, which is well to the left of the Paschen curve (fig.1.2) on the steeply rising portion (pxd_{min} is $\sim$ 1), so that the breakdown voltage is high. This means that large pulsed voltages with fast time characteristics have to be applied to the electrodes.

b. The relatively weak field of the main gap is unlikely to capture electrons from the high field in the auxiliary gap.

c. Distortion of the main field is caused by the introduction of auxiliary electrodes.

3. Localised breakdown of the gas by focussing a Q-switched laser beam. This has the advantage of providing initiating electrons at any point in the gap, without the need to introduce material objects into the gap. At atmospheric pressure the incident power density necessary to achieve local breakdown is $\sim 10^{12}$ watts.cm^{-2}; reduction in gas pressure should not affect this value substantially, though it will reduce the number of electrons produced as the electrons initially stripped from the molecules will decrease with the number density, and subsequent ionisation by electron collision after acceleration in the laser field will also be reduced because of the reduced density. A value of 10^{12} watts.cm^{-2} can be achieved by a medium power ruby laser, with a Q-switched pulse of 1 Joule lasting for about 1 nanosecond and a beam divergence of about 10^{-2} radians, using a focussing lens of focal length of 1 cm. This approach was

considered to be financially unsuitable.

4. Constant ultra-violet irradiation of a metal surface held at a positive d.c. potential so that the photo-electrons are recaptured, except during a very short negative pulse applied to the surface (Smith (1967)[A4.1]). This technique, which would seem to be a simple and effective approach to the problem, was not investigated as a successful alternative was already being developed.

5. Photo-electron release from a surface in the gap by irradiation with a short burst of photons of appropriate energy. This is the method that was selected, and details of the experimental work are given in the following section.

A4.2. Production of Initiating Photoelectrons.

A number of fast pulsed ultra-violet sources has been described in the literature and attempts were made to reproduce several of them. However, their unsuitability for this investigation was in some cases immediately evident from the description, and in other cases only evident when they were reproduced. Some devices could not be operated in a triggered mode (D'Alessio et al (1964)[A4.2], Franke and Schmeing (1967)[A4.3], McMahon et al (1966)[A4.4], Preissinger (1967)[A4.5]), others had insufficient ultra-violet intensity (D'Alessio et al, Omuchin (1966)[A4.6], Tawara (1966)[A4.7]), produced too long a pulse (McMahon et al, Preissinger) or required sophisticated facilities for their construction (Fischer (1961)[A4.8]).

The device first reproduced employed a mercury wetted-contact relay, as described by D'Alessio et al. These relays are normally used to switch low currents on a millisecond or faster time-scale, principally in square-wave pulse generators, the reed being driven magnetically by a helical coil surrounding the relay. The relay consists of a nickel-iron reed and electrode, the reed dipping into a mercury pool which wets the contacts and permits fast switching as well as prolonging the life of the electrodes; the whole is sealed into a glass capsule which is filled with hydrogen to a pressure of 18 atmospheres.

Application of an overvoltage will cause this gap to break down with an accompanying emission of light, the breakdown voltage being about 6kV . To obtain a short pulse of light, the self-capacitance of the relay is charged through a resistance of 250 megohms to give successive pulses at a repetition rate which can be controlled either by altering the charging resistance or by varying the overvoltage. The self-capacitance of the gap was estimated to be 10^{-13}F, giving an energy storage at 6kV of 2×10^{-6} Joules. If this is released in 10^{-8} seconds, the instantaneous power is about 200 watts, equivalent to about 10^{13} photons per pulse if it is assumed that all the energy is radiant.

The relay used was the Adams-Westlake P46-60000. D'Alessio et al had access to the manufacturers facilities and were able to produce a relay in a quartz envelope; in the commercially available form the envelope is glass and, since the high pressure hydrogen

filling precluded any attempts at manufacture in the laboratory, the glass envelope variety had to be used. The consequences of this will be mentioned later, and the data given refers to visible and not ultra-violet radiation.

The temporal characteristics of the lamp were determined using an RCA 1P21 photomultiplier without any additional spectral discrimination, feeding the signal into two different oscilloscope configurations -

1. A Tektronix 519 oscilloscope; this has a bandwidth of 1000Mc/s, but a vertical sensitivity of only 10 volts/cm, with an input impedance of 125 ohms. The photomultiplier output was fed through a 125 ohm cable directly into the oscilloscope input impedance, which formed the anode load, to give a time-constant of 1.3 nanoseconds (the anode-dynode capacitance of the 1P21 is 10.4pF). The minimum signal that could be detected on the oscilloscope was 2 volts, corresponding to a photomultiplier anode current of 16mA, whilst the maximum average current rating for the 1P21 is 0.1mA, so the tube was being heavily over-run even in pulsed operation. The overall voltage applied was 1250 volts to give a gain of 10^7.

Under these conditions the observed temporal characteristics of the lamp were a rise-time of 2 nanoseconds, and a half-width of 10 nanoseconds. Under ideal conditions, the photomultiplier has a rise-time of 1.9 nanoseconds, so that the actual rise-time is $T = (T_o^2 - T_r^2)^{\frac{1}{2}} = (2.0^2 - 1.9^2)^{\frac{1}{2}} = 0.63$ nanoseconds, according to first-

-order pulse theory. The calculated photon output over the range 3100 - 6800Å was 10^8 photons.sterad^{-1}.nanosecond^{-1}, using the manufacturer's characteristics for the photomultiplier.

2. A Tektronix 545A, with type N sampling plug-in unit and type 110 pulse generator; this extends the bandwidth of the 545A oscilloscope from 30Mc/s to the 1000 Mc/s range, with an input sensitivity of 20 millivolts/cm into an impedance of 50 ohms, provided a repetitive waveform is available. This arrangement was employed as the degree of overrunning necessary to provide a sufficient signal from the photomultiplier to operate the 519 oscilloscope slows the response of the photomultiplier.

In practice the maximum sensitivity that could be used was 200 millivolts/cm, due to electrical pick-up from the pulse, requiring an instantaneous anode current of 4mA for a deflection of 1cm. Under these conditions a rise-time of 2.0 nanoseconds and a half-width of 7.5 nanoseconds was observed. Correction of the rise-time again yields a calculated value of 0.63 nanoseconds (the values claimed by D'Alessio et al are rise-time 0.4 ns , half-width 0.5ns). The life of the source would appear to be indefinite, though a small amount of electrode sputtering was apparent, made evident by the tendency of mercury droplets to stick to the glass walls after many hours of operation at repetition rates of about 10^3 p.p.s.

Although a spark in a hydrogen atmosphere using mercury electrodes has a spectrum rich in ultra-violet, as previously mentioned

the only relays available had glass envelopes, so it was necessary to introduce a low work-function surface into the experimental tube to release photo-electrons. This technique, which is briefly described in Section A4.3, was unsuccessful insofar as no photo-electrons were detected, and this type of pulsed lamp was abandoned. Nevertheless, the mercury relay is a useful source of very fast, fairly intense, visible light pulses, and is particularly appropriate for testing the frequency response of photo-electric devices.

A4.3. Attempt to release photo-electrons with visible radiation.

An experimental tube was constructed such that, at the centre of a plane-parallel gap, the tip of a light-guide was coated with a film of strontium. The light pulse from the mercury relay passed down the light-guide onto the strontium film from which, by virtue of its low work function (between 2.06 and 2.47 eV, equivalent to between 6000 and 4500Å), it was intended that photo-electrons should be released. However, no evidence of photo-electrons could be found, and because of the difficulties involved in depositing the film this method was not pursued further.

The deposition technique required that strontium was loaded into the gun whilst immersed in carbon tetrachloride to prevent oxidation, and that the gun was then sealed into the experimental tube and the tube pumped down before the carbon tetrachloride evaporated. The gun was fired by radio-frequency induction heating, and to ensure that the strontium was only deposited on the tip of the light guide it was

necessary to arrange for the gun to be moved into and out of the gap.

The reason for the lack of a detectable photo-electron current, tested with a continuous light source and an electrometer, is not known, but it is presumed that a pure strontium film was not deposited and that the consequent work-function was too high. Alternatively, if the highest value for the work-function of strontium is taken (2.74eV or 4500Å) then, since the transmittance of the tube envelope starts to fall off at 4350Å, very little effective radiation would be incident on the film.

A4.4. Fast Atmospheric Spark Light Sources.

The spectrum of a high voltage spark in air has a considerable ultra-violet content, and several types of device employing an atmospheric spark were constructed. The primary requirement for fast temporal characteristics is that the inductance of the circuit, which almost invariably appears predominantly in the electrode region of the device, should be kept as small as possible, whilst the design must also allow for adequate energy storage if a reasonable spark intensity is to be achieved.

A4.4.1. Coaxial cable devices.

A device of this type was constructed, and consisted simply of a length of coaxial cable with a spark gap inserted in the inner conductor in such a way that the continuity of the cable was disturbed as little as possible. The cable on one side of the spark gap stored

electrical energy, and was charged from a high voltage source through a charging resistance until the gap broke down, when a voltage pulse propagated through the spark gap into the remaining cable, to be absorbed by a matched termination at the far end of the cable. The shape of the light pulse followed fairly closely the shape of the voltage pulse unless the voltage pulse was very short. This device produced a light pulse having a rise time of 10 nsec and a halfwidth of 22 nsec. The intensity was low, and increasing the length of the cable to give greater energy storage also increased the length of the light pulse proportionately, whilst the charging voltage was already in excess of the maximum voltage rating for the cable. The further problem of making this device operate in a triggered low-jitter mode was not attacked, nor was any attempt made to construct an aritificial line with lumped elements.

A4.4.2. Capacitor devices.

A commercially available pulsed ultra-violet source, known as the "Nanolite", prompted the development of the second type of device; the stated risetime of the Nanolite is 2 nsec and the halfwidth 8 nsec. The Nanolite was originally described by Fischer, and consists essentially of a coaxial capacitor of about 500 pF, tapering hemispherically at one end. An electrode pin from the tip of the inner hemisphere passes through a hole in the outer hemisphere to form a coaxial spark gap with a total inductance claimed to be less than 1 nanohenry. The dielectric is PTFE of thickness 0.1mm, machined to fit exactly the contours of the electrodes. The machining of this PTFE shell was beyond the resources

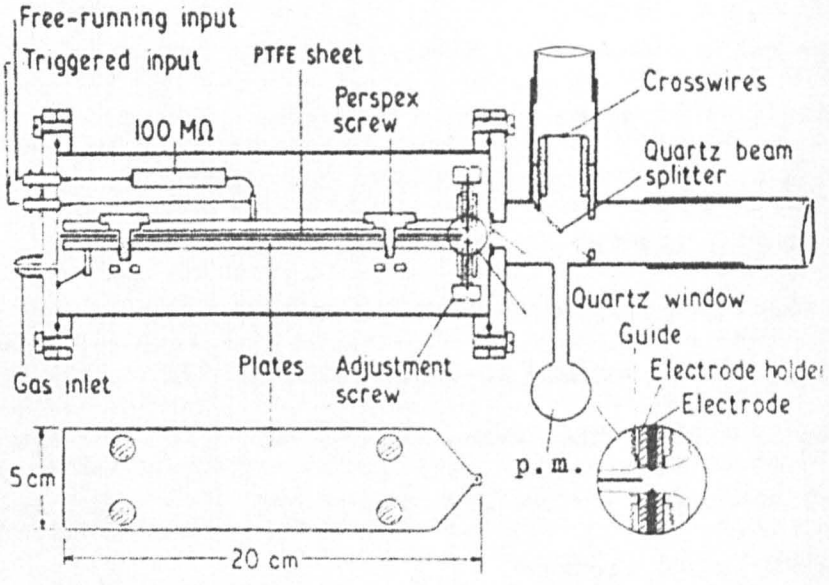

Fig. A4.1

The pulsed light source.

available during the investigation so that the Nanolite could not be reproduced, and the commercially available version was financially unattractive.

The coaxial construction of the Nanolite is an unnecessary artefact, and Fischer's remarks relating the electrical properties to transmission line theory imply erroneously that the fast characteristics of the device arise from its resemblance to a transmission line. In fact it is far too short ($7\frac{1}{2}$ cm) to be treated as a distributed circuit and the hemispherical taper is too abrupt to permit undistorted propagation of a wave; also it is misleading to quote the line inductance of less than 1 nanohenry when the inductance of the spark gap circuit totals about 7 nanohenries (which is still commendably low). Electrically the device can best be described as a high voltage capacitor of minimum inductance, discharging through the inductive-resistive load formed by the spark and the electrodes. Many geometrical configurations will satisfy these criteria, the most obvious possibly being a circular plane-parallel capacitor with an annular spark gap in the centre of one plate. In this investigation the requirements were for a precisely located, intense spark between electrodes that could be easily adjusted or renewed, and for physical dimensions that were not too cumbersome, together with simple and inexpensive fabrication. To satisfy these conditions, a plane-parallel design as shown in fig. A4.1. was chosen.

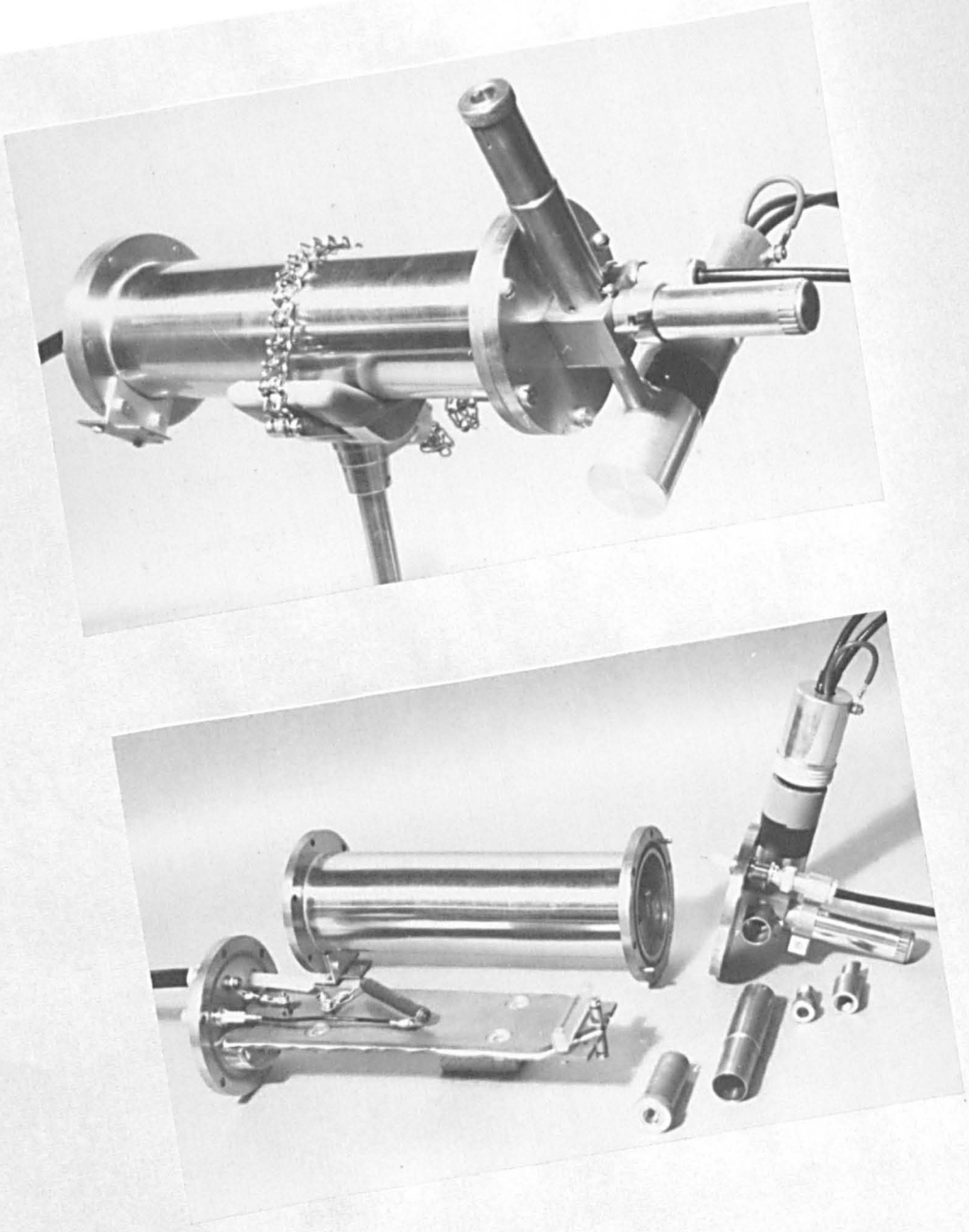

Fig. A4.2

The pulsed ultra-violet source.

The low inductance capacitor was very simply constructed from two copper plates, each of thickness 0.3 cm and of common area 95cm^2, machined flat on the inner surfaces and with radiussed edges to eliminate local high electric fields, and separated by a thin sheet of PTFE (ε = 2.0) for which a thickness of 0.012 cm was normally used, being sufficiently resistant to electrical puncturing, though 0.005cm was also used. These thicknesses represent a compromise between the achievement of high energy storage by designing a capacitor to withstand high voltages, with the accompanying problems of high voltage pulse techniques,and a capacitor of maximum capacity operating at a lower voltage. The electrodes were 0.1 cm diameter tungsten rods, ground to a point having an included angle of 90°, the tip being slightly radiussed to minimise erosion. It was essential to obtain a tight push-fit between the tungsten electrode, the electrode-holder and the guide to maintain the low inductance and resistance path between the plates. The perspex clamping screws were also machined to a push-fit to ensure accurate location of the electrodes, and the guides were carefully drilled so that the electrode tips were directly opposed at all adjustments. This design permits rapid adjustment or renewal of the electrodes. The spark cavity was kept as small as possible to minimise the self-inductance of the circuit, and each plate was recessed to a depth of 0.06 cm. The capacitor was mounted on perspex, for electrical isolation, inside a brass container that could withstand pressures of at least ten atmospheres and also provided electrical screening. After passing through a quartz window, the light pulse was focussed by a simple

quartz lens of focal length 15 cm. Difficulty was experienced in focusing and positioning the light pulse on the polished metal surfaces used in the experimental tube, and the alignment optics was added to the device.

The optics was initially adjusted under favourable viewing and ambient light conditions, after which it was only necessary to sight the target through the optics so that it lay on the cross-wires and was in focus. The initial adjustment of the optics was made by focussing the light output under subdued ambient lighting onto a translucent screen marked with a cross, and then adjusting the beam-splitter and the cross-wires so that the image of the cross coincided with the cross-wires without parallax. The beam-splitter, having two partially reflecting surfaces, produced a double image, and it was necessary always to use the same image. A 931A photomultiplier was attached to the side of the optics opposite to the eyepiece, and was used to monitor the fraction of the light output reflected onto it by the beam-splitter; attenuators had to be placed in front of the photomultiplier to prevent gross overloading. The signal from this arrangement was used for the provision of timing marks and to trigger the oscilloscope, but not to determine the temporal characteristics of the pulsed ultra-violet source.

The u.v. source could either be used in a free-running mode, when the capacitor was simply charged through a limiting resistor of 10^6 ohms until the sparking potential was reached, so that the repetition

rate depended on the applied voltage, or in a low-jitter triggered mode by applying a negative pulse of amplitude 2000 volts, rise-time 50 nsec (fig. A4.3d) generated by the circuit described in section 4.3.

It was found that the optimum electrode spacing was about 6×10^{-3} cm, which gave moderate intensity with reliable operation and the minimum of electrode erosion; the corresponding sparking potential was 500 volts, and the gap could be rapidly adjusted to this value. More than 10^4 pulses could be obtained before unreliable operation made adjustment of the electrodes necessary.

The inductance of the device was not measured, but if the spark gap is approximated to a circle of diameter 0.12 cm the inductance, given by $L = \frac{1}{2}\mu_o \pi r$, is 1.2×10^{-9} henries. The resistance of the spark channel is variable and difficult to estimate, but is probably $\sim$ 1 ohm at peak current. The capacitance is discharged through the series resistance and inductance to give a damped oscillatory current of period $T = 2\pi(LC)^{\frac{1}{2}} = 8.3$ nsec, the condition for critical damping being R = 1.8 ohms. Thus the model assumed is that of a slightly over-damped series LCR circuit, and this was supported by the waveform of the electrical pick-up from the spark, though the current transients were not measured directly. If the light output follows the current closely, a rise-time of 0.4 nsec and a half-width of 1.6 nsec are predicted at critical damping. The measured values of 3.0 and 7.5 nsec are in reasonable agreement in view of the uncertainty in the value of R.

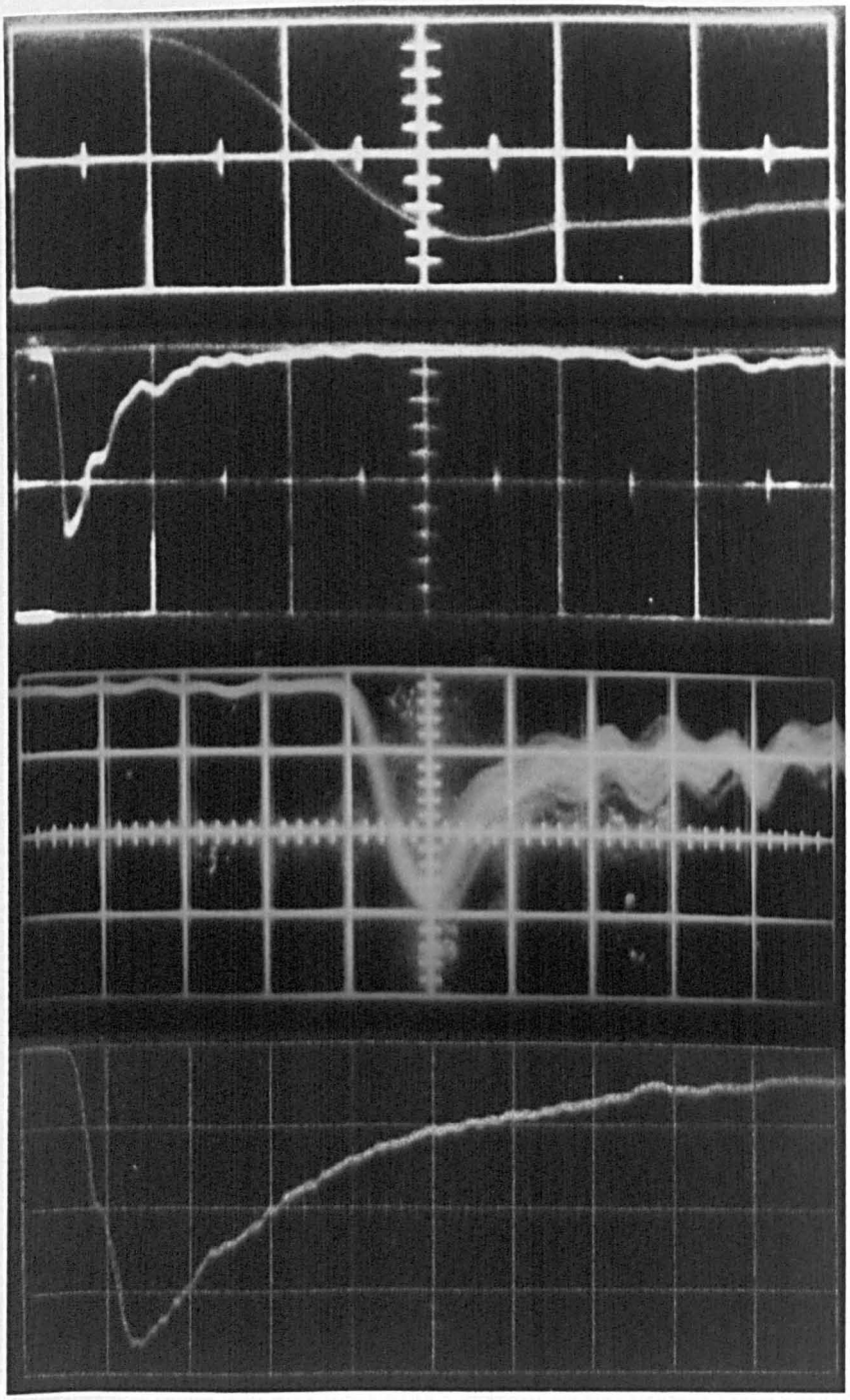

(a)
2ns/div.
10 pulses

(b)
20ns/div.
1 pulse

(c)
20ns/div.
40 pulses

(d)
100ns/div.
1 pulse

Fig. A4.3

Light source traces

(a) & (b) free-running u.v. pulses, (c) triggered u.v. pulse, (d) voltage pulse.

To further shorten the predicted temporal characteristics, keeping the capacitance large for adequate energy storage and having no control over the spark resistance, it would be necessary to further decrease the inductance by more careful design and construction of the gap.

A4.4.3. Light Source Characteristics.

The output of the light source, after suitable attenuation to prevent overloading, was measured by a Philips 56AVP photomultiplier with the output signal developed directly across the 125 ohm input resistance of a Tektronix 519 oscilloscope. The photomultiplier rise-time was 2 nsec for small signals, whilst that of the oscilloscope was only 0.35 nsec and so did not impose any limitations. The 56AVP photomultiplier can be operated at a gain of 10^8 and the maximum anode current is 100mA, which is adequate to drive the input stage of the 519 oscilloscope.

Figs A4.3a and A4.3b show the shape of the free-running ultra-violet pulse, indicating a half-width of 8.0 nsec and a rise-time of 3.6 nsec; if a correction is applied for the detector bandwidth, these values become 7.5 and 3.0 nsec. In this mode, provided the electrodes are not badly eroded, the reproducibility is good, as indicated by the 10 superimposed pulses in fig.A4.3c. In the triggered mode the rise-time remains the same, but the half-width becomes 23 nsec, which was adequate for this investigation, though it is considered that

attention paid to shortening of the electrical firing pulse (rise-time 50 nsec, and half-width 250 nsec - fig. A4.3d) could result in shortening of the ultra-violet pulse. Fig. A4.3c, which was obtained with a different detection system (931A photomultiplier and 545A oscilloscope) and does not illustrate the true shape of the u.v. pulse, shows that the jitter is ±3.5 nsec over 40 pulses, with respect to the triggering pulse applied to the grid of the XH3-045 thyratron (see fig. 4.11), and that the reproducibility is good on the leading edge and fair on the trailing edge. The tail of the pulse falls more rapidly than shown, and the 10%-10% width is 35 nsec.

The output energy did not vary appreciably between the free-running and the triggered modes, and the data following is for the free-running mode at a sparking potential of 500 volts. The total output between 2000Å and 7000Å was approximately 10^9 photons per pulse, emanating from a virtual point (the spark channel length was 6×10^{-3} cm and the diameter 1×10^{-2} cm), of which 88% lay between 2000Å and 3000Å. This is equivalent to a surface brightness of 50 watts.cm^{-2} and a mean power of 10^{-2} watts during the pulse. In the triggered mode the total output depended on the electrical energy available from the driving circuit, and with 0.005 μF at 2.5 kV, the output was a factor of two to three greater than in the free-running mode.

The spectrum was recorded photographically on Agfa Isopan-Record film using a Bausch and Lomb 1.5 metre grating spectrograph. Even with this fast film (800 ASA when developed for maximum speed), long exposures of about 30 minutes at pulse repetition rates of 20 sec^{-1} were

needed for adequate exposure because of the very small duty cycle of the lamp; the integrated exposure time under these conditions was only about 0.3 millisec. The observed spectrum consisted of a continuum extending from 2300Å to 6800Å, the limits of the photographic emulsion, with a number of lines superimposed, amongst which were identified tungsten, molybdenum and neodymium. These are the basic material and impurities present in the electrodes, indicating that an arc was formed. The continuum is presumed to be that of an atmospheric spark. Time-resolved spectroscopy was beyond the scope of the available facilities. The temporal characteristics of the light pulse were measured in the visible region using the 56AVP photomultiplier, but measurements made with an ultra-violet sensitive 1P28 photomultiplier indicated no appreciable difference, though the 1P28 suffers some loss of frequency response when drawing the large currents necessary to drive the 519 oscilloscope.

Excited state lifetimes in air at atmospheric pressure are about 1 nsec, but it was thought that a small improvement in the temporal characteristics might be achieved by pressurisation of the spark gap, and a range of pressures between 0.1 and 8 atmospheres in nitrogen was investigated. The half-width of the ultra-violet pulse was slightly decreased to 6.5 nsec at 0.5 atmospheres, but overall there was a roughly linear increase to 30 nsec at 2.5 atmospheres, above which it remained constant at 30 nsec. From a superficial investigation it appears that, in the linear region, the half-width is a function of the sparking potential V_s, and therefore of the (pxd)

product, since if V_s was kept constant by adjustment of p and d, the half-width remained constant. It is suggested that this increase of half-width with pressure, which is also recorded by Onuchin, can be attributed to the increasing spark resistance with pressure, which results in increasing over-damping of the LCR circuit. The only advantage to be derived from pressurisation is increased light output at the expense of accelerated electrode erosion.

Appendix 5

A MODEL FOR ELECTRON AVALANCHE RUNAWAY

Runaway can either be partial, when energy is lost by collision at a rate unequal to that at which it is gained from the field, or total, when there are no loss processes. The latter case is trivial, being a description of an electron freely accelerating in a uniform electric field. Thermal velocities ($\simeq 1.2\times10^{7}$cm.sec^{-1} at 300°K) and therefore diffusion, and also the initial velocity are relatively small and can be neglected, so that the transit time is given by

$$t_{-} = (2md/eE)^{\frac{1}{2}} = d(2m/eV_a)^{\frac{1}{2}} .$$

Thus $$v_{-app} = d/t_{-} = (\tfrac{1}{2}eV_a/m)^{\frac{1}{2}} ,$$

and v_{-app} is expected to be proportional to $(V_a)^{\frac{1}{2}}$ only.

For the case of partial runaway, consider a very short pulse of electrons released at the cathode of a uniform field drift space (E volts.cm^{-1}) with average energy ε_o, about which the spread of energy is assumed to be negligible. A Langevin type model is adopted, in which the electrons drift in the field direction, suffering identical collisions with gas molecules at equal distance intervals, and losing an equal fraction of their energy at each collision. The Ramsauer effect is neglected.

Let f = fractional energy loss on collision

λ = electron mean free path in field direction

d = total drift distance

V = total applied voltage = $E \times d$

ε_o, v_o = initial energy, velocity

ε_n, v_n = energy, velocity before nth collision

ε'_n, v'_n = energy, velocity after nth collision

ε = energy acquired between collisions = $eV\lambda/d$.

Then

$$\varepsilon'_1 = (1 - f)(\varepsilon_o + \varepsilon) ,$$

$$\varepsilon'_2 = (1 - f)^2\varepsilon_o + \left[(1 - f)^2 + (1 - f)\right]\varepsilon ,$$

$$\varepsilon'_n = (1 - f)^n\varepsilon_o + \left[(1 - f)^n + \ldots. + (1 - f)\right]\varepsilon ,$$

and $$\varepsilon_n = (1 - f)^{n-1}\varepsilon_o + \left[(1 - f)^{n-1} + \ldots. + (1 - f) + 1\right]\varepsilon .$$

Now the time spent between the (n-1)th and nth collisions is

$$t_n = \frac{md}{eV}(v_n - v'_{n-1}) .$$

Also

$$\begin{cases} \frac{1}{2}mv'^2_{n-1} = \varepsilon'_{n-1} \rightarrow v'_{n-1} = \left(\frac{2}{m} \cdot \varepsilon'_{n-1}\right)^{\frac{1}{2}} \\ \frac{1}{2}mv^2_n = \varepsilon_n \rightarrow v_n = \left(\frac{2}{m} \cdot \varepsilon_n\right)^{\frac{1}{2}} \end{cases}$$

so that

$$t_n = \left(\frac{2md^2}{e^2V^2}\right)^{\frac{1}{2}} \cdot \left[(\varepsilon_n)^{\frac{1}{2}} - (\varepsilon'_{n-1})^{\frac{1}{2}}\right].$$

Assuming that the interaction time is negligible compared with the time between collisions, the electron transit time is given by

$$t_- = \sum_{n=1}^{d/\lambda} t_n .$$

Thus $$v_{-app} = d/\Sigma t_n$$

where

$$\Sigma t_n = \left(\frac{2md^2}{eV^2}\right)^{\frac{1}{2}} \cdot \sum_{n=1}^{d/\lambda} \left[V_o(1-f)^n + V\frac{\lambda}{d}\left(\frac{1-(1-f)^n}{f(1-f)}\right)\right]^{\frac{1}{2}} - \left[V_o(1-f)^{n-2} + V\frac{\lambda}{d}\left(\frac{1-(1-f)^{n-2}}{f(1-f)} + 1\right)\right]^{\frac{1}{2}}$$

since $$(1-f)^n + \ldots + (1-f) = \frac{1-(1-f)^n}{f(1-f)} .$$

special case 1 : f = 1

$$\Sigma t_n = \left(\frac{2md^2}{eV^2}\right)^{\frac{1}{2}} \cdot \sum\left(V.\frac{\lambda}{d}\right)^{\frac{1}{2}} = \left(\frac{2md^2}{eV^2}\right)^{\frac{1}{2}} \left(\frac{d}{\lambda} = 2\right)\left(V\frac{\lambda}{d}\right)^{\frac{1}{2}}$$

$$\rightarrow \quad v_{-app} = \left(\tfrac{1}{2}.\frac{eV\lambda}{md}\right)^{\frac{1}{2}} \qquad \text{if } d >> \lambda \qquad (A5.1)$$

(c.f. the mean velocity between collisions $\bar{v} = \frac{1}{2}v = (\frac{1}{2}eV\lambda/md)^{\frac{1}{2}}$, since $\frac{1}{2}mv^2 = eV\lambda/d$.)

special case 2 : f = 0

$$\Sigma t_n = \left(\frac{2md^2}{eV^2}\right)^{\frac{1}{2}} \cdot \sum\left[(V_o + V)^{\frac{1}{2}} + (V_o)^{\frac{1}{2}}\right] \quad \text{since } \lambda \simeq d$$

$$\rightarrow \quad v_{-app} = \frac{\lambda}{d}\left(\tfrac{1}{2}\frac{e}{m}\right)^{\frac{1}{2}} \cdot \frac{V}{(V_o+V)^{\frac{1}{2}}+V_o^{\frac{1}{2}}}$$

$$\simeq \left(\tfrac{1}{2}.\frac{eV}{m}\right)^{\frac{1}{2}} \qquad \text{if } V >> V_o \qquad \text{(A5.2)}$$

(c.f. the mean velocity of an electron freely accelerating through a potential V is $v = (\frac{1}{2}eV/m)^{\frac{1}{2}}$.)

special case 3 : $V_o << V$, $f \neq 0$ or 1

$$\Sigma t_n = \left(\frac{2md^2}{eV^2} .V \frac{\lambda}{d}\right)^{\frac{1}{2}} \cdot \sum\left[\left(\frac{1-(1-f)^n}{f(1-f)}\right)^{\frac{1}{2}} - \left(\frac{1-(1-f)^{n-2}}{f(1-f)} + 1\right)^{\frac{1}{2}}\right]$$

$$= \left(\frac{2md\lambda}{eV}\right)^{\frac{1}{2}} \cdot F\left(\frac{d}{\lambda}, f\right) \qquad \text{since } n = \frac{d}{\lambda},$$

so that

$$v_{-app} = \left(\tfrac{1}{2}\frac{e}{m}\frac{d}{\lambda}V\right)^{\frac{1}{2}} . G\left(\frac{d}{\lambda}, f\right) \qquad \text{(A5.3)}$$

where $G(d/\lambda, f) = 1/F(d/\lambda, f)$.

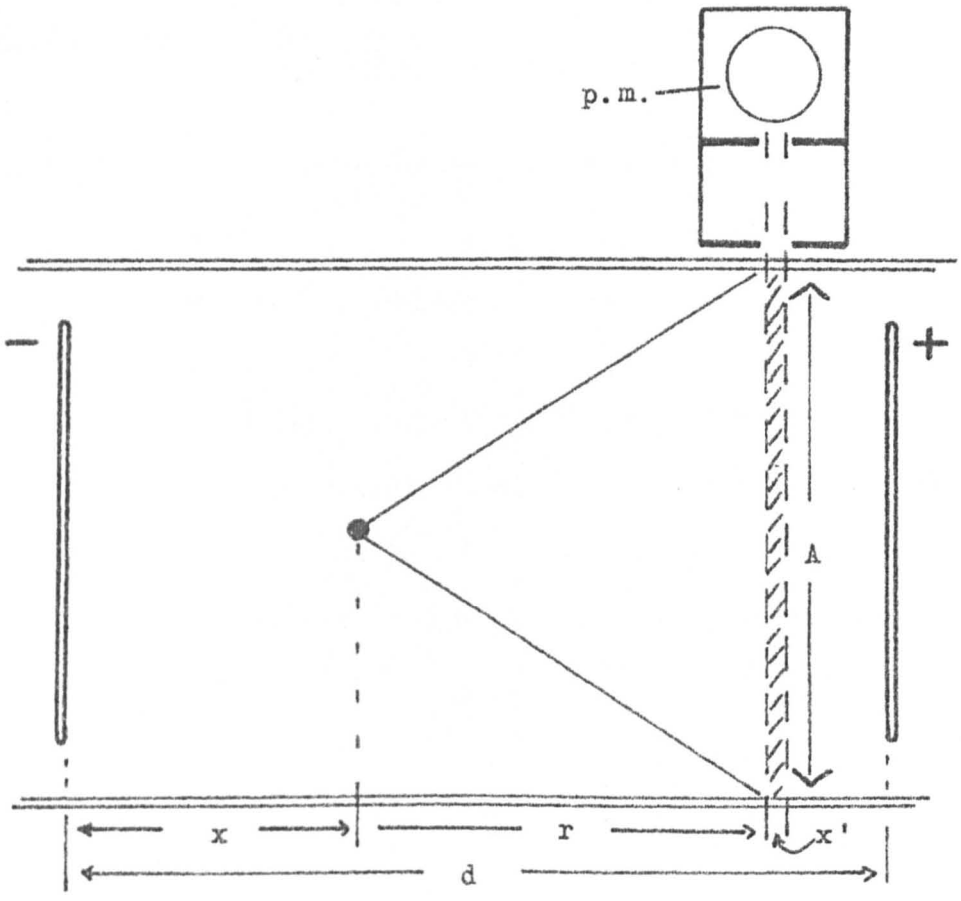

Fig. A6.1

Experimental geometry for the resonance radiation model.

Appendix 6

A MODEL FOR THE RESONANCE SCATTER OF PHOTONS INTO THE PHOTOMULTIPLIERS

Suppose that the experimental geometry (fig. A6.1) is such that, in the shaded region viewed by the photo-multiplier, there is a number N.A.δx of uniformly distributed excited molecules, which emit radiation isotropically on decay, and that the fraction which is detected is given by a factor g. Let there be δ/α exciting collisions per ionising collision, and suppose that there is an avalanche of $n = n_o \exp(\alpha x)$ electrons at a distance r from the shaded region. Then the number of photons which intercept the shaded region is given by

$$n_p = (A/4\pi r^2)\ (\delta/\alpha)\ n_o \exp(\alpha x).$$

If σ is the differential absorption cross-section, the number of photons absorbed in this region is

$$n_p' = NAx'\sigma(\delta A/4\pi r^2\alpha)n_o \exp(\alpha x),$$

so that the number detected on re-radiation is given by

$$n_p'' = f.g.n_o.A.N.\sigma.\delta.x'.\exp(\alpha x)/4\pi r^2\alpha$$

where f is the fluorescence conversion efficiency to "detectable" radiation.

Now, for constant gas temperature and volume, N α p, to give

$$n''_p = K.g.\sigma.\delta.p.n_o \exp(\alpha x)/ (d-x)^2$$

where r = (d-x), and K is a constant.

The number of photons detected from a true avalanche is

$$n_t = g.\delta.n_o \exp(\alpha d)/\alpha \quad ,$$

so a spurious signal would be detected when $n''_p = n_t$, that is when

$$(d-x)^2.\exp(f(\frac{E}{p}).p(d-x)) = K.\delta.p \qquad (A6.1)$$

Solution of this equation for x would allow the true drift velocity to be calculated from $v_- = x/t_{-app}$. The ratio of the true and apparent drift velocities is given by

$$v_{-app}/v_- = d/x.$$

It is possible to quickly ascertain the nature of the solution for x under certain conditions, and thus to calculate how v_{-app}/v_- will vary.

1. E/p, d, σ constant $\rightarrow$ $x \alpha (1/p).\ln(1/p)$

so that $v_{-app}/v_- \alpha p/\ln(1/p)$ (A6.2)

2. E/p, p, σ constant $\rightarrow$ x = d + constant

so that $v_{-app}/v_{-} = d/(d + \text{const}) \propto d$ (A6.3)

3. p,d, σ constant $\rightarrow$ $x \propto f(E/p) = \alpha/p$

so that $v_{-app}/v_{-} \propto 1/f(E/p)$ (A6.4)

and since $v_{-} = g(E/p)$, $v_{-app} = h(E/p)$ (A6.5).

The form of $h(E/p) = g(E/p)/f(E/p)$ is shown in fig. 5.8.

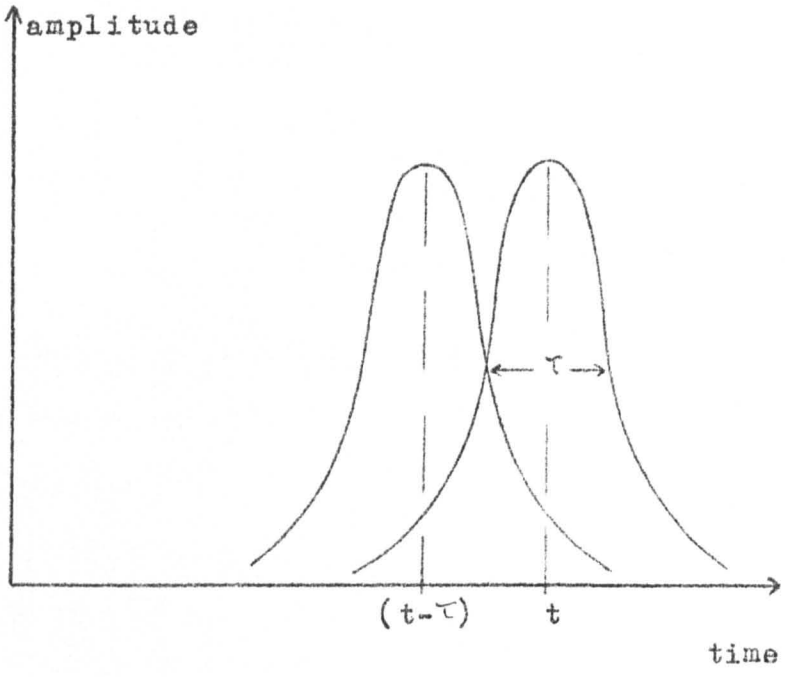

Fig. A7.1

Resolution of two avalanches.

Appendix 7

CRITERION FOR THE RESOLUTION OF PRIMARY AND SECONDARY AVALANCHES

The only secondary process that is sufficiently rapid to cause merging of primary and secondary avalanches is the release of photo-electrons from the cathode.

The criterion adopted for resolution of two avalanches (fig. A7.1) is that, if the peaks of the avalanches are separated by τ, the width of each avalanche (in units of time), the peak amplitude of the secondary avalanche should be less than that of the primary.

At time t, the number of electrons in the primary avalanche is given by

$$n_1 = n_o \exp(\alpha v_- t) ,$$

and the number in the secondary avalanche by

$$n_2 = n_o' \exp(\alpha v_- (t - \tau))$$

$$= \frac{\delta'}{\alpha} n_o \exp(\alpha v_- (t - \tau)),$$

where δ'/α is the ratio of secondary photo-electrons to ionising collisions in the gas.

Thus the condition for resolution is

$$n_1 > n_2$$

i.e. $$n_o \exp(\alpha v_- t) > \frac{\delta'}{\alpha} n_o \exp(\alpha v_-(t - \tau))$$

or $$\frac{\delta'}{\alpha} < \exp(\alpha v_- \tau).$$

Summary of

electron multiplier data						photo-								
E/P v/cm/t.	V_c v	P torr	$e^{\alpha d}$	p.d t.cm	$v_x 10^7$ cm/sec	E/P v/cm/t.	V_c v	P torr	$e^{\alpha d}$	p.d t.cm	$v_x 10^7$ cm/sec	E/P v/cm/t	V_c v	P torr
55	571	.95	9	11.3	2.71	27	1135	3.50	4	40.2	7.61	40	1262	2.64
60	531	.80	11	9.5	2.82	30	958	2.64	5	30.4	5.53	41	1160	2.41
70	504	.66	17	7.8	3.66	34	831	2.08	6	23.9	4.36	45	446	1.86
82	503	.56	34	6.6	5.33	36	749	1.77	8	20.4	3.78	53	916	1.66
118	535	.41	60	4.9	6.76	39	703	1.50	14	17.2	2.75	56	872	1.30
151	583	.35	100	4.2	7.50	46	623	1.13	30	13.0	2.07	70	821	.98
186	650	.32	181	3.8	9.19	49	571	.97	33	11.1	1.90	82	813	.83
202	711	.32	270	3.8	9.90	58	541	.79	67	9.1	1.59	117	860	.62
236	667	.30	299	3.6	10.41	68	509	.63	134	7.2	2.07	145	933	.54
364	1033	.26	492	3.1	13.10	83	502	.51	330	5.9	2.81	170	1049	.52
40	1188	2.73	19	32.4	2.20	107	536	.42	880	4.8	4.63	196	1167	.50
56	1088	1.77	13	21.0	2.76	144	582	.34	2430	3.9	5.27	32	1188	3.13
56	663	1.08	8	12.8	2.47	153	582	.32	2520	3.7	5.11	33	1012	2.61
65	1004	1.42	10	16.9	3.12	199	711	.30	9480	3.4	6.67	36	903	2.10
85	1009	1.08	8	12.8	4.24	230	766	.28	2.16^4	3.2	7.13	39	846	1.83
97	489	0.46	3	5.5	4.62	300	890	.25	1.38^4	2.9	8.62	45	745	1.40
131	663	0.46	3	5.5	6.98	362	1032	.24	1.87^4	2.8	6.04	50	693	1.16
200	1009	0.46	3	5.5	9.90	165	649	.33	6530	3.8	6.24	56	660	1.00
-	-	-	-	-	-	39	1242	2.71	74	31.2	12.26	71	622	.74

the Experimental Data.

multiplier data															
$e^{\alpha d}$	p.d t.cm	$V_a 10^7$ cm/sec	E/p v/cm/t	V_a v	p torr	$e^{\alpha d}$	p.d t.cm	$V_a 10^7$ cm/sec	E/p v/cm/t	V_a v	p torr	$e^{\alpha d}$	p.d t.cm	$V_a 10^7$ cm/sec
110	30.4	12.42	85	617	.61	1210	7.0	2.64	231	1100	.40	6.04^5	4.6	6.98
110	27.7	11.48	114	651	.48	6.30^4	5.5	3.61	28	1135	3.42	2	22.2	5.47
200	21.4	8.56	161	705	.42	1.07^4	4.8	4.44	28	958	2.86	2	18.6	2.56
493	16.8	7.30	171	774	.38	3.52^4	4.4	4.99	32	831	2.15	3	14.0	2.01
3590	14.9	6.75	194	853	.37	6.46^4	4.2	5.20	36	749	1.75	4	11.4	2.18
9860	11.3	5.28	239	907	.32	527^4	3.7	4.99	39	703	1.51	5	9.8	2.53
9620	9.5	5.60	297	1096	.31	1.31^5	3.6	5.20	44	623	1.18	6	7.7	3.09
6.22^4	7.1	5.91	36	1207	2.55	30	32.8	11.73	52	570	.93	10	6.0	2.03
2.38^5	6.2	6.79	37	1070	2.06	27	28.3	9.61	54	541	.84	10	5.5	2.82
1.67^6	5.9	8.15	39	989	2.13	36	24.5	8.17	65	509	.66	17	4.3	2.62
3.56^6	5.7	7.72	46	867	1.60	100	18.4	6.18	81	503	.52	29	3.4	3.58
11	36.0	9.74	50	802	1.34	164	15.4	5.37	120	535	.37	60	2.4	5.24
9	30.0	7.74	58	761	1.11	403	12.8	4.62	139	583	.35	110	2.3	6.06
15	24.1	8.05	70	721	.87	898	10.0	3.68	160	649	.36	200	2.2	7.20
21	21.0	5.76	85	717	.71	3890	8.2	4.14	193	711	.31	221	2.0	6.99
45	16.1	3.95	115	753	.55	1.53^4	6.3	4.74	246	767	.26	245	1.7	8.84
148	13.3	3.24	146	818	.47	5.79^4	5.4	5.30	294	890	.25	330	1.6	7.71
134	11.5	2.57	172	903	.44	1.96^5	5.1	6.22	362	1033	.24	403	1.7	12.97
493	8.5	2.20	201	1002	.42	3.35^5	4.8	6.76	-	-	-	-	-	-

REFERENCES

1.1. Townsend, J.S. "The Theory of Ionisation of Gases by Collision". Methuen. 18. 1910.

1.2. Von Engel, A. "Handbuch der Physik". Springer. 21. 504. 1956.

1.3. Smith, D. B.J.A.P. 16. 697. 1965.

1.4. Brown, S.C. "Introduction to Electrical Discharges in Gases". Wiley. 99. 1966.

1.5. Emeleus, K.G.
Lunt, R.W.
Meek, C.A. Proc.Roy.Soc. A156. 394. 1936.

1.6. Blevin, H.A.
Haydon, S.C. Aust.J.Phys. 10. 590. 1957.

1.7. Blevin, H.A.
Haydon, S.C.
Somerville, J.M. Nature. 179. 38. 1957.

1.8. Rose, D.J.
DeBitetto, D.J.
Fisher, L. Nature. 1771 945. 1956.

1.9. Schram, B.L.
Boerboom, A.J.H.
Kleine, W.
Kistemaker, J. Physica. 32. 749. 1966.

1.10. Bartholomeyczyk, W. Z.fur Phys. 116. 235. 1940.

1.11. Dutton, J.
Haydon, S.C.
Llewellyn Jones, F.
Davidson, P.M. B.J.A.P. 4. 170. 1953.

Davidson, P.M. Phys. Rev. 99. 1072. 1955.

Davidson, P.M. Phys. Rev. 103. 1897. 1956.

1.12. Davies, D.K
Llewellyn Jones, F.
Morgan, C.G. Proc.Phys.Soc. 81. 677. 1963.
and
Proc.Phys.Soc. 83. 137. 1964.

1.13. Betts, B.P. Ph.D. Thesis, Keele Univ. 1965.

1.14. Morgan, C.G.
Williams, W.T.
Proc.Phys.Soc. 85. 443. 1965.

1.15. Evans, G.
Ph.D. Thesis, Keele Univ. 1967.

1.16. Willis, B.A.
Morgan, C.G.
J.Phys.D. 2. 1567. 1969.

1.17. Davies, D.E.
Smith, D.
Myatt, J.
Proc.5th.Int.Conf. Ion Phen.in Gases. 678. 1961.

1.18. Overton, G.D.N.
Smith, D.
Davies, D.E.
B.J.A.P. 16. 731. 1965.

1.19. Loeb, L.B.
"Basic Processes of Gaseous Electronics". U.C.P. 1955.

1.20. Raether, H.
Z.fur Phys. 112. 464. 1939.

1.21. Hasted, J.B.
"Physics of Atomic Collisions". Butterworth. 360. 1964.

1.22. Dawson, G.A.
Z.fur Phys. 183. 172. 1965.

1.23. Dawson, G.A.
Winn, W.P.
Z.fur Phys. 183. 159. 1965.

1.24. Tholl, H.
Z.fur Phys. 172. 536. 1963.

1.25. Kruithoff, A.A.
Penning, F.M.
Physica 3. 515. 1936.

1.26. Chanin, L.M.
Rork, G.D.
Phys.Rev. 135. 71. 1964.

2.1. Schulz, G.J.
Westinghouse Research Report 64-928-113-P1. 1964.

2.2. Herzberg, G.
"Molecular Spectra and Molecular Structure". Van Nostrand. 1950.

2.3. Von Engel, A.
"Ionised Gases". Oxford. 1965.

2.4. Langevin, P.
Ann.Chim.& Phys. 28. 317. 1903.

2.5. Langevin, P.
Ann. Chim.& Phys. 5. 245. 1905.

2.6. Thomson, J.J.
Phil.Mag. 47. 337. 1924.

2.7. Frost, L.S.
Phelps, A.V.
Westinghouse Research Report 62-908-113-P1. 1962.

2.8. Englander-Golden, P. Rapp, D. — Lockheed Report. LMSC 6-74-64-12. 1964.

2.9. Morse, P.M. — Phys.Rev. 90. 51. 1953.

2.10. Gerjuoy, E. Stein, S. — Phys.Rev. 98. 1848. 1955.

2.11. Frost, L.S. Phelps, A.V. — Proc.5th.Int.Conf. Ion Phen.in Gases 192. 1961.

2.12. Pidduck, F.B. — Proc.Roy.Soc. A88. 296. 1913.

2.13. Compton, K.T. — Rev.Mod.Phys. 2. 210. 1925. (Review article, original 1918).

2.14. Hertz, G. — Z.fur Phys. 32. 298. 1925.

2.15. Druyvesteyn, M.J. — Physica. 10. 61. 1930.

2.16. Morse, P.M. Allis, W.P. Lamar, E.S. — Phys.Rev. 48. 412. 1935.

2.17. Allis, W.P. Allen, H.W. — Phys. Rev. 52. 703. 1937.

2.18. Davydov, B. — Phys.Z.Sowjet. 8. 59. 1935.

2.19. Smit, J.A. — Physica. 3. 543. 1937.

2.20. Healey, R.H. Read, J.W. — "The Behaviour of Slow Electrons in Gases". A.W.A. Sydney. 1941.

2.21. Yarnold, G.D. — Phil.Mag. 38. 186. 1947.

2.22. Holstein, T.R. — Phys.Rev. 82. 567. 1951.

2.23. Barbiere, D. — Phys.Rev. 84. 653. 1951.

2.24. Huxley, L.G.H. — Aust.J.Phys. 13. 578. 1960.

2.25. Huxley, L.G.H. — Aust.J.Phys. 13. 718. 1960.

2.26. Huxley, L.G.H. Crompton, R.W. — "Atomic and Molecular Processes" ed. D.R.Bates. Acad.Press. 1962.

2.27. Allis, W.P. — "Handbuch der Physik". Springer. 21. 383. 1956.

2.28. Arthurs, A.M. Dalgarno, A. — Proc.Roy.Soc. A256. 552. 1960.

2.29. Heylen, A.E.D. — Proc.Phys.Soc. 76. 779. 1960.

2.30. Demetriades, A. Hill, J.H. — J.Appl.Phys. 36. 747. 1965.

2.31. Ward, A.L. — J.Appl.Phys. 36. 1291. 1965.

2.32. Lawson, P.A. Lucas, J. — Proc.Phys.Soc. 85. 177. 1965.

2.33. Lawson, P.A. Lucas, J. — B.J.A.P. 16. 1813. 1965.

3.1. Townsend, J.S. Tizard, H.T. — Proc.Roy.Soc. A88. 336. 1913.

3.2. Hershey, A.V. — Phys.Rev. 54. 237. 1938.

3.3. Huxley, L.G.H.(e.g.) Zaazou, A.A. — Proc.Roy.Soc. A196. 402. 1949.

3.4. Townsend, J.S.(e.g.) Bailey, V.A. — Phil.Mag. 47. 873. 1921.

3.5. Crompton, R.W. Elford, M.T. Gascoigne, J. — Aust.J.Phys. 18. 409. 1965.

3.6. Liley, B.S. — Aust.J.Phys. 20. 527. 1967.

3.7. Bradbury, N.E. Nielsen, R.A. — Phys.Rev. 49. 388. 1936.

3.8. Loeb, L.B. — Phys.Rev. 48. 684. 1935.

3.9. Lusk, H.F. — M.Sc.Thesis, Univ.of Cal. 1927.

3.10. Cravath, A.M. — Phys.Rev. 34. 605. 1929.

3.11. Van de Graaff, R.J. — Phil.Mag. 6. 210. 1929.

3.12. Loeb, L.B. — Phys.Rev. 19. 24. 1927.

3.13. Compton, K.T. — Rev.Mod.Phys. 2. 123. 1930.

3.14. Pack, J.L. Phelps, A.V. — Phys.Rev. 121. 798. 1961.

3.15. Prasad, A.N. Smeaton, G.P. — B.J.A.P. 18. 371. 1967.

3.16. Wahlin, H.B. — Phys.Rev. 37. 260. 1931.

3.17. Allis, W.P. — "Handbuch der Physik". Springer. 21. 413. 1956.

3.18.	Lowke, J.J.	Aust.J.Phys.	16.	115.	1963.
3.19.	Legler, W.	Z.fur Phys.	173.	169.	1963.
3.20.	Dibbern, U.	Z.fur Phys.	163.	582.	1961.
3.21.	Frommhold, L.	Z.fur Phys.	160.	554.	1960.
3.22.	Rose, D.J.	Phys.Rev.	104.	273.	1956.
3.23.	Masch, K.	Ark.Electrotech.	26.	587.	1932.
3.24.	Jager, G. Otto, W.	Z.fur Phys.	169.	517.	1962.
3.25.	De la Rue, W. Muller, W.H.	Phil.Trans.Roy. Soc.	171.	109.	1880.
3.26.	Paschen, F.	Weid.Ann.	37.	69.	1889.
3.27.	Carr, W.R.	Phil.Trans.	A201.	403.	1903.
3.28.	Engstrom, R.W. Huxford, W.S.	Phys.Rev.	58.	67.	1940.
3.29.	Von Gugelberg, E.L.	Helv.Phys.Acta.	20.	307.	1947.
3.30.	Bartholomeyczyk, W.	Z.fur Phys.	116.	235.	1940.
3.31.	Davies, D.K. Llewellyn Jones, F. Morgan, C.G.	Proc.Phys.Soc. and Proc.Phys.Soc.	81. 83.	677. 137.	1963. 1964.
3.32.	Williams, W.T. Morgan, C.G.	Proc.Phys.Soc.	85.	443.	1965.
3.33.	Betts, B.P.	Ph.D. Thesis, Keele Univ.			1965.
3.34.	Willis, B.A. Morgan, C.G.	J.Phys.D.	2.	1567.	1969.
3.35.	Davidson, P.M.	B.J.A.P.	4.	171.	1953.
3.36.	Molnar, J.P.	Phys.Rev.	83.	933.	1951.
3.37.	Hornbeck, J.A.	Phys.Rev. Phys.Rev.	80. 83.	297. 374.	1950. 1951.
3.38.	Newton, R.R.	Phys.Rev.	73.	570.	1948.
3.39.	Varney, R.N.	Phys.Rev.	93.	1156.	1954.
3.40.	Loeb, L.B.	"Basic Processes of Gaseous Electronics". U.C.P.			1955.

3.41. Raether, H. — Z.fur Phys. 107. 90. 1937.
Z.Techn.Phys. 12. 564. 1937.

3.42. Riemann, W. — Z.fur Phys. 120. 16. 1942.
Z.fur Phys. 122. 216. 1944.

3.43. Allen, K.R.
Phillips, K. — J.Elect.& Contr. 8. 273. 1960.

3.44. Breare, J.M.
Von Engel, A. — Proc.Roy.Soc. A282. 390. 1964.

3.45. Corrigan, S.J.B.
Von Engel, A. — Proc.Roy.Soc. A245. 335. 1958.

3.46. Schlumbohm, H. — Z.fur Phys. 182. 306. 1965.
Z.fur Phys. 182. 317. 1965.

3.47. Wagner, E.B.
Davis, F.J.
Hurst, G.S. — J.Chem.Phys. 47. 3138. 1967.

3.48. Hurst, G.S.
O'Kelly, L.B.
Wagner, E.B.
Stockdale, J.A. — J.Chem.Phys. 39. 1341. 1963.

3.49. Hurst, G.S.
Parks, J.E. — J.Chem.Phys. 45. 282. 1966.

3.50. Pederson, P.O. — Ann.der Phys. 71. 317. 1923.

3.51. Tam, R. — Archiv.f.Electr. 19. 235. 1928.

3.52. Beams, J.W. — J.Frank.Inst. 206. 809. 1928.

3.53. Wilson, R.R. — Phys.Rev. 50. 1082. 1936.

3.54. White, H.J. — Phys.Rev. 49. 507. 1936.

3.55. Newman, M. — Phys.Rev. 52. 652. 1937.

3.56. Fletcher, R.C. — Phys.Rev. 76. 1501. 1949.

3.57. Dawson, G.A.
Davies, D.E. — B.J.A.P. 14. 155. 1963.

3.58. Dawson, G.A. — Ph.D. Thesis, Keele Univ. 1963.

3.59. Betts, B.P.
Davies, D.E. — J.Phys.D. 1. 1852. 1968.

4.1.	Bedford, D.K.	J.Phys.E.	3.	77.	1970.
4.2.	Baley, E.G.C.	Phil.Mag.	35.	200.	1893.
4.3.	Druyvesteyn, M.J.	Physica.	2.	255.	1935.
4.4.	Riesz, R. Dieke, G.H.	J.Appl.Phys.	25.	196.	1954.
4.5.	Loeb, L.B.	J.Appl.Phys.	29.	1369.	1958.
4.6.	Mittelstadt, V.R. Oskam, H.J.	Rev.Sci.Instr.	32.	1408.	1961.
4.7.	Miller, J.C.	J.Appl.Phys.	35.	1745.	1964.
4.8.	Schmeltekopf, A.L.	J.Appl.Phys.	35.	1712.	1964.
4.9.	Smith, D.	Private Communication.			1969.
4.10.	Strong, J. (ed.)	"Modern Physical Laboratory Practice". London.			1948.
4.11.	Ishii, H. Nakayama, K.	8th.Nat.Vac.Sci.Symp.	1.	519.	1961.
5.1.	Hornbeck, J.A.	Phys.Rev.	80.	297.	1950.
5.2.	Evans, G.	Ph.D. Thesis, Keele Univ.			1967.
5.3.	Amin, M.R.	J.Appl.Phys.	25.	358.	1954.
5.4.	Hudson, G.G. Loeb, L.B.	Phys.Rev.	123.	29.	1961.
5.5.	Dawson, G.A.	Z.fur Phys.	183.	172.	1965.
5.6.	Przybylski, A.	Z.fur Phys.	168.	504.	1962.
5.7.	Geballe, R.	Phys.Rev.	66.	316.	1944.
5.8.	Legler, W.	Z.fur Phys.	173.	169.	1963.
5.9.	Bhalla, M.S. Craggs, J.D. Meek, J.M.	Proc.5th.Int.Conf. Ion Phen.in Gases.		315.	1961.
5.10.	Raju, G.R.G. Harrison, J.A. Meek, J.M.	B.J.A.P.	16.	933.	1965.

5.11.	McDaniel, E.W.	"Collision Phenomena in Ionised Gases". Wiley.		352.	1964.
	Po Lee	Astrophys.J.	115.	570.	1952.
	Weissler, G.L.				
	Wainfan, N.	Phys.Rev.	99.	542.	1955.
	Walker, W.C.				
	Weissler, G.L.				
	Bunch, S.M. et al.	J.Chem.Phys.	28.	740.	1958.
	Schonheit, E.	Z.Naturforsch.	15A.	841.	1960.
5.12.	Kouri, D.J.	J.Chem.Phys.	45.	154.	1966.
5.13.	Taylor, H.S.	J.Chem.Phys.	45.	2872.	1966.
	Nazaroff, G.V.				
	Golebiewski, A.				
5.14.	Eliezer, I.	J.Chem.Phys.	47.	2165.	1967.
	Taylor, H.S.				
	Williams, J.K.				
5.15.	Golden, D.E.	Phys.Rev.Lett.	14.	1010.	1965.
	Bandel, H.W.				
5.16.	Rapp, D.E.	Phys.Rev.Lett.	14.	533.	1965.
	Sharp, T.E.				
	Briglia, D.P.				
5.17.	Schulz, G.J.	Phys.Rev.Lett.	15.	946.	1965.
	Asundi, R.K.				
5.18.	Frommhold, L.	Phys.Rev.	172.	118.	1968.
5.19.	Kouri, D.J.	Phys.Rev.	184.	252.	1969.
	Sams, W.N.				
	Frommhold, L.				
5.20.	Ecker, G.	Z.Naturforsch.	16a.	246.	1961.
	Muller, K.G.				
5.21.	Muller, K.G.	Z.fur Phys.	169.	432.	1962.
5.22.	Muller, K.G.	Z.fur Phys.	179.	52.	1964.
	Wahle, P.				
5.23.	Fletcher, J.	Aust.J.Phys.	19.	615.	1966.
	Haydon, S.C.				
5.24.	Bagnall, F.T.	M.Sc. Thesis, Uni.New Engl.			1964.
5.25.	Chanin, L.M.	Phys.Rev.	132.	2547.	1963.
	Rork, G.D.				

5.26.	Haydon, S.C. Stock, H.M.P.	Aust.J.Phys.	19.	795.	1966.
5.27.	Llewellyn Jones,F. Davies, D.E.	Proc.Phys.Soc.	B64.	519.	1951.
5.28.	Davies, D.E. Dawson, G.A. Gozna, C.F.	Proc.5th.Int.Conf. Ion Phen.in Gases.		671.	1961.
5.29.	Morgan, C.G. Williams, W.T.	Proc.Phys.Soc.	85.	443.	1965.
5.30.	Massey, H.S.W. Burhop, E.H.S.	"Electronic and Ionic Impact Phenomena". Oxford.			1952.
5.31.	Kontaratos, A.N.	J.Appl.Sci.Res.	B12.	27.	1965.
A1.1.	Huxley, L.G.H. Crompton, R.W. Elford, M.T.	B.J.A.P.	17.	1237.	1966.
A1.2.	Editor.	B.J.A.P.	18.	691.	1967.
A4.1.	Smith, D.	Private communication.			1967.
A4.2.	D'Alessio, J.T. Ludwig, P.K. Burton, M.	Rev.Sci.Instr.	35.	1015.	1964.
A4.3.	Franke, H.G. Schmeing, H.	Nucl.Instr.Meth.	52.	171.	1967.
A4.4.	McMahon, D.H. Franklin, D.H. Carleton, H.R.	Rev.Sci.Instr.	37.	1142.	1966.
A4.5.	Preissinger, H.	Z.Angew.Phys.	22.	225.	1967.
A4.6.	Onuchin, A.P.	Instr.Exp.Tech.	4.	866.	1966.
A4.7.	Tawara, H.	Nucl.Instr.Meth.	42.	318.	1966.
A4.8.	Fischer, H.	J.Opt.Soc.Am.	51.	543.	1961.